The role of the microtubule-severing enzyme katanin in development, memory formation and consolidation

Dissertation

with the aim of achieving a doctoral degree at the Faculty of Mathematics, Informatics and Natural Sciences. Department of Biology of University of Hamburg

Submitted by

Franco Luis Lombino

from Mendoza, Argentina

Hamburg 2018

Evaluators:

Prof. Dr. Matthias Kneussel

Prof. Dr Christian Lohr

Date of defense: 05.10.2018

Declaration on oath

I hereby declare, on oath, that I have written the present dissertation by my own and have not used other than the acknowledged resources and aids.

Hamburg, 12th July 2018 _____

signature

“Keep your eyes on the goal,
use your heart along the road”

Table of contents

1. Summary

Microtubules (MTs) are dynamic polymers of α- and β-tubulin and their network plays essential roles during cell division. MTs establish contacts with kinetochores and participate in the segregation of genetic material, generate mechanical forces and contribute to spindle positioning. During cell division, the MT network is organized by the centrosomes and during interphase, MTs can be either stable or dynamic. They have been involved in cell migration, cellular morphology and intracellular cargo transport.

MT-severing enzymes are known to disassemble MT filaments and the first characterized MT-severing enzyme was katanin. Katanin is a heterodimeric complex formed by a regulatory subunit, p80, and a catalytic subunit, p60. P60 severing activity is regulated by ATP hydrolysis and the regulatory subunit, p80, targets p60 to the centrosome, suggesting that p60 katanin plays a role in cell division. Besides, previously reported data showed that p60 katanin severs MTs from their plus-ends, regulating cellular motility and mice lacking p80 katanin show malformations in the brain cortex. Little is known about MT-severing by katanin in non-mitotic cells, although it has been shown that inhibition of p60 affects neuronal morphology.

In this study, two main questions were addressed. First, focus was on the roles of the catalytic subunit of katanin, p60 in early processes of brain development and adult neurogenesis in *mus musculus*. Second, I described a new role of MT-severing by p60 in adult neurons, with special attention to post-synaptic compartments and synaptic transmission.

In order to address the first question, a previously generated constitutive *knockout* mouse for p60 katanin was used. The initial results showed that p60 is required for embryonic survival and proper neuronal development. Using cell biology and *in vivo* techniques, I showed that a downregulation of p60 in heterozygous *knockout* animals leads to an accumulation of cells in the ventricular zone (VZ) during embryonic corticogenesis and in the subgranular zone (SGZ) during adult neurogenesis. Additionally, during adult neurogenesis cell proliferation was impaired in the SGZ, which resulted in an increase of the progenitor pool size in heterozygous *knockout* animals. In agreement with previously reported findings

about the impact of SGZ adult neurogenesis *in vivo*, a minimal effect was observed at the behavioral level.

In the second set of data, I found that inhibition of p60 function with an ATPase-defective clone (p60-DEID) that acts as a dominant negative, alters MT dynamics and intracellular transport in neurons *in vitro* indicating that p60 plays a role in cargo distribution inside the cell by regulating the MT cytoskeleton. In order to assess p60 function at the synapse level, conditional depletion was required. Previously generated floxed mice were crossed with a time- and region-specific CRE-driver line. Electrophysiological data showed that stimulation of CA3 promotes an increased induction in Long-Term Potentiation at the CA1 region of the hippocampus of p60 conditional *knockout* mice, suggesting that p60 katanin is involved in early phases of synaptic plasticity. Besides, cell biology experiments showed that p60 katanin is present in post-synaptic compartments. MTs are known to enter dendritic spines and play a role in spine morphology, but inhibition of p60 function with p60-DEID decreased the number of MT +Tip in dendritic spines. Interestingly, spine growth was shown to occur upon long-term potentiation, but locally stimulated dendritic spines failed to undergo structural plasticity upon p60-DEID overexpression.

Altogether, this study showed a fundamental role for p60 in mammalian embryo survival and cell division during adult neurogenesis in the hippocampus, supporting previous data that connects p60 with cell proliferation. Finally, an active function of p60 katanin in synaptic compartments facilitating MT-entry in dendritic spines and participating in structural modifications during synaptic plasticity was shown in this study.

2. Zusammenfassung

Mikrotubuli (MT) sind dynamische Polymere die aus α- und β-Tubulin Dimeren aufgebaut sind. Sie spielen unter anderem in der Zellteilung eine wichtige Rolle, wobei sie sich mit Kinetochoren verbinden, zur Trennung des genetischen Materials beitragen, mechanische Kräfte erzeugen und bei der Positionierung der Spindel helfen. Während der Zellteilung wird das MT Netzwerk durch die Zentrosome organisiert und in der Interphase können die MT zwischen einem stabilen und einem dynamischen Zustand wechseln. Außerdem sind sie in die Zellmigration, die Zellmorphologie und den intrazellulären Transport involviert.

Es existieren mehrere Enzyme die MT schneiden und dafür bekannt sind, dass sie zum Abbau der MT Filamente beitragen. Das zuerst charakterisierte MT schneidende Enzym ist Katanin. Es liegt als heterodimerischer Komplex in der Zelle vor und besteht aus einer regulatorischen Untereinheit, genannt p80, und einer katalytischen Untereinheit, genannt p60. Die katalytische Untereinheit p60 schneidet MT, welches durch ATP Hydrolyse reguliert wird und die regulatorische Untereinheit p80 sorgt für die Lokalisation von p60 zum Zentrosom. Dies legt nahe, dass p60 Katanin eine Rolle in der Zellteilung spielt. Außerdem konnte gezeigt werden, dass p60 Katanin MT vom plus Ende her schneidet und damit Zellbewegung regulieren kann. Mithilfe eines Mausmodels konnte nachgewiesen werden, dass Mäuse denen p80 Katanin fehlt, Fehlbildungen des Kortex zeigen. In Zellen, die sich nicht teilen ist jedoch wenig über den Abbau von MT durch Katanin bekannt. Obwohl gezeigt wurde, dass eine Inhibition von p60 Katanin die Morphologie von Neuronen beeinflusst.

In dieser Studie werden zwei Hauptfragestellungen untersucht. Zum einen, liegt der Fokus auf der Rolle der katalytischen Untereinheit, p60 Katanin, in der frühen Gehirnentwicklung und der adulten Neurogenese in Mäusen (*mus musculus*). Zum anderen, untersuche ich eine bisher unerforschte Rolle des MT Filament Abbaus durch p60 Katanin in adulten Neuronen, mit einem genaueren Augenmerk auf Post-Synaptische Regionen und synaptischer Signalübertragung.

Um die erste Frage zu beantworten, wurde ein schon generiertes konstitutives *Knockout* Mausmodell für p60 Katanin genutzt. Die ersten Ergebnisse zeigen,

dass p60 Katanin für das embryonale Überleben und die neuronale Entwicklung wichtig ist. Durch zellbiologische und *in vivo* Techniken konnte ich zeigen, dass eine herunter Regulierung von p60 Katanin in heterozygoten *Knockout* Tieren zu einer Ansammlung von Zellen in der ventrikulären Zone (VZ) während der embryonalen Kortex Entwicklung und in der subgranulären Zone (SGZ) während der adulten Neurogenese führt. Zusätzlich ist die Zellvermehrung in der SGZ bei der adulten Neurogenese behindert, was zu einer Vergrößerung der Stammzellpools in heterozygoten *knockout* Tieren führt. Übereinstimmend mit bereits veröffentlichten Ergebnissen über den Einfluss der adulten Neurogenese in der SGZ *in vivo*, wurde ein minimaler Effekt bei Verhaltensexperimenten beobachtet.

In Bezug auf die zweite Fragestellung, konnte ich nachweisen, dass die Inhibition der p60 Funktion mittels eines Klons (p60-DEID) der nicht durch ATPase aktiviert werden kann und somit als dominant negatives Protein fungiert, die MT Dynamik und den intrazellulären Transport in Neuronen *in vitro* beeinträchtigt. Dies weist darauf hin, dass p60 durch die Regulation des MT Zytoskeletts indirekt eine Rolle in der Verteilung von Kargo innerhalb der Zelle spielt. Um die Funktion von p60 auf dem synaptischen Level zu beurteilen, ist ein konditionaler Abbau erforderlich. Hierfür wurden bereits generierte gefloxte Mäuse mit einer Zeit- und Region spezifischen CRE-driver Linie gekreuzt. Elektrophysiologische Daten zeigen, dass die Stimulation der CA3 Region eine erhöhte Induktion der Langzeit Potenzierung in der CA1 Region des Hippocampus von p60 konditionalen *knockout* Mäusen induziert. Dies weist darauf hin, dass p60 Katanin in die frühe Phase synaptischer Plastizität involviert ist. Außerdem konnten Zellbiologische Experimente zeigen, dass p60 Katanin in postsynaptischen Kompartimenten vorhanden ist. MT sind dafür bekannt, dendritische Spines zu enervieren und eine Rolle in der Spinemorphologie zu spielen. Die Inhibition der p60 Funktion mittels p60-DEID verringert jedoch die Anzahl an MT Plus-Enden in dendritischen Spines. Interessanterweise wurde nachgewiesen, dass Spines durch Langzeit Potenzierung wachsen, lokal stimulierte Spines nach p60-DEID Überexpression jedoch keine strukturelle Plastizität zeigen.

Zusammenfassend, zeigt diese Studie die fundamentale Rolle von p60 Katanin für das Überleben von Säugetierembryonen und für die Zellteilung während der adulten Neurogenese im Hippocampus, was bereits publizierte Daten unterstützt,

wonach p60 mit Zellteilung in Zusammenhang gebracht wird. Schlussendlich konnte gezeigt werden, dass die aktive Funktion von p60 Katanin in Synapsen den Eintritt von MT in dendritische Spines erleichtert und während synaptischer Plastizität eine Rolle in der strukturellen Modifikation spielt.

3. Introduction

3.1. The Central Nervous System

The Central Nervous System (CNS) is a structure composed of the brain and the spinal cord. It is also known to be the part of the Nervous System that integrates and processes information. The computational units of the CNS are neurons, and together with other cell types, they contribute to the achievement of complex activities and brain processes such as memory storage. Neurons are polarized cells consisting of many dendrites, a cell soma and a long axon. This asymmetrical structure allows them to receive inputs from many cells, elaborate them, and transmit complex signals to the next unit in the circuit. Each neuron is part of a larger neuronal network and forms precise connections with numerous neurons, allowing the system to accomplish a very high complexity. In order to achieve this, neurons must be born, form their connections, and re-define them across time (Fig. 1) (Alberts B. et al., 2002).

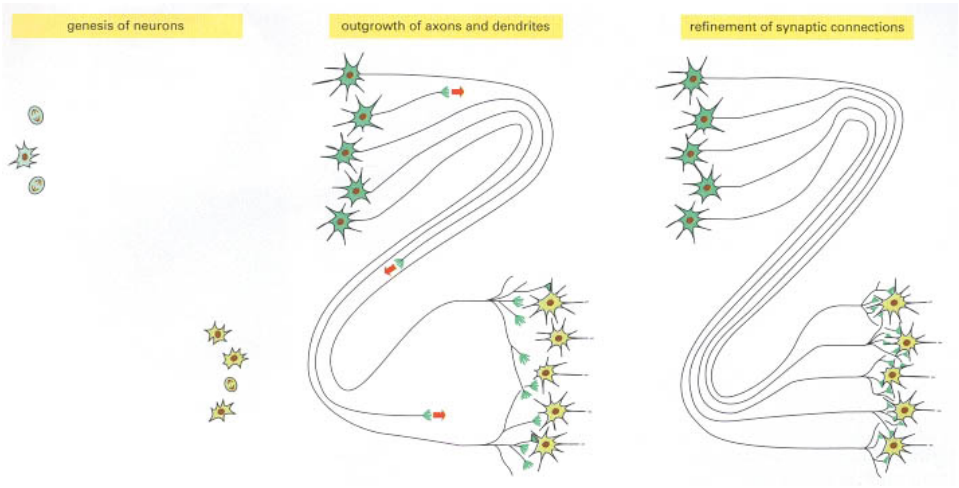

Figure 1. ***Phases of Neuronal development.*** After neurons are born, they start growing dendrites and axons. This allows them to make connections with other neuronal units. These connections are then specified. ***(Alberts B. et al., 2002).***

3.2. Embryonic brain development

During early embryonic development, a key step in defining the future organism's general architecture is gastrulation. During this process, three well-defined layers are formed, and are termed as endoderm, mesoderm, and ectoderm; gastrulation also promotes the formation of a midline and anterior and posterior axes (Solnica-Krezel L. and Sepich D. S., 2012). The notable result of this process is the presence of the notochord that extends along the midline. The region of the ectoderm located above the notochord is known as the neuroectoderm. The notochord plays an important role in brain formation, and indeed, molecular signals from this structure promote neuroectodermal cell differentiation into neuronal precursor cells. This process is known as neurulation and it leads to the formation of the neural plate (Purves D. et al., 2001).

The neural plate, through a layer invagination, gives rise to the neural tube. Neurulation can be differentiated into primary and secondary neurulation, and it shares common features in reptiles, birds and mammals. In mammals, primary neurulation forms three different groups of cells: cells that form the internal neural tube, which will form the brain and spinal cord; cells for the external epidermis of the skin; and the neural crest cells (Gilbert SF., 2000).

The neural tube is the structure that eventually leads to the formation of the brain and the spinal chord. Indeed, two subsets of stem cells are present in the neural tube: the ventral region stem cells, which give rise to motor neurons, and another group that is located further apart from the ventral region, which leads to the production of sensory neurons.

On the dorsal part of the neural tube, the presence of a third group of stem cells is evident. They form a structure called the neural crest. Neural crest cells migrate away from the neural tube and give rise to a variety of neuronal and non-neuronal cells (Fig. 2) (Purves D et al., 2001).

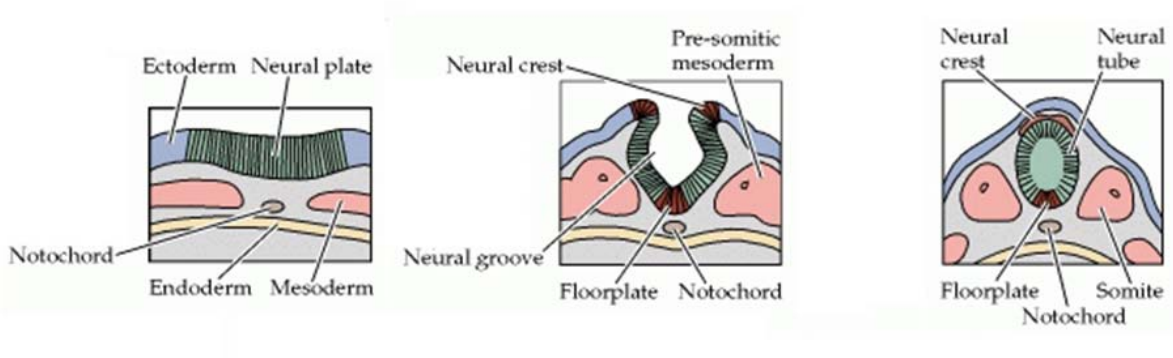

Figure 2. ***Structure and development of the neural tube.*** **(adapted from Purves D. et al. 2001).**

In this respect, other groups have extensively contributed to the field by showing that molecules have a fundamental function in conferring an identity to the distinct neural tube cell populations (Echelard Y. et al., 1993; Marti E. et al., 1995; Ericson J. et al., 1997; Briscoe J. et al., 2000). One example is the Sonic Hedgehog (SHH) signaling factor that promotes the ventral characterization on the neural tube in a gradient-like expression pattern (Patten I. and Placzek M., 2000).

Once the neural tube is formed, an additional level of differentiation takes place: The tube starts to partition through movements and constrictions and forms three different regions called forebrain, midbrain and hindbrain. At the neural tube's most caudal region, the spinal chord starts developing too. It is widely known that in neural tube partitioning, important and widely studied transcription factors are involved. A clear example is the homeobox (Hox) genes family, whose expression corresponds to or anticipates many region-specific processes (Philippidou P. and Dasen J. S., 2013). It is important to note that these genes by themselves do not directly determine the identity of a region. Rather they contribute to a cascade of events that eventually leads to the structural specification (Purves D et al., 2001).

An important region for subsequent steps is the ventricular zone (VZ), which is the inner layer of cells within the neural tube and contains precursors that could lead to neuronal or glial cells (Levitt P. et al., 1981).

Stem cells in the VZ can to give rise to many post-mitotic neurons or to renew the stem cell pool. They do so by dividing while performing stereotyped movements in

the VZ area. These movements are well characterized and correspond to specific cell cycle steps (Fig. 3) (Purves D et al., 2001).

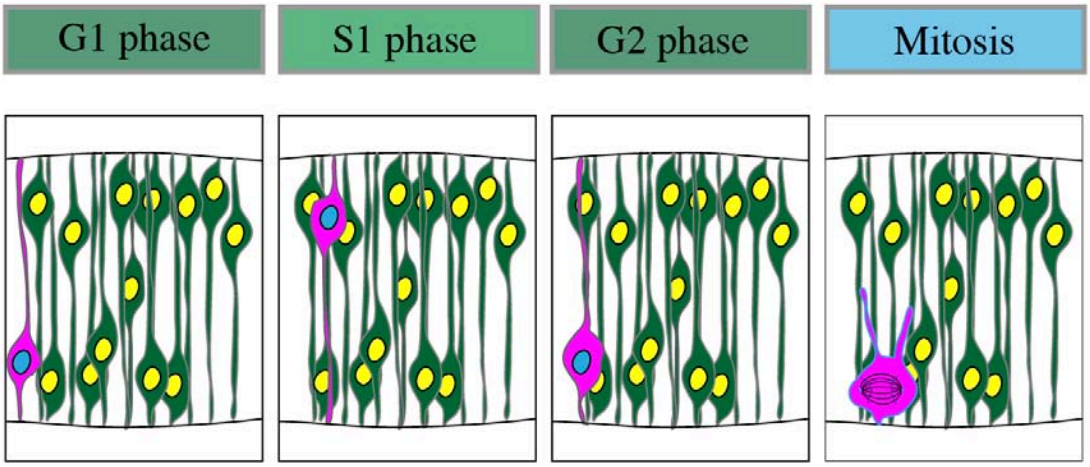

Figure 3. ***Cell proliferation in the ventricular zone during embryonic cortical development.*** Stem cells that undergo cell division manifest a sequence of stereotyped movements that have been well characterized in the field. Before mitosis, cells undergo a series of growing steps coupled to cytokinetic processes.
(Cartoon by F. L. Lombino adapted from Purves D. 2001).

3.2.1. Neuronal Development

After they are born, neurons display specific developmental patterns. However, since dissociated neurons are a common tool for research, it is worth mentioning that *in vivo* and *in vitro* neuronal development differs drastically.
In vitro, neurons are first dissociated from the whole tissue and then seeded in a laboratory dish. On the other hand, *in vivo*, neurons start their development right after they are born. Here, I aim to summarize the main characteristics of neuronal development in order to facilitate results interpretation.
One key processes during neuronal development both *in vitro* and *in vivo* is neuronal polarization. This is one of the initial processes that confer directionality to all neuronal functions (De Anda F. C. et al., 2005; Takano T. et al., 2015). *In vitro*, neuronal polarization and acquisition of the typical structure of a mature

neuron was first described by Dotti and colleagues (Dotti CG. et al., 1988). In their work, they plated hippocampal neurons from embryonic rats and followed their development until both axon and dendrites were fully developed. What they showed is that after 24 to 48 hours in culture, cells display a major process that later on becomes the mature axon, and minor processes that grow at a slower rate that will form the dendritic tree. *In vivo*, the situation is far more complex. Neuronal development differs from one brain region to the other (Hall A. C. et al., 2003). For example, excitatory cortical neurons are born in the VZ and migrate to their respective layer in the cortical plate (Tan X. and Shi S-H., 2013). In order to achieve this, they transit from a multipolar state with many protrusions, to a bipolar migrating state in which a longer trailing neurite and a long leading protrusion exist. Subsequently, trailing and leading processes will become the axon and dendrite, respectively (Miyata et al., 2004; Noctor et al., 2004). Neuronal polarization is regulated by many molecular and macromolecular processes. Among others, the neuronal cytoskeleton plays a fundamental role (Stiess M. and Bradke F., 2011). It is widely known that the actin and the MT cytoskeleton are involved during the entire neuronal polarity process in different ways (reviewed by Takano T. et al., 2015). It has been shown that destabilization of the actin cytoskeleton in the growth cone is required for axonal specification (Bradke F. and Dotti C. C., 1999). Opposite to that but in an orchestrated manner, a higher MT stability in the growing axon is also needed (Witte H. et al., 2008) (Fig. 4). Moreover, Microtubule-associated Proteins (MAPs) have been linked to such a mechanism (Umeda K. et al., 2000) although some data is still controversial.

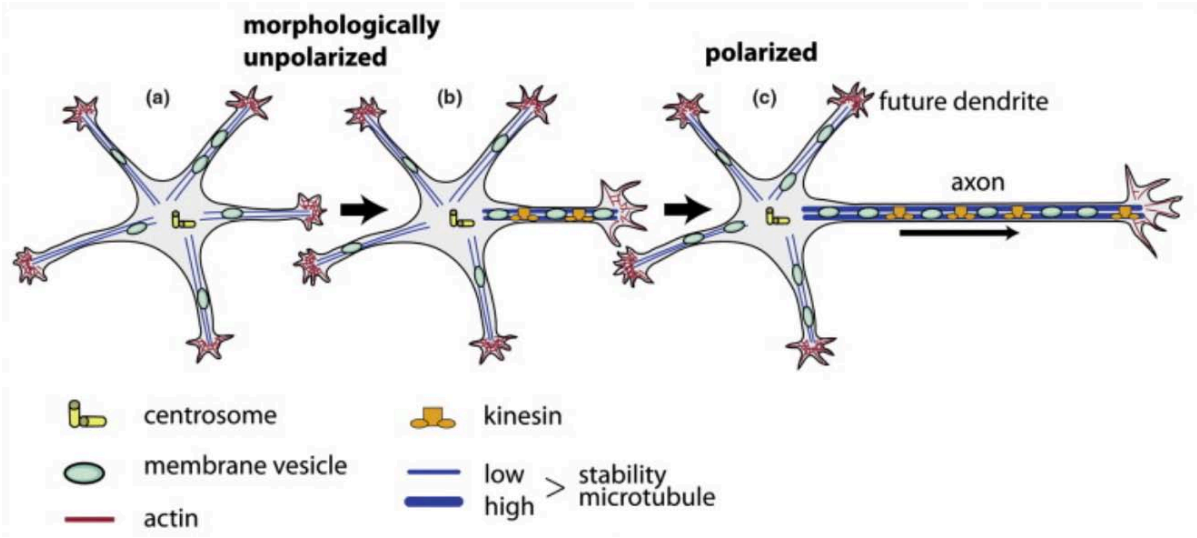

Figure 4. ***Involvement of the cytoskeleton in neuronal polarization.*** An important player during neuronal polarization is the MT cytoskeleton. An orchestrated stability and instability of MTs in growing neurites, leads to the specification of the neuronal axon. ***(Witte H. and Bradke F. 2008).***

3.2.2. Embryonic Cortical Development

The mammalian cerebral cortex is composed mainly of two neuronal subtypes: Pyramidal excitatory neurons that have long projections and non-pyramidal inhibitory interneurons (Molnár Z. et al., 2006). Cortical development is an intriguing aspect of embryogenesis. Defects in this process have been related to pathological conditions (Pang T. et al., 2008).

Cell division during corticogenesis is tightly regulated, with cells shown to transit from a symmetrical to an asymmetrical division (Paridaen J. T. M. L. and Huttner W. B. 2014). Dysregulation of this switch has been linked with tumorigenesis in other tissues (Knoblich J. A. 2010). One of the main players in regulating cell division is the spindle pole (Lancaster M. A. and Knoblich J. A. 2012). The position of the spindle regulates the size (McNally F.J. 2013) and fate (Horvitz H. R. and Herskowitz I., 1992) of daughter cells and the MT cytoskeleton is known to regulate this process (Kaltschmidt J. A. and Brand A. H., 2002; Pearson C. G. and Bloom K., 2004; McNally F.J. 2013).

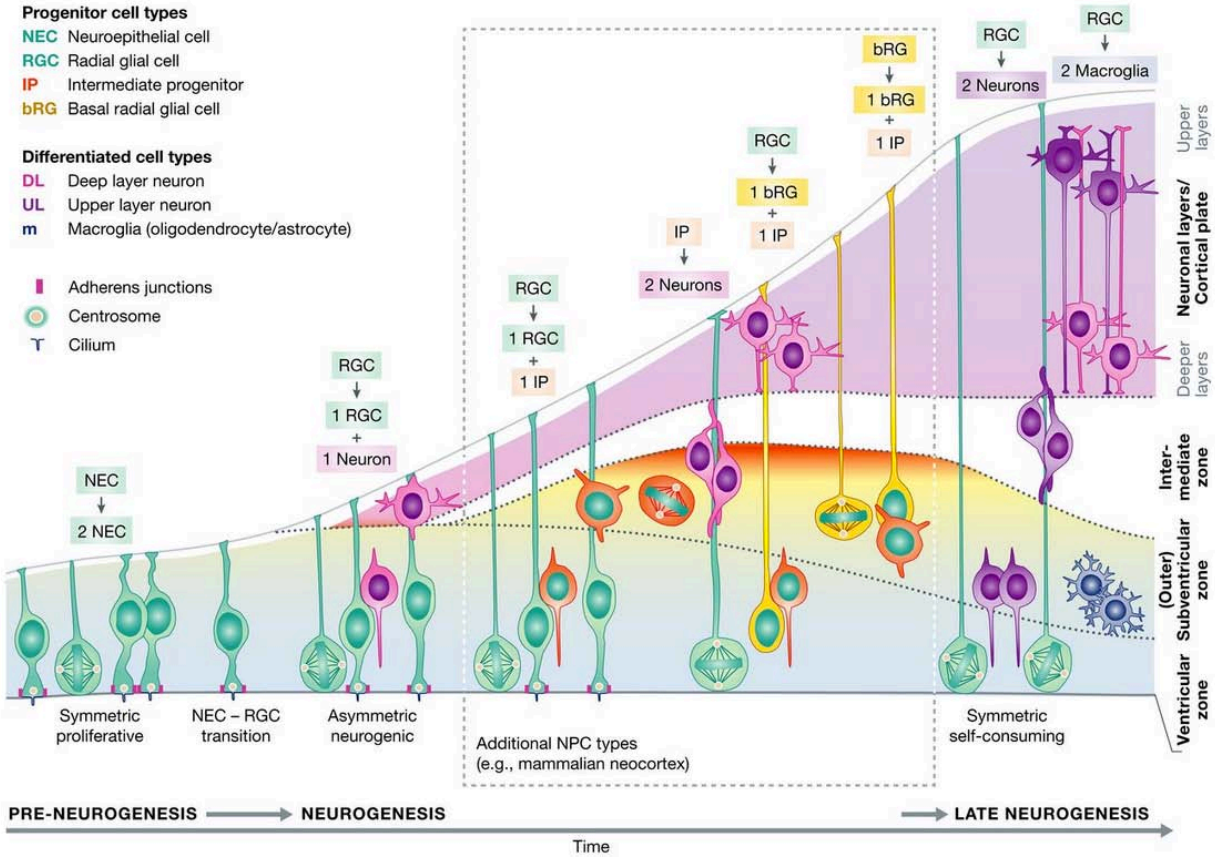

Figure 5. ***Symmetric and asymmetric cell division during embryonic corticogenesis.*** During the formation of the neocortex, dividing cells must transit from a symmetric division pattern, to an asymmetric one, leading to the formation of precursors and adult neurons. ***(Paridaen J. T. M. L. and Huttner W. B. 2014).***

In rodents, from early stages of cortex development til embryonic day 13 (E.13), the most prominent niche for newborn neurons is the VZ. Later on, at around E.15, the subventricular zone (SVZ) takes over to become the major secondary niche for post-mitotic neuron generation (Smart I. H. M., 1973; Smart I. H. M. and McSherry G. M., 1982).

Cortical neurons are generated from radial glial cells (RGC) (Malatesta P. et al., 2000), short neural precursors (SNP) that reside in the VZ (Gal J. S. et al., 2006), and intermediate progenitors (IPC) found in the SVZ (Noctor S. C. et al., 2004). At the beginning of neurogenesis, RGCs start dividing asymmetrically to generate a

RGC and a differentiating neuron. (Paridaen J. T. M. L. and Huttner W. B. 2014). RGCs eventually undergo asymmetric cell division to originate a daughter RGC and an IPC. IPCs in the SVZ consequently divide symmetrically and give rise to two differentiating neurons (Paridaen J. T. M. L. and Huttner W. B. 2014) (Fig. 5). Interestingly, RGCs who are also called apical progenitors, exhibit a bipolar morphology with an elongated neurite that crosses the cortical formation, while SNPs appear to have only a short anchoring basal process (Gal J. S. et al., 2006). Although inhibitory interneurons are thought to originate in the medial and caudal ganglionic eminence of the newly formed brain and undergo long tangential migration (Lavdas et al., 1999; Sussel et al., 1999; Wichterle et al., 1999), pyramidal neurons migrate radially and to generate the different cortical layers in an inside-out gradient (Rakic P. 1995) (Fig. 6).

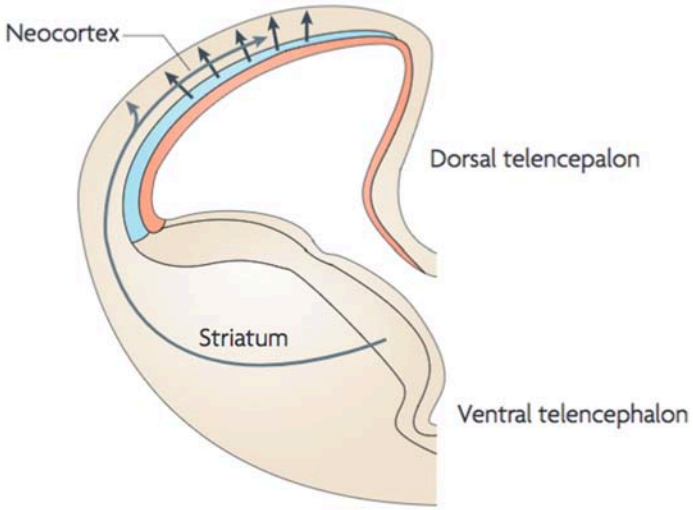

Figure 6. ***Pyramidal neurons and non-pyramidal interneurons migration patterns.*** Dark-gray arrows indicate origin and radial migration of excitatory cortical neurons. Light-gray arrow indicates interneurons that migrate from the ventral telencephalon to their cortical destination in a tangential migration pattern. **(Dehay C. and Kennedy H. 2007).**

During cortical migration, neurons give rise to what is known as the preplate (PP). In the PP, neurons split into the Marginal Zone and Subplate (MZ and SP, respectively) to give rise to the Cortical Plate (CP). MZ and CP will originate what in the mature cortex is a well-defined 6-layered structure (Meyer G. et al., 2000; Marin-Padilla M., 1978; Smart I. H. M. and McSherry G. M., 1982; Smart I. H. M. and Smart M., 1982; Luskin M. B. and Shatz C. J., 1985). Following the previously described inside-out migration paradigm during corticogenesis, older neurons reside in deeper layers of the newly formed cortex (Fig. 7).

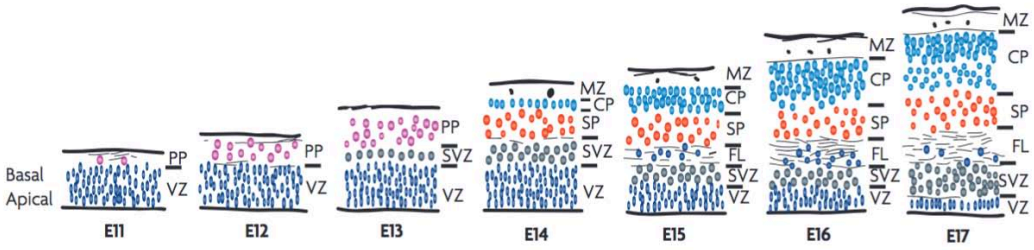

Figure 7. ***Cortical migration in rodents.*** The cortex in rodents is developed in an inside-out paradigm. Neurons are born in the VZ and migrate radially to upper layers of the neocortex. In this way, younger neurons form upper cortical layers. ***(adapted from Smart I. H. et al., 2002)***

3.2.3. Adult Neurogenesis

It is more than fifty years since Altman first described the presence of dividing neurons in the mammalian post-natal brain (Altman J., 1962). Altman made use of [3-H]-thymidine (tritiated thymidine) autoradiography and challenged the dogmatic theory that excludes the possibility of neurogenesis in the adult brain. His findings demonstrated that glial proliferation took place after an acute brain lesion. Furthermore, he observed the presence of proliferating neuroblasts, glial cells and neurons in brain regions close to the lesion site. Altogether, his data was a new open era for a new research, which has an incredible potential for clinical applications. However, his findings did not receive much attention at the time due to the limitations of the techniques used. It was Kaplan, fifteen years later, who

supported Altman's findings using tritiated thymidine and electron microscopy (E.M.) (Kaplan, M.S. & Hinds, J.W., 1977). Nowadays, the field has developed extensively. New techniques including the characterization of bromodeoxyuridine (BrdU) (Kuhn H.G. et al., 1996), has allowed many groups to investigate and manipulate the process in more detail. Because of these contributions, we know now that in the adult brain and under normal conditions, neurogenesis takes place in at least two major regions: the sub-ventricular zone (SVZ) that provides the Olfactory Bulb (OB) with newborn interneurons (Lois C. and Alvarez-Buylla A., 1994) and the sub-granular zone (SGZ) of the dentate gyrus (DG) (Gage F.H., 2000). Importantly, newborn cells have been shown to differentiate (Lois C. and Alvarez-Buylla A., 1993) and integrate functionally into the pre-existing circuit (Paton J. A. and Nottebohm F. N., 1984). Adult neurogenesis is demonstrated to occur also in the adult human brain (Eriksson P. S. et al., 1998; Knoth R. et al., 2010, Boldrini M. et al., 2018), although others have challenged this hypothesis (Sorrells S. F. et al., 2018). Sorrells and colleagues (2018) have recently failed to identify newborn neurons in adult human brains.

It is suggested based on previous studies that quiescent multipotent stem cells are mainly radial glia-like cells that generate granule post-mitotic neurons in the SGZ, and interneurons and oligodendrocytes in the SVZ. The migratory path will then drive the SVZ-originated cells to the olfactory bulb (OB) and corpus callosum, respectively (reviewed by Guo-li M. and Hongjun S., 2011).

In this study, focus was mainly on adult neurogenesis in the SGZ, although a brief background of SVZ neurogenesis will be provided as well.

SVZ neurogenesis

In a region along the walls of the adult brain lateral ventricles, there is a niche of proliferating cells that undergo long-range migration via the Rostral Migratory Stream (RMS) to the OB (Fig. 8). Here, they get integrated and differentiate into post-mitotic interneurons (Lim D.A. and Alvarez-Buylla A., 2018). In the SVZ, type B1 cells are considered to be the Neuronal Precursor Cells (NPCs). From type B1 cells, type C or transit-amplifying precursors are generated. They are responsible for generating new neuroblasts or type A cells. Nowadays, Doublecortin (DCX) is used to label type A cells (Doetsch et al. 1997).

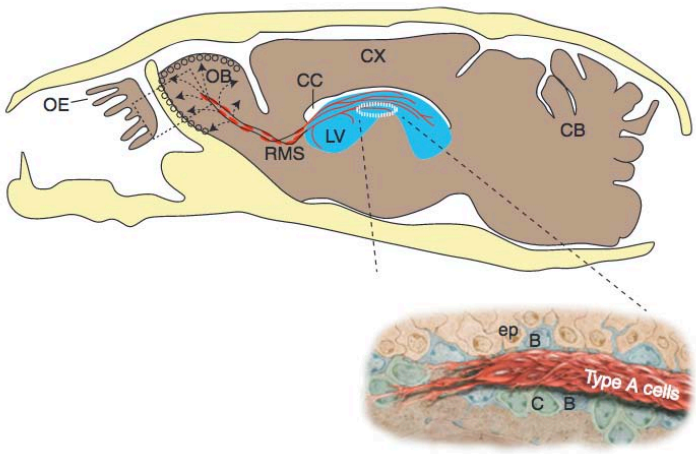

Figure 8. ***Adult neurogenesis in the SVZ.*** The SVZ is one of the neurogenic niches of the adult brain. Neurons originated in this region undergo long-range migration via the RMS and integrate in the olfactory bulb region as interneurons. ***(Lim D.A. and Alvarez-Buylla A. 2018).***

Interestingly, not all the type B1 cells are the same. Instead, their position in the SVZ determines their characteristics leading to different types of interneurons in the OB (Merkle et al. 2007; Alvarez-Buylla et al. 2008).

SGZ neurogenesis

As outlined before adult neurogenesis was first characterized by J. Altman over 50 years ago (Altman J., 1962). Despite initial skepticism, his findings are now widely accepted. . His experiments using tritiated thymidine that was incorporated in dividing cells have extraordinary potential for the possible impact of newborn neurons in hippocampal connectivity. Indeed, many hypotheses have been made regarding the functions of such an intriguing homeostatic brain process (Aimone J. B. et al., 2006; Braun S. M. G. and Jessberger S., 2014; Apple D. M. et al., 2017).

In the SGZ, NPCs originate from Neuronal Stem Cells (NSCs) to give rise to immature neurons. A brief radial migration of immature neurons allows them to integrate into the Granule Cell Layer (GCL) and become part of the hippocampal circuitry (Aimone J.B. et al., 2014).

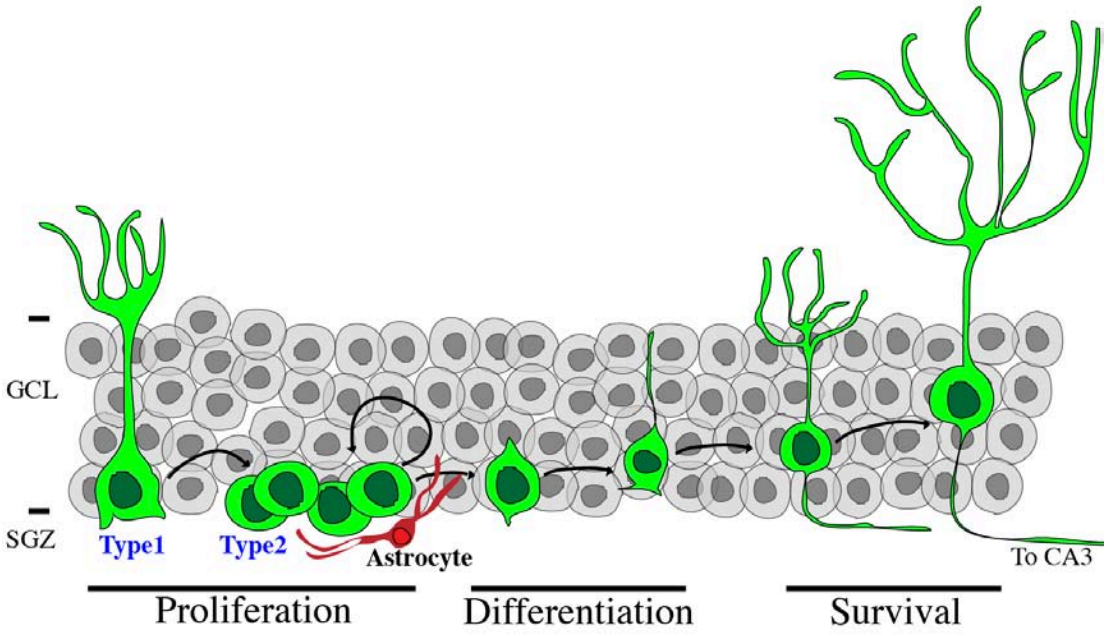

Figure 9. ***Adult neurogenesis in the DG.*** Adult neurogenesis in the SGZ involves the generation of cells through a well characterized sequence of events. Type 1 cells undergo meiotic cell division and generate intermediate precursor cells IPCs. Neuroblasts do not proliferate further but rather differentiate and migrate radially over a short distance to the Granular Layer of the DG. The result of this process is the integration into the hippocampal circuitry of a new cellular unit that receives inputs from the perforant path and projects its axon to the CA3 formation therefore participating in hippocampal connectivity. ***(Cartoon by F. L. Lombino, adapted from Aimone JB et al., 2014)***

In details, Radial Glia-like cells (RGLs) are Type 1 cells and considered to be the NSCs that generate intermediate precursor cells (IPCs) or Type 2 cells. After another division step, IPCs can give rise to Type 3 cells or neuroblasts that mature and migrate to the GCL (Gonçalves J. T. et al., 2016) (Fig. 9). The identity of Type 1 cells of the SGZ is an intriguing topic. It is shown that different sub-populations of cells coexist in this microenvironment, which can be identified based on the specific expression of GFAP (Seri B. et al., 2001), Nestin (Lendahl U. et al., 1990) and Sox2 (Ellis P. et al., 2004). It is also possible that the differential expression of these proteins influences their self-renewal versus differentiation capabilities (Gonçalves T.J. et al., 2016). As discussed later, proliferating cells in the SGZ are selectively identified based on the combination of molecular markers that these cells express (Zhang J. and Jiao J., 2015) (Fig. 10).

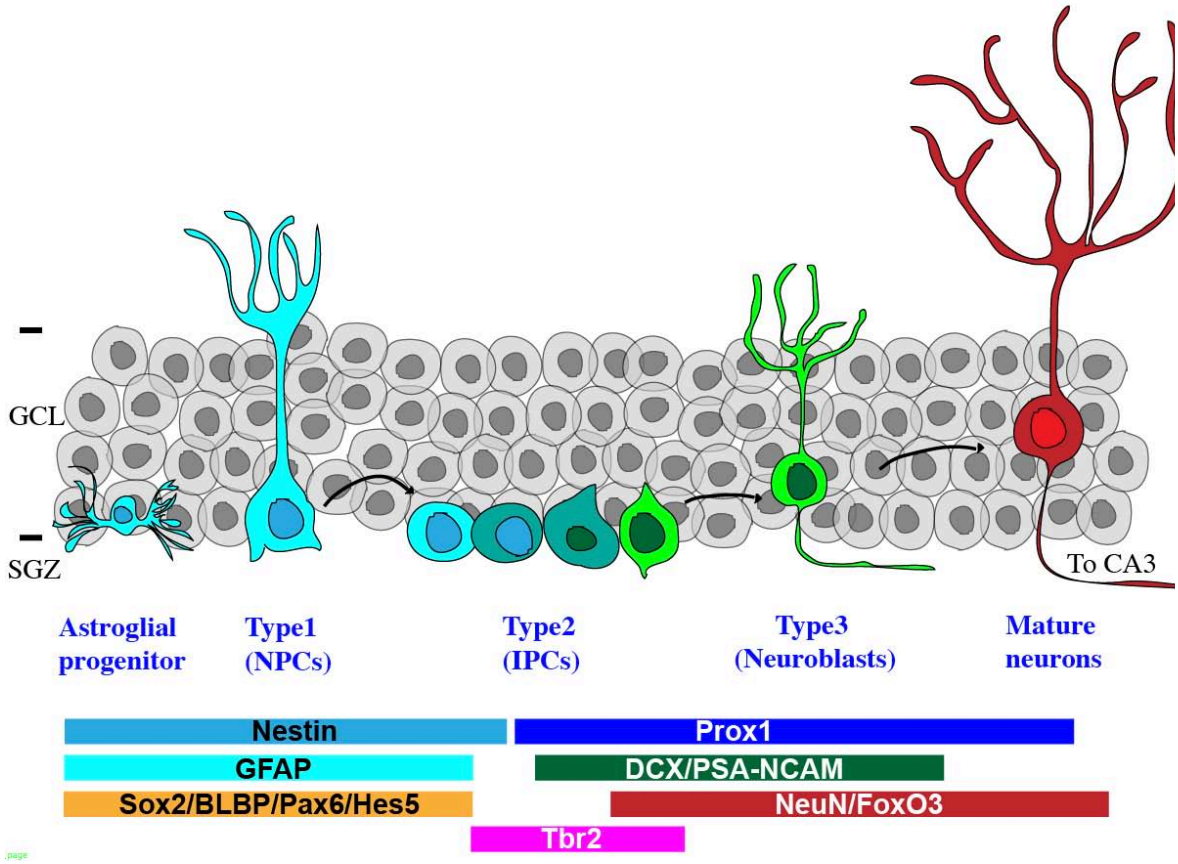

Figure 10. ***Differential marker expression of distinct cell populations in the SGZ.*** Adult neurogenesis takes place in the SGZ of the DG. Astroglial progenitors give rise to Type 1 cells, which in turn generate Type 2 Intermediate progenitors. Finally Neuroblasts are generated which undergo differentiation, migration and maturation to form adult neurons that integrate into the hippocampal circuitry. Notably, it is possible to identify cells in each proliferative stage based on the expression, absence of expression, or combination of multiple molecular markers. For example, Neuronal Progenitor cells can be identified based on the combined expression of GFAP/Sox2, while Neuroblasts typically express DCX. ***(cartoon by F. L. Lombino adapted from Zhang J. 2015)***

The niche of NSCs at the SGZ is tightly regulated by intrinsic and extrinsic factors such as supporting cells, extracellular matrix and blood vessels (Ferraro F. F. et al., 2010). At the molecular level, one of the key players in maintaining the SGZ homeostasis is Notch and its signaling pathway. Some studies state that Notch is involved in maintaining the undifferentiated state of NSCs and acts in a context-

and time-dependent manner, influencing parameters like proliferation and cell-cycle exit (Breunig et al., 2007). Another group of molecules that has been shown to participate in SGZ homeostasis is sonic hedgehog (SHH) specifically in the expansion of progenitors (Breunig et al., 2008). However, other molecular pathways have also been shown to be involved in different stages of cell proliferation (Liu H. and Song N., 2016). It is known from a study performed by Spalding who used ^{14}C to show that around 700 neurons are born every day, suggesting that adult neurogenesis plays a critical role in maintaining brain connectivity (Spalding K.L. et al., 2013). However, there is no consensus in the field about the possible function of these cells.

3.2.4. Roles of Adult Neurogenesis

As stated before, the roles of adult neurogenesis in the mammalian brain are still under debate. Many conflicting data exist, possibly due several factors such as animal strains used (Clark P. J. et al., 2011), age of the animals in which the experiments are carried out (Martinez-Canabal A. et al., 2013) and variations of the protocols employed for the tests (Drew M. R. et al., 2010). Also, neurogenesis can be manipulated in different ways: it can be positively regulated via exercise (Wolf S. A. et al., 2011; So J. H. et al., 2017) and environmental enrichment (Monteiro B. M. et al., 2014), or negatively affected via irradiation (Wojtowicz J. A., 2006), genetically (one example is Saxe M. D. et al., 2006) or subjecting the animals to aversive conditions such as chronic stress (Lucassen P. J. et al., 2009). It is therefore clear that the different manipulations used can impact the magnitude of adult neurogenesis, leading to different outcomes and interpretations. This has led to challenges in forming strong conclusions on the on the role of adult neurogenesis. In this study I adhere to a general knowledge in which DG neurogenesis has been shown to play a role in rodents by many groups.

From the connectivity point of view, the hippocampus receives inputs from the entorhinal cortex (EC) via the perforant path (Köhler C. 1985) and its intrinsic circuitry is composed of three synapses: the DG receives inputs from the EC and projects its mossy fibers to the CA3 (Jonas P. and Lisman J., 2014). Finally, CA3 Schaffer collateral axons project to CA1 pyramidal neurons (Amaral DG. And Witter MP., 1989).

In order to elucidate the function of the hippocampus, it is useful to consider reports of patients in which this region has been damaged or animal models that show compromised hippocampal function. Scoville and Milner published a milestone case report (Scoville WB. and Milner B., 1957) in which patient H.M. was reported to have retrograde memory impairments following lesions of the temporal lobe, including the hippocampus. Since then, the hippocampus has been linked to memory formation and consolidation. In 1971, electrophysiological recordings from cells in the dorsal hippocampus gave rise to an important study published by O'Keefe and Dostrovsky. The authors showed in behaving rats that special firing patterns could be observed during head turns or in response to external stimuli (O'Keefe J. and Dostrovsky J., 1971; O'Keefe J, 1976). This was the first evidence showing that the hippocampus played a role in spatial mapping. This idea was investigated further by several groups, which has led to the discovery of grid cells, head direction cells and place cells that contribute to different aspects of mapped navigation (reviewed by Moser E.I. et al., 2017). The concept of the hippocampus as a reference map during spatial navigation was consolidated (O'Keefe J and Nadel, 1978).

Within the hippocampal circuitry, the DG plays a major role in processing inputs from the enthorinal cortex before projecting to the CA3 (Jonas P. and Lisman J., 2014). Mature granule cells in the DG receive glutamatergic excitatory inputs from the EC and inhibitory inputs from DG interneurons (Zhao C. et al., 2008). The DG is organized into layers that correspond to Molecular Layer, Granule Layer and Hilus, from the top to the bottom (Witter MP et al., 1989).

Although the role of newborn cells in the SGZ of the adult hippocampus is still controversial, studies have shown that these cells are involved in a variety of processes. In a study that used methylazoxymethanol acetate (MAM), a drug that methylates DNA to reduce neurogenesis, the authors found that reduced number of newborn neurons impaired hippocampal-dependent associative fear memory (Shors T. J. et al., 2001), suggesting a role for these cells in hippocampal memory. Likewise, ablation of adult neurogenesis after learning impairs spatial memory in specific paradigms (Arruda-Carvalho M. et al., 2011). Other studies have connected newborn neurons in the SGZ to social-avoidance and paternal recognition (Lagace D. C. et al., 2010; Mak G. K. and Weiss S., 2010), although adult neurogenesis in the OB also plays a major role in social recognition tasks.

Recent findings indicate that adult generated neurons might be involved in discriminating similar or ambiguous inputs in a process known as pattern separation (Kheirbek M. A. et al., 2012). In this respect, studies demonstrated that by increasing adult generated neurons, the capacity to discriminate between similar contexts was increased (Sahay A. et al., 2011).

3.3. Neuronal Connectivity: Synapse formation and Synaptic transmission

Luigi Galvani demonstrated the existence of synaptic transmission when he induced muscle contraction in a frog and first described the concept of “animal electricity” (Galvani L. 1791; Piccolino M. 1997; Cowen WM. and Kandel ER. 2001). Later on, Ramon y Cajal showed that neurons are unique structures that connect with each other, and that electric communication has a directionality that starts in dendrites and finishes at the axon. For their work, Ramon y Cajal and Camillo Golgi were awarded the Nobel Prize in 1906. Two interconnected cells communicate via synapses, which are currently classified into two main types: chemical and electrical synapses. Electrical synapses are predominantly formed by gap-junctions (Bennett M. V. L., 1997). Gap-junctions are physical contacts between two adjacent cells in which connexins are the most relevant family of proteins (Söhl G. and Willecke K., 2004). The function of these synapses appears to be the electric synchronization of a connected network of neurons (Nagy JI. et al. 2017).

On the other hand, chemical synapses are characterized by the presence of a synaptic cleft, which is the space between the pre- and post-synaptic compartments and where messenger molecules or neurotransmitters are released (Purves D. et al., 2001). During synaptic transmission, the pre-synaptic compartment, in this case an axon terminal, releases neuropeptides or neurotransmitter into the synaptic cleft which is then captured or binds to the post-synaptic compartment (Levitan IB. and Kaczmarek LK. 1997). Chemical synapse identity and subsequent output depends on the predominant neurotransmitter type

at the pre-synapse and the availability of corresponding post-synaptic receptors (Spitzer N. C., 2015). Additional features also contribute to the function of the whole synaptic machinery such as the pre-synaptic re-uptake of the released neurotransmitter and the presence of astrocytes that bridge these connections (Chung W. S. et al., 2015).

Synapse formation, also known as “synaptogenesis”, has been addressed by many. It has been suggested that the release of neurochemicals from a pre-synaptic terminal helps to specify the post-synaptic site (Sanes J.R. and Lichtman J.W., 1999). However, others suggest that the process is not only dependent on pre-synaptic terminal influence on the post-synaptic compartment, but rather an orchestrated communication between both terminals (Nimchinsky E.A., Sabatini B.L. and Svoboda K., 2002). Physical contact between pre- and post-compartments during synapse formation is known to occur due to membrane proteins expressed at both compartments that belong to a big family of cell adhesion molecules (CAMs) (reviewed by Petzoldt A.G. ad Sigrist S.J., 2014). After synapse formation, synaptic transmission at functional synapses is currently known to involve two main events and numerous molecules. At the pre-synaptic terminal, synaptic vesicles bind and fuse with the pre-synaptic membrane in a region known as the active zone in order to release neurotransmitters in the synaptic cleft (Südhof T.C., 2012). At the adjacent post-synaptic terminal, receptors are geographically organized to receive the signal. The most studied post-synaptic receptors are AMPA and NMDA receptors, which belong to the family of ionotropic glutamate receptors (Okabe S., 2007).

Synapses are not static structures and are indeed known to undergo remodeling under certain conditions. For example, the process known as synaptic plasticity involves modifications of the strength of synaptic connections after certain learning episodes (Citri A. and Malenka R.C. 2008). Synaptic plasticity exists in different forms depending on the time the synaptic changes last, and can therefore be classified into Short-Term Plasticity or Long-Term Plasticity. Importantly, these are activity-dependent phenomena, so that the type of activity itself determines the sort of modifications that synapses undergo. Short-Term plasticity is characterized by changes in synaptic strength which last minutes (Zucker R.S. and Regehr

W.G., 2002), while Long-Term plasticity can last for hours or days. Evidence for long-lasting changes comes from the discovery of Long-Term Potentiation (LTP), which involves synaptic strengthening upon repeated stimulation (Bliss T.V. and Lømo T., 1973). In summary, the formation, strengthening and maintenance of synaptic connections depend on neuronal activity, and these processes are shown to be impaired in several neurological disorders (Colon-Ramos DA. 2009; Lin YC. and Koleske AJ. 2010). In this study, focus was on chemical synapses and how the microtubule network can influence their structure, protein composition and function.

3.4. The Neuronal Cytoskeleton

The neuronal cytoskeleton is a fundamental structure during neuronal development and in the mature brain. Cytoskeletal formations can be distinguished as microtubules (MTs), actin filaments (AF) and intermediate filaments (IF) (Siegel G.J. et al., 1999).

In this study, focus was on the AFs and MTs, since hypotheses and experimental procedures mainly addressed these two structures. Although is worth mentioning that IFs are fundamental in maintaining cellular structure and provide resistance to cellular tension and compression. Several groups are currently investigating their function given their role in heart and skin-related diseases (Fletcher DA. and Mullins RD., 2010 and reviewed by Goldmann WH., 2018).

Neuronal properties and functions require a tight organization. They are excitable and polarized cells that collect inputs through their dendritic arborization and are able to transmit them to neighboring cells via axonal terminals. These compartmentalized functions are made possible by a variety of localized features (reviewed by Craig AM. and Banker G., 1994). Among the factors that allow compartmentalization in neurons, molecular motors and the MTs and actin cytoskeletons play a key role.

3.4.1. The Neuronal Actin Cytoskeleton

The actin cytoskeleton plays a fundamental role in establishing neuronal polarity. This highly dynamic structure is formed by polymerization of actin monomers, also known as globular actin (G-actin) into filamentous actin (F-actin). Actin polymerization is reversible and becomes relevant when coordinated in a spatio-temporal dimension, which leads to the description of barbed end and a pointed end for each single actin filament (reviewed by Skruber K. et al., 2018). Actin polymerization is a highly unfavorable biochemical process, which requires nucleation and elongation steps during which actin monomers bind to or detach from both ends of the filament (Pollard TD. 1986). In a simplistic model, elongation of actin filaments occurs at the barbed end, and de-polymerization at the pointed end. Through this mechanism, filaments polymerize and de-polymerize in a treadmilling fashion (Wegner A., 1976; Pollard T. D. and Mooseker M. S., 1981). Biochemically, free G-actin is bound to the nucleotide adenosine 5'-triphospate (ATP) and upon polymerization, once in an F-actin state, ATP is converted to adenosine 5'-diphosphate (ADP) via hydrolysis. ADP-bound F-actin is thought to stabilize the filaments (Korn ED. et al., 1987). However, each step of the actin polymerization process is regulated by additional proteins.

Dendritic spines are protrusions that form the post-synaptic compartment of excitatory synapses (Nimchisky E. A. et al., 2002). , F-actin is the main structural component of dendritic spines (Halpain S., 2000; Hotulainen P. and Hoogenraad C. C., 2010) (Fig. 11). Interestingly, dendritic spines undergo structural and molecular re-arrangements, and F-actin is a central component in this process (Okamoto KI. et al., 2004). Furthermore, it has been recently described that actin can also form ring-like structures at the dendritic spine neck contributing to its morphology (Bär J. et al., 2016). Although the function of a ring-like organization of actin is not yet known, this study shed light on the importance of actin filament distribution in different subcellular compartments.

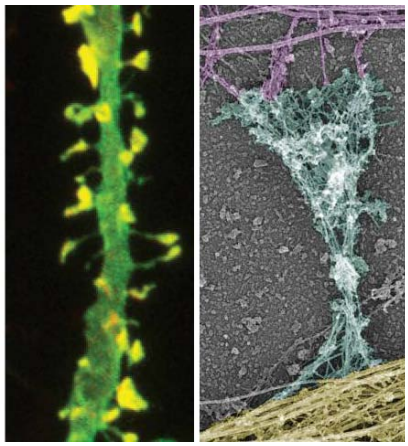

Figure 11. ***F-actin and dendritic spines***. Dendritic spines are the key structure of the post-synaptic compartment. It is now known that these structures are enriched with F-actin that provides structural support and is involved in cargo trafficking. *(adapted from Hotulainen P. and Hoogenraad C. 2017).*

3.4.2. Tubulin and the Neuronal Microtubule Cytoskeleton

Monomers of α- and β- Tubulin polymerize to form tubular filaments known as microtubules (MTs). Tubulin isoforms arise from a large and well-conserved family of proteins (reviewed by Ludueña R., 1998). Different Tubulin isoforms, together with specific post-translational modifications (PTMs) generate MTs with different properties. One notable detail about the conserved Tubulin monomer is its 3D structure: although the amino acid sequence differs between Tubulin isotypes, a globular structure coupled to a negatively charged carboxy-tail is shared within the family (reviewed by Chakraborti S. et al., 2016) (Fig. 12).

During Tubulin polymerization, heterodimers of α- and β-Tubulin bind in a head-to-tail arrangement, giving rise to a proto-filament with a minus- and a plus-end (+Tip). A hollow tube-like structure is formed when 13 protofilaments bind laterally. Importantly, Tubulin polymerization is GTP-dependent (Sternlicht H. et al., 1987). Indeed, only GTP-bound Tubulin is incorporated at the +Tip of the new filament. Once tubulin dimers are bound to the MT, a hydrolysis step takes place and the nucleotide is converted from GTP to GDP. Interestingly, this modification appears to alter MTs structure and stability. The equilibrium between polymerization and

de-polymerization of MTs is known as “dynamic instability” (reviewed by Sept D. 2007).

The highly dynamic nature of MTs means that MTs filaments with different properties can coexist. Indeed, MTs dynamics and stability are influenced by several factors, among which are: the incorporation of different Tubulin isoforms, the presence of Tubulin PTMs (The tubulin code, *see next paragraph*) and the interaction of MTs with MTs-associated proteins (MAPs) (reviewed by Wloga D. et al., 2017).

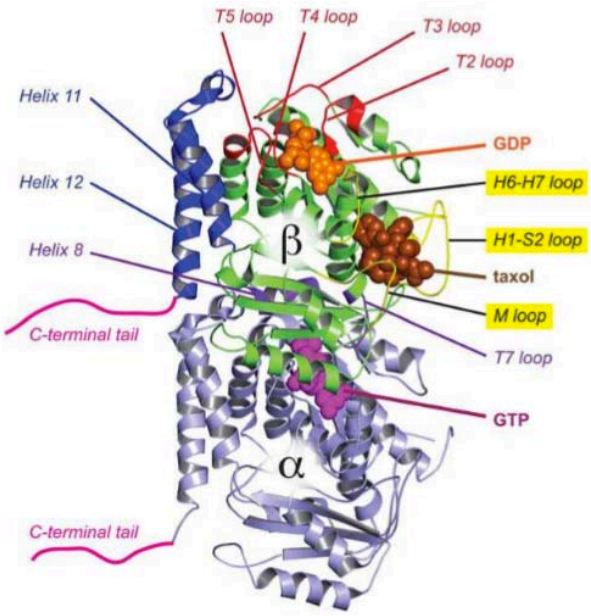

Figure 12. The *tubulin dimer 3-dimensional structure.* The cartoon depicts the 3-dimensional structure of an α- and β-Tubulin dimer bound to GTP and GDP in orange. In brown, taxol, a MT stabilizing drug binds to b-Tubulin. The C-terminal tails of α– and β-Tubulin are depicted in pink and notably point away from the structure. ***(Chakraborti S. 2016).***

The stability, rapid polymerization and de-polymerization allow MTs to modify their structure and influence a wide variety of cellular processes. In highly polarized post-mitotic neurons, MTs display a very specific arrangement. The MT

cytoskeleton provides mature neurons with architectural support and tracks for cargo transport across different compartments of the cell. Although MTs display mixed orientation in dendrites, with the +Tips pointing towards the nucleus or distal part of the dendrite, in axons MTs orientation is uniform, with the +Tips always facing the axonal terminal (reviewed by Conde C. and Caceres A., 2009). Although a lot of effort is invested to understand the mechanisms that underlie neuronal polarization, this process remains unclear. However, sufficient evidence suggests that MT organization and stabilization play a central role in determining where the future axon will be formed. Indeed, it has been shown that hippocampal cultures at developmental stage-2 (provided with only short neurites) show a highly stabilized MT array in a single dendrite that subsequently becomes the future axon (Witte H. et al., 2008; reviewed by Conde C. and Caceres A., 2009).

3.5. The Tubulin code

In order to regulate specific functions, MTs become specialized across a tight regulation at different levels. First, tubulin isotypes have different properties and therefore confer MT filaments with different characteristics (Vemu A. et al., 2017). Second, MTs can be post-translationally modified (PTM) by enzymes that acetylate, phosphorylate, glutamylate, and detyrosinate MTs (Wloga D. and Gaertig J., 2010). Because of these modifications MTs interact with a variety of proteins such as MT-associated proteins (MAPs), motor proteins, and severing enzymes (reviewed by Gadadhar S. et al., 2017).

3.5.1. Tubulin isotypes

Tubulin isotypes share high sequence homology although small sequence variations can result in unique characteristics, which subsequently influence properties of the MT filament. For example, it is interesting that TUBA4A is the only Tubulin isoform that lacks the C-terminal tail Tyrosine (Gadadhar S. et al, 2017), which can influence the affinity and function of proteins that bind to MTs. Moreover, single residue modifications in the tubulin sequence have been associated with a spectrum of diseases. For instance, mutations on the TUBB3 gene impair axon guidance and survival (Tischfield MA. et al., 2010; reviewed by Gadadhar S. et al, 2017).

3.5.2. Tubulin PTMs

Post-translational modifications influence the properties and function of MTs, with most of them occurring at the C-terminal tail of tubulin. Since numerous PTMs exist, here I discuss PTMs that were most relevant to my study

Tubulin acetylation is a well-characterized PTM that can take place two major sites. One acetylation site is Lysine-40 (K40) of α–tubulin, which is catalyzed by the alpha-tubulin acetyltransferase (ATAT) enzyme (Akella J. S. et al., 2010), and reversed by histone deacetylase 6 (HDAC6) (Hubbert C. et al., 2002). Interestingly, K40 acetylation occurs in the lumen of MTs and appears to influence the activity of the MT-severing enzyme, katanin (Li L. and Yang X-J., 2015; Sudo H. and Baas P. W., 2010). The second acetylation site is in Lysine-252 (K252) of b-Tubulin at the interface between the α– and β–Tubulin dimer. However, only K40 acetylation appears to occur in polymerized MTs (Li L. and Yang X-J., 2015).

Tubulin Polyglutamylation (polyE) is a strong MT modification that occurs in the C-terminal tail of both a- and b-Tubulin and consists of the addition of glutamate residues by the enzymes TTLL1, 6, 11 and 13. . Glutamate residues form branches from pre-existing glutamates in the C-terminal tail (Yu I et al., 2015). Besides, Tubulin-polyE is involved in MT stability (Wloga D. et al., 2010) and MT interaction with binding partners (Bonnet C. et al., 2001).

3.6. Microtubule-associated Proteins (MAPs)

MAPs are well-known MT interacting proteins mainly due to their involvement and therapeutic potential in Alzheimer's disease (AD) (Gong C. X. and Iqbal K., 2008) and Frontotemporal dementia (FTD) (Ghetti B. et al., 2015). MAPs include a variety of proteins that are believed to be involved in processes like cell division, transport and cellular morphology (Mandelkow E. and Mandelkow E. M., 1995). For example, Tau is a MAP that binds to and stabilizes MTs (Kadavath H. et al., 2015), and therefore also impacts motor protein processivity (Dixit R. et al., 2008). Under physiological conditions, Tau can be phosphorylated in multiple sites (Pierre M. and Nunez J., 1983) but in AD, Tau appears to be hyper-phosphorylated (Grundke-Iqbal I. et al., 1987). It is well established that during neurodegeneration hyper-phosphorylated Tau forms fibrils known as paired helical

filaments (PHF) (Grundke-Iqbal I. et al., 1986), and together with Amyloid-Precursor Protein metabolites, promotes cytotoxicity and ultimately neuronal cell death.

3.7. Microtubule-severing Proteins

MT severing is one of the characteristics that determine a dynamic cytoskeleton system. In mammals, MT severing has multiple functions and can be regulated in different ways. Currently, there are three enzymes known to disassemble the MT filaments and are referred to as: spastin, katanin and fidgetin. A common characteristic is that they belong to the triple AAA-ATPase family of enzymes and therefore rely on the hydrolysis of ATP to ADP + P_i to perform their functions. Fidgetin has been shown to be involved in dendritic degeneration (Tao J. et al., 2016) and spontaneous mutations in the fidgetin gene (*Fidget*) lead to strong behavioral aberrations in mice (Grüneberg H. 1943). Mutations in the gene that encodes for spastin have been associated with autosomal dominant forms of Hereditary Spastic Paraplegia, a highly incapacitating disease that starts with muscle weakness and shows cognitive impairments on its later stages (Hazan J. et al., 1999). Here, we depleted the catalytic subunit of katanin, p60, and aimed to elucidate its function in brain development and synaptic connectivity.

3.7.1 The Microtubule-severing enzyme Katanin

Katanin is a complex composed of a catalytic subunit, p60; and a regulatory subunit, p80 (reviewed by Luptovčiak I. et al., 2017). Katanin was the first MT-severing enzyme to be isolated and characterized from *Xenopus laevis* extracts (Vale RD. 1991; McNally FJ. and Vale RD., 1993). McNally and Vale (1993) showed that katanin was a heterodimeric complex since a 60 kDa and a 81 kDa (named p81 by the authors and referred here as p80) polypeptides co-eluted from a chromatography column. The authors suggested that both subunits precipitate in a 1:1 ratio and showed that in the presence of 1mM MgATP, katanin was able to disassemble immobilized MTs (Fig. 13).

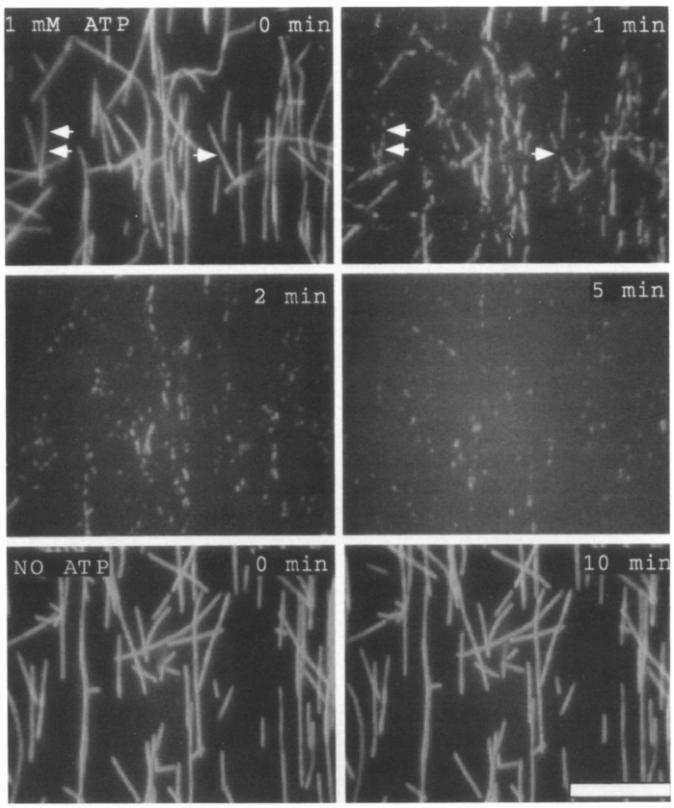

Figure 13. ATP-dependent function of p60 katanin. Katanin disassembles Immobilized MTs on a glass coverslip only in the presence of ATP. Image adopted from ***McNally FJ and Vale, 1993.***

Notably, the study also demonstrated that the byproducts of katanin-mediated depolymerization are indeed tubulin dimers, and that the depolymerization action was reversible since ATP depletion led to MT repolymerization (Fig. 13). Also, the authors showed that tubulin polymers and the presence of ADP increased the affinity of katanin for MT, but ATP hydrolysis was required to promote MT severing. Altogether, the findings reported in this outstanding study demonstrated in biochemical detail how the disassembling of MTs is achieved by katanin. Furthermore, it established the basis for further investigation on how the MT network is remodeled during different cellular processes.

Subsequent studies using Fluorescence Resonance Energy Transfer (FRET) have shown that p60 katanin requires ATP to oligomerize and that the presence of MT filaments enhances this oligomerization (Hartman JJ. and Vale RD. 1999). Also, purification through chromatography confirmed the elution of a polymer built of 6 katanin subunits (Hartman JJ. and Vale RD. 1999). Taken together, both studies suggest a scenario where single ADP-bound p60 subunits bind to MT and oligomerize *in situ* owing to the presence of MT polymers and ATP. ATP hydrolysis is the factor that eventually drives MT-disassembly. Zehr and colleagues shed light on this possibility when they first published the X-ray structure of p60 katanin and a cryo-EM reconstruction of the hexameric ring (Zehr E. et al., 2017; Fig. 14).

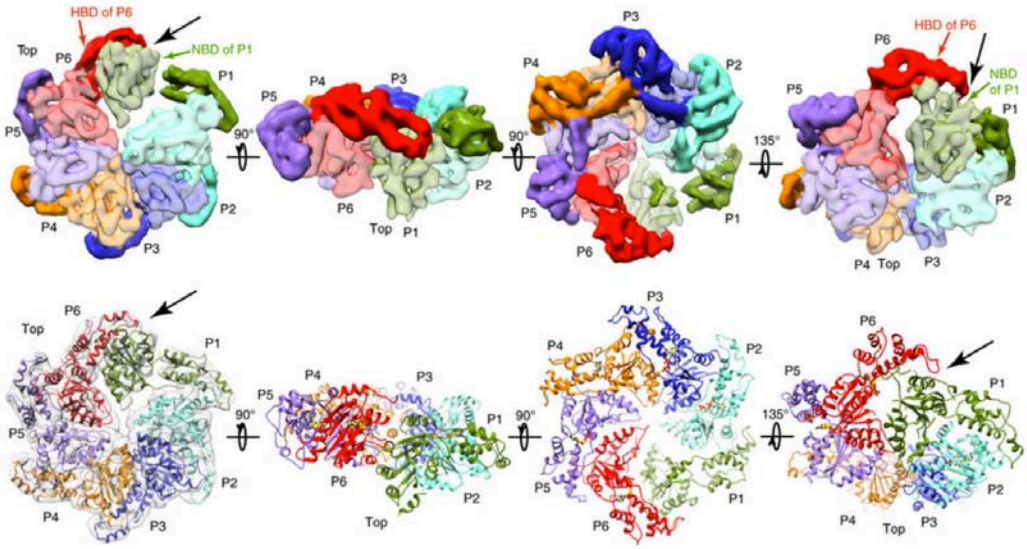

Figure 14. ***Surface (above) and atomic (below) structures of the katanin ring.*** In their study, the authors demonstrate that the transition between spiral and ring conformations of the katanin hexameric module is driven by protomer 1, and this mediates MT severing. **(Zehr E. et al., 2017).**

The C-terminal region of the p80 regulatory subunit binds the N-terminal region of p60 (McNally KP et al., 2000). Studies have shown that the p80 regulatory subunit potentiates p60-severing activity, increases p60 affinity for MT, and that p80 targets p60 to the centrosome via its WD40 repeats positioned at the N-terminal

(Hartman J.J. et al. 1998) (Fig. 15). In mammals, three p60 isoforms are expressed (KATNA1A, KATNAL1 and KATNAL2), while two different p80 subunits are expressed. Katanin forms heterohexameric rings that bind the C-terminal tails of tubulin. Katanin ATP hydrolysis promotes conformational changes that enable p60 to pull off the targeted tubulin subunit, thus creating a break in the MT filament and ultimately leading to the depolymerization of MTs. Katanin is positively regulated by tubulin acetylation (Sudo H and Baas P.W. 2010) and negatively by the binding of Tau to MTs (Qiang L. et al., 2006). This is particularly relevant in the context of AD and Tauopathies (Sudo H and Baas P.W. 2011). Indeed, Peter Baas has proposed that hyperphosphorylation of Tau gives free access for katanin to depolymerize MTs in a process that eventually results in neuronal cell death.

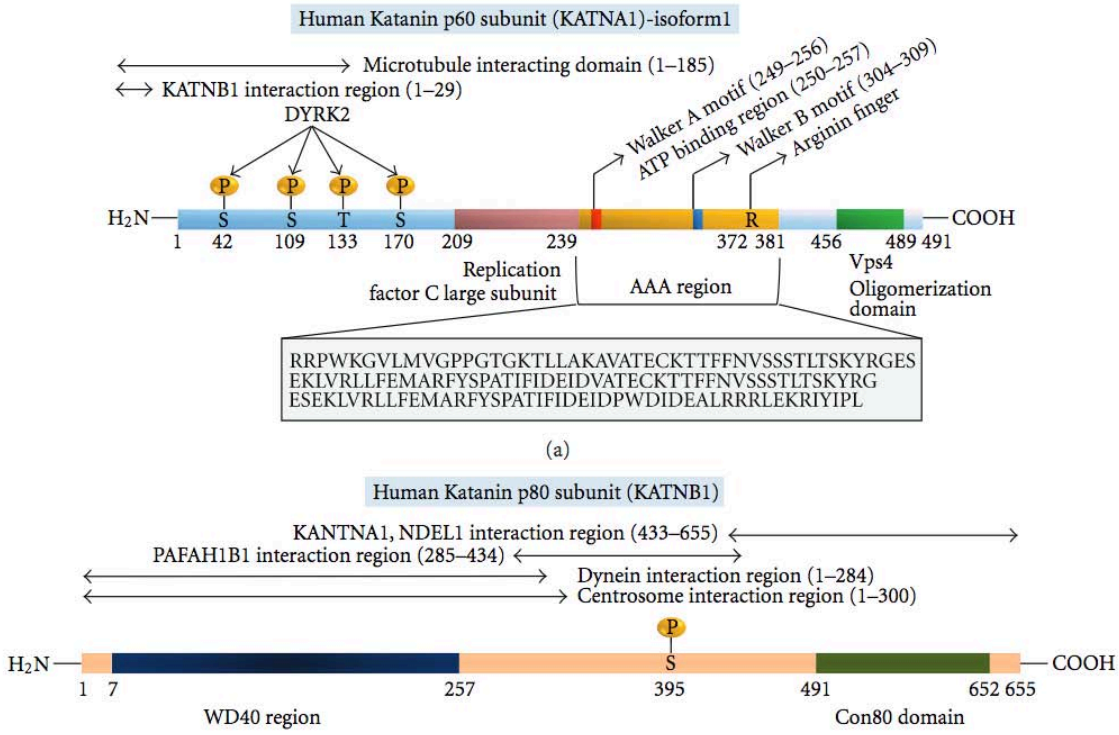

Figure 15. ***General structure of p60 and p80 katanin subunits.*** Human p60 (above) interacts with MTs via its N-terminal domain. A p60 oligomerization domain is depicted at the C-terminal (in green).. In yellow is the AAA-ATPase domain. The human p80 subunit (below) contains an N-terminal WD40 domain for centrosomal targeting. Interaction with p60 katanin takes place at the C-terminal of p80. ***(Kumar Ghosh D. et al., 2012).***

3.8. Aims of the study

During my research project, I investigated the role of p60 katanin in brain development and synaptic transmission. In order to dissect the roles of p60 in the developing brain, constitutive p60 heterozygous knockout mice were used. Given previously described functions of katanin in cell division and the importance of MT-severing during this process, focus was primarily on embryonic development and adult neurogenesis.

To understand the functions of p60 in adult neurons, conditional knockout animals were generated. The aim was to overcome developmental effects of p60 depletion in neurons. For that a CRE driver line was used in which expression of CRE was driven by the CamkII-a promoter. Besides, an ATPase-defective p60 katanin clone was used to perform cell biology experiments and unravel the importance of MT-severing in intracellular cargo transport and adaptive changes during neuronal activity.

4. Materials and Methods

4.1. Chemicals

All chemicals were purchased from:

SIGMA-Aldrich	**Taufkirchen, Germany**
Roche	**Mannheim, Germany**
Roth	**Karlsruhe, Germany**
VWR	**Darmstadt, Germany**
Life Techologies	**Darmstadt, Germany**
Applichem	**Darmstadt, Germany**
Merk	**Darmstadt, Germany**

Table 1 ***List of chemicals suppliers***

4.2. Solutions

NAME	COMPOSITION
10X PBS	1.37M NaCl / 27mM KCl / 100mM Na_2HPO_4 / 18mM KH_2PO_4
10X TBS-T	200mM Tris-Base / 1.5M NaCl / 1% Tween
50X TAE	For 1L 242g Tris-Base / 57.1ml glacial Ac. Acid / 0.5M EDTA pH=8
10X SDS-Running Buffer	250mM Tris / 2.5M Glycine / 15% SDS / fill up to 1L with ddH_2O / pH=8.3
SDS-Transfer Buffer	25mM Tris / 192mM Glycine / 20% MeOH
5X SDS-Loading Buffer	5% BME / 0.02% Bromophenol Blue / 30% Glycerol / 10% SDS / 250mM Tris-HCl.
PBS/Triton Lysis Buffer	PBS / Triton X-100 1% + prot./phosp. inhibtors
Sucrose Buffer 1	320mM Sucrose / 1mM $NaHCO_3$ / 1mM $MgCl_2$ / 500mM $CaCl_2$ / 1mM PMSF

Phem Buffer	60mM Pipes / 25mM HEPES / 10mM EGTA / 2mM $MgCl_2$ / pH=6.9
IF Blocking Buffer	PBS / 1% BSA
IF Permeabilization Buffer	PBS / 0.2% Triton X-100
IF Fixation Buffer	PBS / 4% Formaldehyde
IF Antibody incubation buffer	PBS / 1% BSA
Saline	ddH_2O / 0.09% NaCl
Perfusion buff for IHC	PBS / 4% PFA
Perfusion buff for Sholl	PBS / 4% PFA / 0.... Glutaraldehyde
IHC Blocking Buffer	PBS / 1% BSA / 10% goat Serum
IHC Permeabilization Buffer	PBS / 0.5% Triton X-100
IHC Antibody Incubation buffer	PBS / 1% BSA / 3% goat Serum
Ringer Solution	
HEPES Buffer for Time Lapse	10mM HEPES / pH=7.4 / 135mM NaCl / 5mM KCl / 2mM $CaCl_2$ / 2mM $MgCl_2$ / 15mM Glucose
2XHBS	280mM NaCl / 10mM KCl / 1.5mM Na_2HPO_4 / ddH_2O / 12mM dextrose / 50mM HEPES / pH=7.5 adjusted with 0.5M NaOH.
$CaCl_2$	1molar $CaCl_2$
Resting solution	110mM choline chloride, 25mM $NaHCO_3$, 25mM D-glucose, 11.6mM sodium L-ascorbate, 7mM $MgSO_4$, 1.25mM NaH_2PO_4, 2.5mM KCl, 0.5mM $CaCl_2$, pH 7.4, 310-315 mOsm/Kg, saturated with 95% O_2 / 5% CO_2
ACSF	140mM NaCl, 26mM $NaHCO_3$, 26mM D-glucose, 1mM $MgSO_4$, 1mM NaH_2PO_4, 4mM KCl, 2.4mM $CaCl_2$, pH 7.4, 302-305 mOsm/kg, saturated with 95% O_2 / 5% CO_2
Basic alcohol solution	1% Sodium hydroxide, 80% EtOH

Table 2 ***List of solutions and their composition.***

4.3. Other reagents

NAME	Cat. number	COMPANY
DNA ladder	15615-016	Invitrogen
Protein ladder	MWP04/03	NIPPON Genetics
3,3'-Diaminobenzidine tablets	D4418-5SET	Sigma-Aldrich
Antigen Retrieval reagents	CTS013 to 016	R&D Systems
BSA	A3156	Sigma-Aldrich
DMEM	61965026	Thermo Fisher
dNTPs	U1240	Promega
Donkey Serum	Ab7475	Abcam
FLUORO-JADE C	AG325-30MG	MILLIPORE
Goat Serum	Ab156046	Abcam
HBSS	14170-088	Invitrogen
Mitotracker CMXRos	M7512	Invitrogen
MNI-caged-L-glutamate	1490	TOCRIS bioscience
DH5-alpha	C2989K	New England BioLabs
Neuronal medium, Neurocult	05712	Stemcell technologies
Phosphatase inhibitors set	04906845001	Sigma-Aldrich
Pierce ECL Western Blotting Substrate	32106 / 32109 / 32209	Thermo Scientific
Poly-D-Lysine	P7886	Sigma-Aldrich
Protease complete inhibitors mini	04693132001	Sigma-Aldrich
Protease inhibitors set	1206893	Roche
Rhodamine Phalloidin	PHDR1	Cytoskeleton

Tetrodotoxin citrate	Ab120055	Abcam
Aqua Poly Mount 1	18606-20	(Polysciences, Eppelheim, Germany).
Trypsin/EDTA	25300054	Invitrogen

Table 3 ***List of reagents***

4.4. Oligos and Primers

FUNCTION	NAME	SEQUENCE
P60-katanin PCR forward	PRL-170	CAAGATGGCTCATGCAGATAGATGTA
P60-katanin PCR reverse	PRL-94	ACTTTGGCTTCTGTTTATCTCCTTTCCT
CRE Genotyping PCR forward	CRE1	TAACATTCTCCCACCGCTAGTACG
CRE Genotyping PCR reverse	CRE2	AAACGTTGATGCCGGTGAACGTGC
P60 katanin sequencing 1	FL-35	GACCCTGAAGTTCATCTGCA
P60 katanin sequencing 2	FL-36	AGCTGAAGGGCATCGACTTC
P60 katanin sequencing 3	FL-37	CTATGACTCTGCGATGGTC
P60 katanin sequencing 4	FL-38	CCAGGACCTAGAAAACGCC
P60 katanin sequencing 5	FL-39	GCAGTAACAGAACCAGAGAC
P60 katanin sequencing 6	FL-40	CAGAGGAGAATCTGAGAAGC
P60 katanin sequencing 7	FL-41	GTTGACCTTGCAAGTATAGC
P60 katanin sequencing 8	FL-42	CCTCTACAAATGTGGTATGGC

Table 4 ***Oligonucleotides list***

4.5. Plasmids and virus

GFP	pmaxGFP	Lonza
td-Tomato-C1	632533	Clontech
P60-katanin-DEID-EGFP	McNally F. J.	McNally K.P. et al., 2000
P60-katanin-wt-EGFP	McNally F. J.	McNally K.P. et al., 2000

EB3-tomato	Jennifer Radwitz	ZMNH, Hamburg, Germany

Table 5 ***List of plasmids***

4.6. Primary Antibodies

TARGET	SPECIES	Clone/Cat. number	COMPANY
α-Acetylated-Tubulin	Mouse	T7451	Sigma
α-alpha-Tubulin	Mouse	DM1A, T9026	Sigma
α-beta-actin	Mouse	AC15, A5441	Sigma
α-BrdU	Rat	OBT0030S	Bio-Rad
α-Doublecortin (DCX)	Goat	C-18, sc-8066	Santa Cruz
α-Doublecortin (DCX)	Guinea pig	ab2253	Millipore
α-EB3	Rat	Ab53360	Abcam
α-gamma-Tubulin	Mouse	GTU-88	Sigma
α-GAPDH	Mouse	6C5, Gtx28245	GeneTex
α-NeuN	Mouse	MAB377	Millipore
α-p60-katanin	Rabbit	McNally	-
α-PARP	Rabbit	9542	Cell signaling
α-Spastin	Mouse	Sp6C6, ab77144	Abcam
α-Tau	Rabbit	A0024	Dako
α-Tau	Guinea pig	314004	Syn. Systems
α-Tubulin-βIII	Rabbit	T2200	Sigma
α-Sox2	Rabbit	ab5603	Millipore
α-GFAP	Mouse	G3893	Sigma
α-GFP	Rabbit	A-11122	Thermo Fisher scientific

Table 6 ***List of primary antibodies***

4.7. Secondary Antibodies

Product	Cat. number	COMPANY
Alexa 488 α-Guinea pig	a11073	Invitrogen
Alexa 568 α-Mouse	a11031	Invitrogen
Alexa647 α-Rabbit	a21246	Invitrogen
Cy™2-conjugated Donkey α-Rabbit IgG	711-226-152	Dianova
Cy™3-conjugated Donkey α-Mouse IgG	715-165-150	Dianova
Cy™3-conjugated Donkey α-Rabbit IgG	711-166-152	Dianova
Cy™5-conjugated Donkey α-Guinea Pig IgG	706-176-148	Dianova
Cy™5-conjugated Donkey α-Rat IgG	712-175-153	Dianova
Donkey α-Goat Alexa Fluor® 488	705-545-147	Dianova
Donkey α-Mouse IgG (HRP)	Ab98711	Abcam
Donkey α-Rabbit Alexa Fluor® 488	711-545-152	Dianova
Perox-conjugated Donkey α-Guinea Pig IgG	706-035-148	Dianova
Perox-conjugated Donkey α-Mouse IgG	715-036-151	Dianova
Perox-conjugated Donkey α-Rabbit IgG	711-036-152	Dianova
Perox-conjugated Donkey α-Rat Pig IgG	712-036-153	Dianova

Table 7 ***List of secondary antibodies.***

4.8. Equipment

Spinning Disk confocal Microscope	Nikon (Visitron, Puchheim, Germany)
2-photon confocal Microscope	Olympus Fluoview F1000
Confocal Microscope	Olympus Fluoview FV1000 (Hamburg, Germany)
Cryostate	Leica, CM3050 S. Leica Biosystems

DNA-sequencer	ABI Prism® 377 (Applied Biosystems, Darmstadt, Germany.
Tissue Homogenisator	Potter S (Sartorius, Göttingen, Germany)
Western Blot Running Chamber	Mini Protean Tetra (Bio-Rad, Munich, Germany)
Agarose gel imager	Intas Gel Imager (Intas, Göttingen, Germany)
Agarose Gels running chamber	Owl Separation System B2, B1A (Thermo, Asheville, USA)
Plate reader Spectrophotometer	Infinite® 200 PRO NanoQuant (Tecan, Männedorf, Switzerland)
Thermal cycler	PTC-200 (MJ Research, Waltham, USA)
pH-Meter	Toledo320 (Mettler-Toledo, Giessen)
Bacterial plates incubator	
Bacterial shaker	W 560 K, Mytron
Centrifuge	Beckman Coulter Avanti J-26 XP
Centrifuge	5804R, Eppendorf
Microcentrifuge	5430, Eppendorf
Microcentrifuge	5430R, Eppendorf
Cell culture incubator	HeraCell 150/150i (Thermo, Massachusetts, US)
Cell culture hood	SterilGARD Class II TypA/B3 (Baker company, Florida, USA); SAFE 2020 (Thermo, Massachusetts, USA)

Table 8 ***List of equipment***

4.9. Softwares

Fluoview	Version 2.1b (Olympus, Hamburg, Germany
Visiview	Visitron Systems (Düsseldorf, Germany)

Photoshop	CS4 11.0.2, Adobe Systems Incorporated
Adobe Illustrator	CS4, 14.0.0, Adobe
ImageJ and Fiji	NIH, Version 2.0.0-rc-23/1.49m
Ethovision	Version XT 8.5, Noldus Technology; The Netherlands
Microsoft Office	2008 for Mac. Microsoft Corporation
SPSS	IBM Corporation Version 23
4 Peaks	By Alexander Griekspoor (Mek) and Tom Groothuis (Tosj) Version 1.7.2
MegAlign	DNA Star/Lasergene 11 Version 11.2.1 (29) Intel
SeqBuilder	DNA Star/Lasergene 11 Version 11.2.1 (29) Intel
SigmaPlot	Version 13. Systat Software Inc. GmbH. Erkrath, Germany

Table 9 ***List of employed softwares***

4.10. Animals

The animals used in this study were both constitutive and conditionally depleted from the catalytic subunit of p60 katanin.

In order to generate constitutive knockout animals for p60 katanin, stem cells Katna1$^{tm1a(KOMP)Wtsi}$ (clone EPD0586_1_A09) were purchased from COMP.

For conditional depletion of p60 katanin, katanin knockout first allele was crossed with Flippase driving line. After recombination, resultant katna1 floxed (katna1 fx/fx) animals were crossed with CRE lines driven by CamkII-a promoter.

4.10.1. Genotyping

DNA extraction was performed from tail snips with Quick Extract Buffer (Biozym Scientific GmbH, Hessisch Oldendorf, Germany). The procedure involved 7 minutes incubation at 65 ^{o}C and inactivation for 2 minutes at 95 ^{o}C.

Genotyping of the animals for *katna1* wt, *katna1 knockout* first and *katna1 flox* alleles, as well as for CRE, was performed with Polymerase Chain Reaction (PCR)

and the resulting amplified DNA was run in agarose gel and checked using INTAS science imaging device.

For p60 katanin constitutive knockout and for CRE-katna1 fx/fx mice:

Primers	**Sequence**
PRL-170	CAAGATGGCTCATGCAGATAGATGTA
PRL-94	ACTTTGGCTTCTGTTTATCTCCTTTCCT
CRE forward	TAACATTCTCCCACCGCTAGTACG
CRE reverse	AAACGTTGATGCCGGTGAACGTGC

Table 10 ***Genotyping oligos***

Stocks	**Reaction recipe (for 50μl)**
10X Loading Buffer	5 μl
dNTPs (2.5 mM)	1 μl
Primer 1 (10mM)	2 μl
Primer 2 (10mM)	2 μl
Taq Polymerase (5U/l)	0.25 μl
DNA	2 μl
ddH_2O	37.75 μl

Table 11 ***Genotyping PCR reaction***

Program	
98°C	30 seconds
98°C	30 seconds
62°C	30 seconds
72°C	2 minutes

72°C	10 minutes
4°C	∞

Table 12 ***Genotyping PCR program***

A 4% agarose in T-BST gel was prepared and 15ml of the PCR reaction was loaded for control.

4.11. Bacteria transformation and DNA purification

E. Coli cells were transformed using heat-shock protocol. In details, 100 uL of bacteria were incubated for 30 minutes in the presence of DNA on ice. Heat shock was achieved by incubating the mix for 45 seconds at 42 °C fast repositioning in ice. After 1 minute, 500 ml of pre-warmed S.O.C. was added and incubated for 30 minutes at 37 °C shaking for recovery.

4.11.1. Midipreps

After growing over night in around 70 ml of LB media supplemented with antibiotics, bacteria was pelleted at 3800 rcf for 12 minutes at 4°C. DNA was isolated using Nucleobond Xtra Midi EF DNA extraction kit (cat.740420.50, Macherey-Nagel, Düren, Germany) and according to the protocol.
After DNA elution from the column, 3.5 ml isopropanol was added and centrifuged 12000g for 30 minutes 4°C. Pellet was washed with 70% EtOH and re-centrifuged at 12000g for 5 minutes at 4°C. It was then dried and resuspended in ddH_2O.

4.12. Messenger RNA quantification

Embryos 15 days after female plugging, were euthanized by decapitation. Their brains were harvested and inmediately frozen in liquid nitrogen.

Miniprep Kit (Agilent) was used for mRNA extraction from the cortex of p60 +/+ and p60 +/- mice. Samples were homogenized with a 1ml syringe in 700ml of Lysis Buffer. DNase treatment and purification were performed following kit instructions. Elution was performed in nuclease-free buffer. Quality control was performed in 1.2% Agarose gel. For reverse transcription, 1mg of RNA was used in combination with oligo dT primers and hexamer primers of the Superscript Reverse Transcription Kit (Life Technologies, Darmstadt, Germany). Primers design was specific to target katna1A gene and excluding katna-like 1 and 2 isoforms. For that, Primer Blast was used (NCBI, U.S. National Library of Medicine 8600 Rockville Pike, Bethesda MD, 20894 USA). QPCR reactions were achieved with Taqman gene expression master mix (Life Technologies) (Ye J. et al., 2012). Primers were desalted and purchased from Metabion International AG (Planegg, Germany). qPCR was performed in HAT Fast Real-Time PCR System (Applied Biosystems, CA, USA) in a 96-wells plate. Conditions were 95 degrees during 15 minutes for activation, two-steps with denaturation for 15 seconds and 94 degrees, 30 seconds at 60 degrees for annealing and extension, and fluorescence collection in 40 cycles. SYBR green was used to check primers characteristics. An incubation at 95 degrees for 15 seconds was followed by melting analysis from 60 to 95 degrees with 2% ramp. Mm00441943_m1 taqman gene expression assay for Transferrin receptor (Life Technologies) was used to normalize mRNA expression.
Self-designed primers were:
katexon11_for-5'-GGAATCTGCCTTAAGTCTTTGAAAA, reverse-5'-TCCAAATCACACCATTATGAAAGTTT; katexon11_probe-5'-FAM—AAATGTAGAA TTT(pdC)AGTGTA CGGAG---ZNA4—BHQ1.
Gene expression was calculated according to Pfaffl method (Pfaffl, M. W. 2001) and REST was used for significance of the differencies (Pfaffl, M. W. et al., 2002).

4.13. Biochemical experiments

All biochemical experiments were performed on ice and in the presence of Protease and Phosphatase inhibitors (04693132001 / 04906845001, Sigma-Aldrich). For embryonic cortical lysates, a pregnant female was sacrificed with CO_2 and embryos were harvested. Embryonic decapitation and brain dissection was

carried out in ice cold PBS or HBSS (14170-088, Invitrogen). For pups or adults hippocampal lysates, mice were sacrificed with CO_2 and decapitation and brain dissection was carried out in ice cold PBS or HBSS.

4.13.1. Post-nuclear brain lysates

S1 (Post-nuclear) fraction was prepared as following: Tissue was resuspended in Sucrose Buffer 1 (320mM Sucrose, 1mM NaHCO3, 1mM MgCl2, 500mM CaCl2, 1uM PMSF) with protease / phosphatase inhibitors (04693132001 / 04906845001, Sigma-Aldrich) and homogenized by potterization at 900 rpm for 12 strokes. Homogenates were then centrifuged at 4C for 10 minutes at 1000g. Supernantants (S1) were quantified with Pierce™ BCA Protein Assay Kit (cat. 23227, Thermo Scientific) and diluted to equal concentrations for each sample using Sucrose Buffer 1. 5X SDS-Loading Buffer was added before loading.

4.13.2. Western Blots

Proteins were separated in custome-made SDS-gels (or PAGE). Gels were casted from the bottom to the top. Separating and Stacking layers were poured respectively. After polymerization, samples were loaded and run in the presence of Running Buffer (for 10X= 250mM Tris / 2.5M Glycine / 15% SDS / pH=8.3). After separation, proteins were transfered to a PVDF membrane previously activated with 100% methanol. Transfer was carried out in wet chambers in the presence of Transfer Buffer (192mM Glycine / 25mM Tris / 20% methanol / water). A blocking step of 30 minutes was performed in 5% milk / TBS-T and primary antibodies were incubated in either 5% milk / TBS-T or 5% BSA / TBS-T for phosphorylated antigens.

Primary antibodies were (in order of appearance) p60 katanin (donated by McNally F. J.), Spastin (ab77144, Abcam), PARP (9542, Cell signaling), α-Tubulin (T9026, Sigma), γ-Tubulin (GTU-88, Sigma), β-Tubulin (T2200, Sigma), NeuN (MAB377, Millipore).

4.14. Histological and Immunohistochemical experiments

For most of the experiments (unless described), animals underwent euthanasia with CO_2 and subsequent cardiac perfusion with PBS / 4% PFA. For BrdU staining, mice were first anesthetized. After fixation, brains were harvested and post-fixed for 24 hours in PBS / 4% PFA. A following dehydration process took place for 48 hours in PBS / 30% sucrose. Brains were then embedded in TissueTek (cat 4583, Sakura Finetek), frozen in dry ice and kept in -80^{o}C until processing. A Leica cryostate was used to collect 18 mM floating sagittal and immediately mounted on SUPERFROST ULTRA PLUS (J3800AMNZ, Thermo Scientific) microscopy slides.

4.14.1. Nissl staining

Sagittal sections were deeped into 95%, 70% and 50% ethanol sequentially. They were then washed twice with water and rinsed for 2 minutes with Cresyl violet. After that, a 1-minute washing step in water and additional incubations in 50% ethanol, 70% acidic ethanol (containing acetic acid), 95% and 100% ethanol were carried out. Mounting was performed with Entellan.

4.14.2. Fluoro Jade C staining.

Sections were deeped in a basic alcohol solution (1% Sodium hydroxide, 80% ethanol) for 5 minutes followed by an incubation in 70% ethanol for 2 minutes. Washing was performed in water for 2 minutes. An incubation for 10 minutes in potassium permanganate 0.06% was carried for 10 minutes. After an additional washing step, sections were incubated in FluoroJadeC solution 0,0001% dissolved in acetic acid 0,1%. Tissue was washed 3 more times and air dried at 50^{o}C. It was then cleared in Xylene for 1 minute and mounted with Aqua Poly Mount 1 (Polysciences, Eppelheim, Germany).

4.14.3. NeuN-DAB staining

18mm sagittal sections were permeabilized with ICH Permeabilization buffer for 20 minutes at room temperature. Subsequently, three washes were performed with PBS. A blocking step with 10% Serum / 1% BSA / PBS was performed for 1 hour at room temperature and NeuN (MAB377, Millipore) primary antibody was incubated over night in wet chamber at 4^{o}C.

The day after, DAB staining was performed according to Vectastain® Universal ABC kit (cat. PK-6200). Briefly, sections were washed for 5 minutes and incubated for 30 minutes with diluted secondary biotinylated antibody. After 5 minues wash, sections were administered with Vectastain® reagent for 30 minutes and washed further for 5 minutes. Subsequently, peroxidase substrate solution was applied until the sections were correctly stained. A deep in H_2O was followed by counterstaining and mounted using Aqua Poly Mount 1.

4.14.4. BrdU-DAB staining

Two months old animals were administered with 1.5mg of BrdU (Sigma B5002-1G) via intraperitoneal injection. Animals were then left resting for 3 hours. Subsequently they underwent terminal anesthesia with Sedaxylan (1.6 mg/ml) and Ketamine (10 mg/ml) via intraperitoneal injection. Mice were then perfused transcardially with 4% PFA/PBS. Their brains were harvested, post-fixed in 4%PFA/PBS and dehydrated in 30% Sucrose/PBS. For tissue collection, 35mM coronal non adjacent sections were obtained with cryostate and were collected every 5th from the previous one. For staining, DNA was first denatured with 2M HCl for 1 hour at 37^{o}C. After 3 washes in PBS, tissue was blocked for 1 hour in TBS (additioned with 0.5% Triton X-100, 5% BSA). Primary antibody (OBT0030S, Bio-Rad) was diluted in 3% Ab incubation buffer (3% BSA, 0.1% Triton X-100, TBS) and incubated over night at 4^{o}C in wet chamber at a concentration of 1:500. The following day, sections were washed twice in PBS for 5 minutes each time and incubated with biotynilated secondary antibody for 1 hour at room temperature.

DAB staining was performed as previously described in NeuN-DAB staining.

4.14.5. Immunohistochemistry.

NeuN-DCX-DAPI staining in the adult SGZ: Sagittal sections were thawed and washed in PBS. Permeabilization was performed in all cases with Triton X-100 / PBS for 20 minutes. After 3 washes with PBS, sections were blocked in 10% Serum / 1% BSA / PBS for 1 hour at room temperature. Primary antibodies where incubated over night in wet chamber at 4^{o}C. The following day 3 washes with PBS and incubation with secondary antibodies was performed for 1 hour at room temperature. Finally, 3 last washing steps were followed by mounting with Aqua Poly Mount 1. Primary antibodies were (in order of appearance) DCX (sc-8066, Santa Cruz), NeuN (MAB377, Millipore). DAPI 1:1000 was added in combination with secondary antibodies for nuclear staining.

Images were taken with FV1000 Olympus confocal microscope. For NeuN / DCX staining, image deconvolution was performed before analysis.

Sox2-GFAP staining in the adult SGZ: Sagittal sections of 50μM thickness were collected in a consecutive way at the level of the RMS. Primary antibodies were incubated over night at 4^{o}C diluted in 0.5% Triton X-100 / 10% goat serum / 1% BSA. The antibodies used were Sox2 (ab5603, Millipore) and GFAP (G3893, Sigma). The day after, washes in PBS were followed by secondary antibody incubation for one hour at room temperature. Hoechst was used to label nuclei (H1399, molecular probes). Later, washes in PBS and mounting was performed.

Images were acquired with FV1000 Olympus confocal microscope. At least 3 stacks of the DG for each section was collected.

4.15. In-utero electroporation

Females pregnant 15 days after plugs received a dose of buprenorphine (0.05-0.01 mg/kg) via injections subcutaneously. 2.5% isoflurane/0.2 via inhalation was used for anesthesia and flow rate of 0.65L/min for oxygen delivery. Isoflurane was

administered via vaporizer (Föhr Medical Instruments, Seeheim-Oberbeerbach, Germany).

A plasmid expressing Venus were microinjected into the lateral ventricle of each embryo after uterine horns were exposed. For electroporation, five pulses (50ms pulse, 950ms interval, 35 mV) were used. After surgery, 2-3 drops of meloxicam (0.1-0.5 mg/kg) were orally administered in combination with soft food for 4 days.

Exactly four days after electroporation, embryos were sacrificed, their brains harvested and post-fixed in 4% PFA/PBS for 24 hours. After fixation a dehydration step was performed in 30% Sucrose/PBS for 48 hours and subsequently frozen using Tissue Tek. Free floating coronal sections were then cut at a thickness of 35 mM and collected sequentially.

For staining, DAPI was used at a concentration of 1:1000 and incubated for 1 hour at room temperature. After that, they were mounted in Aqua Poly Mount 1 (Polysciences, Eppelheim, Germany).

Images were collected using a 10x objective of an FV1000 Olympus confocal microscope. Due to fluorescence variability among slices, adjustment of laser power was used to maximize the number of cells observed and minimize saturation. A total of four subsequent slices were quantified for each embryo with exception of one. Binning of the cortex for quantification was arbitrary decided based on nuclear density. Quantification was performed using ImageJ (NIH) and statistics were performed using SPSS. Mann-Whitney test was applied.

4.16. Tissue cultures

4.16.1. Cell lines culture

N2A cells were mantained in DMEM media 20% serum. Splitting was done in the presence of 0.05% Trypsin by incubation for 5 minutes at 37^{o}C.

4.16.2. Primary hippocampal neurons

Pregnant female was sacrificed and E.16 embryos were harvested. Embryonic decapitation and hippocampal dissection was carried out in ice cold HBSS. Hippocampi were incubated for 5 minutes at 37C in 2.5% Trypsin / EDTA for chemical dissociation. Neurobasal / FBS was used to block trypsin and both were then replaced with 37^{o}C warm HBSS for mechanical dissociation, which was performed with a Pasteur pipette. For immunofluorescence, cells were plated in 24 wells plates containing 12mm glass coverslips pre-coated with poly-D-Lysine (50 μg/ml). Neurons were kept in 1ml of Media. For Time Lapse experiments, cells were seeded in the center of 25mm glass coverslips in 6 wells plates and previously coated with Poly-D-Lysine. Neurons were kept in 3 ml of media until experiments were performed.

4.16.3. Primary neurons and N2A cells transfection

Transfection was performed using Calcium Phosphate method. Briefly, for 12 mm coverslips, a MIX containing around 4 mg DNA, 12.5 ml of 1M $CaCl_2$ and 36 ml of water was prepared. Subsequently, the mix was added to 50 ml of 2X HEPES buffered saline (2xHBS) dropwise. Part of the culture media was removed and saved for following steps. The mix was added to the cells and incubated for 90-120 minutes. Later, 2 washes were performed with HEPES buffer pre-heated to 37^{o}C. The conditioned media saved before, was re-added to the cells.

4.17. Immunocytochemical experiments

4.17.1. *In vitro* cellular morphology and Tubulin acetylation.

DIV6 hippocampal cultures were fixed in 4% Formaldehyde / PBS, washed three times with PBS and permeabilized with PBS / 0.2% Triton X-100. After three washes with PBS, blocking was performed with PBS/1% BSA. Primary antibodies were Tubulin-bIII and acetylated α-Tubulin diluted in PBS/1%BSA and incubated for 1 hour at room temperature. After three additional washes, secondary antibodies were administered in PBS/1%BSA solution and incubated for 1 hour at

room temperature. Three additional washes with PBS were performed prior to mounting with Aqua Poly Mount 1.

Image acquisition was achieved with Olympus FV1000 confocal microscope.

Quantification of acetylated α-Tubulin was performed with Fiji (NIH, Version 2.0.0-rc-23/1.49m) and normalized to Tubulin-βIII levels. For cellular area measurements, images manual threshold was applied and the total area was calculated and normalized to number of nuclei present in the field of view.

4.17.2. Subcellular localization of overexpressed p60 katanin and endogenous p60 katanin.

DIV12 hippocampal cultures (Previously transfected neurons with EGFP-p60 in the case of overexpressed p60) were fixed in 4% Formaldehyde / PBS and washed three times in PBS. A following permeabilization step was performed for 5 minutes with PBS / 0.2% Triton X-100. After three additional washes, blocking was carried out with PBS / 1% BSA for one hour at room temperature. Primary antibody (in the case of endogenous katanin localization) was incubated in PBS / 1% BSA at room temperature for one hour. Three additional washes and secondary antibody (in the case of endogenous katanin localization) plus Rhodamine-Phalloidin were incubated at room temperature. Final washes to eliminate unspecific were also carried out. Coverslips were mounted with Aqua Poly Mount 1 and imaged in Olympus confocal FV1000.

4.17.3. Endogenous EB3 staining.

Primary hippocampal cultures were transfected as described before at DIV10 with td-Tomato as a volume marker in combination with EGFP-p60-DEID or GFP as a control.

Two days after transfection, neurons were fixed in ice cold methanol for 5 minutes, washed once in PBS for 20 minutes and fixed in PBS / PFA Formaldehyde 4%.

After 2 washes for a total of 30 minutes with PBS, a blocking step of 45 minutes was performed with PBS / BSA 1%. Primary antibodies were diluted in Phem buffer (60mM Pipes, 25 mM HEPES, 10mM EGTA, 2mM $MgCl_2$, pH 6.9) and incubated over night in wet chamber. The following day, 3 washes of 10 minutes each in PBS were carried out. Secondary antibodies were incubated for 2 hours at room temperature in Phem Buffer. After washing 3 more times in PBS, mounting was performed using Aqua Poly Mount 1. Rat anti-EB3 from Abcam, was used at a dilution of 1:300.

Imaging was performed with Olympus FV1000. Quantification was done using Fiji (NIH, Version 2.0.0-rc-23/1.49m). Briefly, multiple regions were drawn in Tomato channel on the visible region of as many as possible dendritic spines. Regions were then pasted in EB3 channel and quantified those spines that contained EB3. Criteria adopted for EB3-positive spines was a minimum fluorescence value and the majority of the comet inside the drawn region.

4.18. Time Lapse imaging

4.18.1. Mitochondria movement

Primary hippocampal cultures were transfected at DIV3 as described before with EGFP-p60-DEID or GFP as a control.

24-48 hours later Mitotracker Red (CMXRos cat no. M7512) was administered prior to imaging. Imaging was performed with Spinning Disk Microscope.

Quantification was focused in neuronal axons and manually performed with Fiji, manual tracking (NIH, Version 2.0.0-rc-23/1.49m). Criteria did not include clustering between anterograde and retrograde movement or mitochondria.

4.18.2. EB3 tracking

Hippocampal cultures were co-transfected at DIV3 with EB3-tomato and p60-DEID or GFP as a control.

48 hours after transfection, neurons were imaged with Spinning disk (Nikon). One frame per second was acquired in EB3 channel, while a single acquisition was made for GFP.

For quantification, focus was in neuronal dendrites with no differentiation between anterograde and retrograde movement. Quantification was performed using manual tracking plugin from Fiji (NIH, Version 2.0.0-rc-23/1.49m). Absolute speed was considered for statistical analysis.

4.18.3. Two-photons microscopy for Spine morphology upon Glutammate uncaging

Primary hippocampal cultures at DIV10 were transfected as described before with td-Tomato as a volume marker and EGFP-p60-DEID or GFP as a control. At DIV12, neurons were administered with 1mM TTX diluted in culture media 1 hour prior to experiment.

The experiments were performed in Ringer solution ( ) in the presence of 1mM TTX and 2.5mM Glutamate MNI.

Three regions of interest (ROI) were selected surrounding individual spines and using a single acquisition with 2-photon laser (950nm) as a reference. Uncaging was achieved using 60 pulses of 1.02ms with 100ms interval, with 2-photon laser at a wavelength of 720nm. Baseline were three single plane images obtained with a 5 minutes interval prior to uncaging. Post-stimulation imaging was performed with 559 laser and a single planes of the stimulated regions were obtained every 5 minutes for a total of 12 acquisitions.

For quantification, regions were drawn around the stimulated spines and area was measured with Fiji (NIH, Version 2.0.0-rc-23/1.49m). The average of the measurements from the baseline were set at 100% and all imaging points

(including the baseline) were standardized. Due to focus drift, images in which the stimulated spine was out of focus, an average from previous and subsequent images were calculated.

4.19. Electrophysiological experiments

Experiments were carried out in aggreement with German Law and approved by the Behörde für Gesundheit un Verdraucherschutz Hamburg.
Mice were decapitated after anesthesia with 80% CO_2 / 20% O_2. Brain was harvested and immersed in ice-cold Resting solution (110mM choline chloride, 25mM $NaHCO_3$, 25mM D-glucose, 11.6mM sodium L-ascorbate, 7mM $MgSO_4$, 1.25mM NaH_2PO_4, 2.5mM KCl, 0.5mM $CaCl_2$, pH 7.4, 310-315 mOsm/Kg, saturated with 95% O_2 / 5% CO_2). Lateral surfaces were glued to the support of a Compresstome (VF-200-0Z Microtome, Precisionary Instruments) with cyanoacrylate. 1.2% agarose was used as a support for the tissue, 350mM sections were collected and the excess of agarose, removed.

Recovery of the slices was performed in artificial cerebrospinal fluid (ACSF) (140mM NaCl, 26mM $NaHCO_3$, 26mM D-glucose, 1mM $MgSO_4$, 1mM NaH_2PO_4, 4mM KCl, 2.4mM $CaCl_2$, pH 7.4, 302-305 mOsm/kg, saturated with 95% O_2 / 5% CO_2) at 33^{o}C for 15-minutes. Subsequently, slices were allowed to recover for further 45-minutes at 30^{o}C. Slices were then transferred to a four-chambers Synchroslice (Lohmann Research Equipment) and perfused for 45 minutes with ACSF (flow rate 2.5 ml per minute) at 30^{o}C.

Stimulation electrodes (two), were positioned in *stratum radiatum* at the sides of a bipolar recording electrode placed close to the border with *stratum pyramidale*. Field-excitatory postsynaptic potentials (fEPSPs) were evoked at an amplitude of about 2mV. The stimuli was 200ms and was applied on each electrode with 1 second interval. It was repeated every 30-seconds for a total of 10-minutes. The stimulus intensity was then adjusted to evoke a half of the maximum amplitude of fEPSP for 20-minutes.

Recording was achieved with intervals of 30-seconds for a total time of 30-minutes for the baseline. After, on one stimulation electrode for each slice, theta burst stimulation (TBs, 5 pulses at 100 Hz 10 times at 5 Hz 3 times) was applied, while the other pathway (control electrode) was unstimulated.

Unstable baseline led to exclusion of the recordings from the analysis. Criteria included changes by more than 10% of fEPSP during 30-minutes before TBs (4 of 32 slices). Also, if the control pathway suffered variations by more than 30% after TBs (7 of 32 slices). One slice dried out. For each response, the fEPSP slope was measured (30-70%). Baseline fEPSP slope was the mean of 10 minutes previous to TBs. Post TBs was the mean of 2-minutes following TBs. LTP was assessed 60-60 minutes, 110-120 minutes and 170-180 minutes after TBs. Time course represents mean±S.E.M. normalized to baseline. Statistics were performed with GraphPad Prism (non-parametric). Re-genotyping after experiments was performed to confirm animals assignment. Unblinding occured only after inclusion or exclusion of recordings from the analysis.

4.20. Electron microscopy

Primary hippocampal neurons were plated and grown on Aclar (Ted Pella, Redding, USA). At DIV 7 and 24 hours after transfection with p60-DEID and GFP as a control, neurons were fixed in 4% PFA and 0.1% Glutaraldehyde. Cultures were cryoprotected with 2.3M sucrose and frozen-thawed twice in liquid nitrogen to allow immunoreagents penetration. After washing with PBS, cells were incubated in 10% horse serum, 2% BSA for 15 minutes for blocking. Primary anti-GFP antibody (Invitrogen) was incubated 1:100 in PBS / 1% serum / 0.2% BSA (carrier) over night. A wash with PBS was performed followed by secondary goat anti-rabbit antibody incubation (Vector laboratories, Burlingame, CA, USA) diluted 1:100 in carrier for 90-minutes. After washing, cells were incubated for 90 minutes in ABC reagent (Vector labs) 1:100 in PBS and DAB-H_2O_2 solution (Sigma St. Louis, USA) was applied for 10 minutes. Sodium cacodylate buffer 0.1M (pH7.2-7.4) (Sigma-Aldrich, Buchs, Switzerland) was used for 3x rinsing of the cells followed by 1% osmium tetroxide (Science Services, Munich, Germany) in cacodylate buffer on ice for 20 minutes. Dehydration was performed via ascending concentrations of ethyl

alcohol Stepps and rinsing in propylene oxide (Sigma-Aldrich, Buchs, Switzerland). Embedding was carried out with a solution 2:1 propylene oxide and Epon (Carl-Roth, Karlsruhe, Germany) and with 1:1 of the same solution, folowed by neat Epon. It was then hardened at 60oC for 48 hours. 60nm sections were imaged in a EM902 transmission electron microscope (Zeiss, Germany). Image SP was used as a software (Tröndle, Moorenweis, Germany).

4.21. Behavior

4.21.1. Animals

Animals were bred in a specific-pathogen-free (SPF) facility at the Center for Molecular Neurobiology (ZMNH), University Medical Center Hamburg-Eppendorf, University of Hamburg. Before the experiments, p60 +/+ and +/- mice were housed in a SPF vivarium under controlled humidity (50±5%) and temperature (22±10^{o}C) (Institute of Molecular Neurogenetics, ZMNH). Light/dark cycle was reversed (lights on 19:00 h – 07:00 h). The animals were mantained in groups of 2-4 mice per cage and had food and water was accessible *ad libitum*.

4.21.2. Behavioral experiments

Males and females between 8 and 13 weeks old were considered for experiments. In total, two cohorts of animals were used. For cohort 1: [(+/+) mice: n= (males= , females=); (+/-) mice: n= (males= , females=) and cohort 2 (+/+) mice: n= (males= , females=); (+/-) mice: n= (males= , females=)]. Experiments were carried out during dark phase of the cycle after handling for 1 week. Animals rested for 2-4 days between experiments for less stressful tests and 2-3 weeks for more invasive tests (e.g. Fear conditioning). Experiments were video recorded automatically by a digital camera placed above the mazes, unless stated. Images were visualized via Ethovision (Version XT 8.5, Noldus Technology; The Netherlands) run in a PC. Between trials, mazes were cleaned with 30% EtOH and dried.

4.21.3. Ethics statement

All the experiments were performed according to the German and European Union laws on protection of experimental animals and after approval by the authorities of the City of Hamburg (Committee for Lebensmittelsicherheit und Veterinärwesen, Authority of Soziales, Familie, Gesundheit und Verbraucherschutz Hamburg, Germany, No. 100/13).

4.21.4. Elevated-plus maze (EPM)

EPM is a test for anxiety-related behavior in rodents, and evaluates the natural exploratory tendency conflicting with exposed areas (Handley S. L. and Mithani S., 1984). The arena was made of water proof polyvinyl (PVC) and consisted of 4 interconnected arms, each 30 cm long and 5 cm wide. It was elevated 78 cm from the floor and evenly illuminated with 50 Lux in the open arms. Two opposed arms were closed (closed arms) by opaque PVC walls 16 cm high. The remaining two arms were completely open (open arms) with a 2mm high perimeter in the outer edges. Each animal was subjected to 5 minutes trials and the trial started with the animal in the center of the maze, facing one of the closed arms. After, the mouse was removed from the maze and placed back to the home cage. The percentage of time spent in the open arms (time in open arms/time in all arms x 100%) was used as an index for anxiety-related behavior.

4.21.5. Light-dark transition (LDT)

Anxiety-related behavior was measured with LDT as well. It relies on the natural preference of rodents for dark and closed areas over open and lit areas (Crawley J. and Goodwin F. K., 1980). The experiment was carried out in an opaque box (45cm x 20 cm x 20 cm) made of PVC. The dark compartment was obtained using a smaller dark plastic box (19,5 cm x 19,5 cm x 15 cm) positioned in one of the extremities of the white box. The lit comparment was illuminated with 300 Lux while the dark comparment was dimly illuminated (1 lux). The mouse was allowed to freely navigate between illuminated and dark compartments thanks to an opening in the dark box 7.5 cm x 7.5 cm big. Trials of 10 minutes started with the

animal positioned in the dark compartment. Latency to leave the lit chamber, time spent in the dark compartment and number of transitions between the two compartments were measured.

4.21.6. Open field test

Four animals were tested simultaneously thanks to the presence of multiple arenas made of water proof PVC. Each one was 50 cm x 50 cm x 40 cm and was illuminated with 50 Lux constantly by four lamps placed in a metallic stand above the arenas. Mice were tested in groups of four and counterbalanced across genotype, with two arenas for females and the other two for males. Trials of 40 minutes of free exploration were carried out. Locomotor activity was the distance in 5-minutes bins. The animals were assessed for the time they spent in the central region of the arena 256 cm^2 (9,8% of the total area) as an index of anxiety-related behavior.

4.21.7. Spontaneous alternation in the Y-maze

A Y-maze made with beige opaque Plexiglas with three identical arms was evenly illuminated with 50 Lux. The arms were interconnected at 120 degrees.
Trials of 6-minutes started with the mice positioned in one of the arms. The animals were free to explore the maze undisturbed and the arm-entry sequence was scored manually. Total number of arm entries was a measure of activity, while spontaneous alternation was calculated as following:

Spontaneous alternation (%) = [(Number of alternations)/(Total number of arm entries-2)] x 100.

4.21.8. Y-maze spatial place discrimination and novelty preference.

A symmetrical Y-maze made of plexiglas was positioned 92 cm from the ground. The arms were 50 cm x 9 cm, spaced at 120^o and enclosed by transparent walls 14 cm tall (thickness 1cm). It was located in a dimly illuminated experimental room (50 Lux in the center of the maze) with several extra-maze cues. The maze was

built so to be able to rotate on its central axis. The arms of the maze faced prominent and distinct cues positioned at around 30 cm of distance from the end of each arms. The test consisted of two phases, training and acquisition which lasted 10 minutes each and were separated by around 6 minutes interval.

During acquisition phase, one of the arms was blocked with a plastic door, the animal was placed at the end of the start arm and allowed to navigate between the two open arms. The closed arm was the novel spatial location during the test phase. The position of arms in respect of a specific spatial location was counterbalanced. After a 10 minutes acquisition, the mouse was removed from the maze and placed in a waiting cage located in an adjacent room for around 6 minutes. During this time, the barrier was removed, the maze was properly cleaned and rotated 120^{o} clockwise. During test phase, the animals was introduced in the arm that corresponded to the same spatial location as during training. Test phase lasted 5 minutes and the animals were free to navigate the three arms.

Proportion of time spent in each arm was analyzed and the time in the arm corresponding to the novel spatial location was calculated using the following formula:

(time spent in the novel arm / time spent in all arms) x 100% = index for novelty preference.

4.21.9. Fear conditioniong apparatus

Two identical NIR video fear conditioning systems (MED-VFC-SCT-M, Med associates Inc, VT, USA). Testing chamber was illuminated with a 15 W house light placed above the grid on one side wall. A speaker was placed on the other side wall and used to deliver an acoustic stimulus (conditioned stimulus, CS). Chambers 30 x 24 x 21 cm were made of alluminium walls, a transparent front door made of Plexiglas and located in sound-isolated cabinets. Electric shock (unconditionied stimulus, US) was delivered through a stainless steel grid floor (19 rods, 4 mm diameter and spaced with 1.5 cm) present in the chambers. During testing, video recording of the session was performed via an IEEE 1394a (Firewire 400) processive scan CCD video camera (VID-CAM.MONO-2A) at 30 frames per

second with a visible light filter (VID-LENS-NIR-1). Video Freeze (Med Associates) software was used for visualization in a PC.

4.21.10. Delayed cued fear conditioning, extinction and renewal

On Day 1, *conditioning acquisition* was performed for 813-seconds in Context A. Along the whole trial, light and vanilla scent to provide olfactory cues were also present. A tone representing a conditioned stimulus (CS) (discrete tone of 90 dB, 2.8 kHz) was delivered every 180 seconds and lasted 30-seconds for a total of three times. Right after each CS, an electric foot shock was provided as unconditioned stimulus (US) (0.4 mA foot shock) for 1-second. After the trial, the mice were removed from the chambers and placed in a resting cahe for around 5 minutes before re introducing them to their home cage.

Freezing behavior (cessation of all movement apart from respiration) was a measure for the conditioned response (CR).

On Day 2, a *context test* was carried out. Animals were placed in the same context (context A) in the presence of vanilla scent and light for 360 seconds in order to examine the CR to the background context.

On Day 3, a *CS-test* was performed with the same protocol of Day 1, without US and in a different context (context B) to avoid interference of the conditioned context and assess the efficacy of the CS. A black, triangular acrylic insert and a white smooth acrylic insert instead of the grid floor were placed in the training chambers. During the session the house light was off and the trials were recorded under near infrared (NIR) light. Between trials, the chambers were cleaned with 70%

Extinction was carried out for three consecutive days in context B. Each trial consisted in 10x 30-s CS, with an interval of 20 seconds, and an initial and final phase of 3 minutes reppresenting baseline.

Fear renewal was assessed in the original context A. An 810 seconds trial identical to CS-test protocol was applied. Across the whole experiment,

4.21.11. Context discrimination test

Contexts A (safe) and B (aversive) were different in scent (vanilla or lemon), visual cues and shape. One of the contexts contained an insert that formed a semi-circular shape instead of the alluminium walls of the chamber. The other chamber presented a prominent visual cue covering the deepest wall of the chamber. Chambers were counterbalanced across the sessions.

On day 1 (learning), animals were positioned in Context A for 6 minutes and one hour later, in Context B. In context B animals received three unconditioned stimuli (US) (1 second, 0.4 mA) with intervals of 2 minutes via the floor grid.

On day 2 (test), the animals were positioned again in context A and B for 6 minutes each with an interval of one hour. No US was delivered and the floor grid was covered with a smooth white acrylic insert.

Learning on day 1 was measured as the percentage of time freezing across time-bins.

4.21.12. Statistical analysis

Analysis of variance ANOVA with Genotype (2 levels) and Sex (2 levels) was used between-subject factors. Repeated measures was applied for Trials, Arms, or Time-bins. Two-tailed Type I error rate of $p < 0.05$ was considered as statistically significant. “Statistical Package for Social Science“ (SPSS, ver. 21, SPSS Inc. Chicago IL, USA) was used for statistical analysis. Data are mean ± S.E.M. unless notified.

5. Results

5.1. Katanin p60 is required for embryonic survival and adult neurogenesis

5.1.1. Generation of p60 katanin knockout mice

In order to characterize the function of p60 katanin *in vitro* and *in vivo*, we made use of a mouse model generated by Laura Ruschkies, Dr. Torben J. Hausrat and Dr. Irm Borgmeyer (Transgene facility, ZMNH) in our laboratory at the Universitätsklinikum Hamburg Eppendorf. The mouse is a constitutive *knockout* (*KO*)-first with conditional potential. The *Katna1* KO-first allele contained Lac Z as a reporter gene and neomycin cassette for selection; flanked by 2 flippase (Flp) recognition targets FRT and 2 loxP sites flanking exons 6 and 7 for eventual Cre recombination (Fig. 16A). Long-range PCR was performed following mouse generation (data not shown). Genotyping PCR was performed with oligos e (PRL-170) and f (PLR-94) targeting 5' and 3' regions of the downstream loxP site. The resulting bands were 270 base pairs for the *wt* allele and 236 base pairs for the KO-first allele containing the *loxp* sequence (Fig. 16B).

A

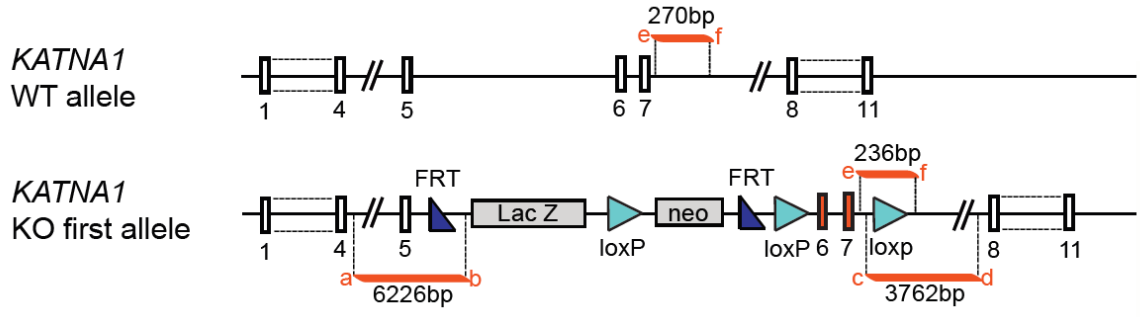

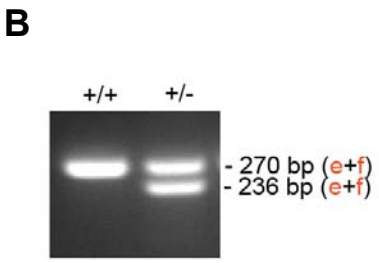

Figure 16. ***Generation of katna1 KO mice.*** The *wildtype* and *knockout first* alleles are shown including Lac Z reporter gene, FRT, neomycin cassette and loxP sites. Binding sites for genotyping oligos is also represented (A). Agarose gel showing genotyping PCR. Oligos *e* + *f* yielded a 270bp band for the wildtype allele and a 236bp band for the *KO*-first allele (B). Oligos *a* + *b* and *c* + *d* were used for Long range PCR (not shown).

5.1.2. *Homozygous Katna1* constitutive knockout mice are not viable

Interestingly, no p60 homozygous *KO* mice were obtained from p60 heterozygous *KO* matings throughout the study (Fig. 17). However, tissue from only a few full *KO* embryos was detected until E.15. The fetus was already undergoing digestion indicating previous embryonic lethality.

These results, underline a fundamental role for P60 katanin during embryonic development. The fact that only a few homozygous p60 *KO* were detected at E.15, suggests that cell division may underlie the embryonic lethality in these mice. P60 katanin functions during development were then elucidated in animals lacking a single *Katna1* allele (*p60 +/-*).

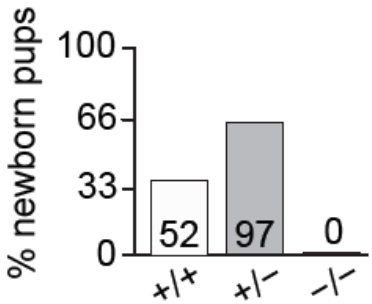

Figure 17. ***No homozygous KO mice were obtained from p60 +/- matings.*** Quantification of the offspring number obtained from heterozygous *KO* matings. Across the whole study, no homozygous *KO* mice were obtained.

5.1.3. *P60 +/-* mice show reduced levels of P60 katanin at the mRNA and protein levels

In order to validate the mouse model and verify if P60 katanin is downregulated in p60 +/- mice, mRNA quantification from brain lysates at E.15 was performed. In details, the oligos used to amplify the target fragments were specifically designed to target *Katna1* and exclude *katna-like 1* and *katna-like 2*, which share a high percentage of homology. The results showed a 50% reduction of *Katna1* mRNA in p60 *+/-* animals when compared to p60 *+/+* (Fig. 18A). P60 katanin protein levels were also assessed in order to exclude translational upregulation. For that, cortical lysates from E.17 embryos were tested with an antibody kindly donated by Prof. Francis J. McNally against human P60 Katanin (McNally F. J. and Thomas S., 1998). As expected, Western Blots showed around 40% decrease in protein expression (Fig. 18B and C). These results confirmed that p60 +/- mice show a significant decrease in P60 katanin protein levels and therefore constitute a reliable experimental model. The fact that only 40% reduction was observed at the protein level in p60 +/- mice could be due to primary antibody specificity which partially recognizes katanin-like proteins.

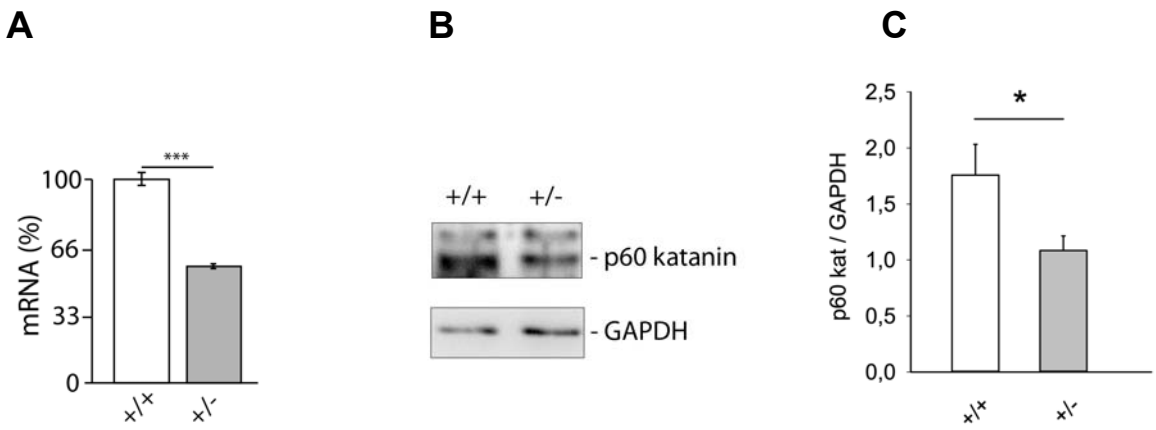

Figure 18. ***Katna1 mRNA and p60 katanin protein levels*.** Quantification of mRNA with qPCR shows a significant decrease of *katna1* mRNA in brain lysates of p60+/- animals (+/+) n=3, (+/-) n=3, from three independent litters. p<0,001 ***, REST© software (Pfaffl, M.W. et al., 2000) (A). Cortical lysates from embryos at E.17 were probed with α–p60 antibody and showed a significant reduction at the protein level. Data represented as mean +/- S.E.M., (+/+) n=3, (+/-) n=3. p<0,05 *, Independent samples T-test (One-tailed) (B).

5.1.4. No major brain abnormalities are present in p60 +/- mice

Previous studies have shown that mutations in the regulatory subunit of katanin, p80, dramatically altered brain morphology (Hu W. F. et al., 2014). The fact that p80 was related to such a strong phenotype suggested that MT-severing by the katanin complex was important for proper brain development. Since a downregulation of the catalytic subunit p60 could lead to similar results, I performed a gross analysis of brain morphology in 2-month old mice. No evident changes in brain dimensions and alteration on *Nissl* staining were observed (Fig. 19A-D). Although low levels of P80 katanin lead to brain malformations, downregulated p60 katanin does not lead to visible alterations. Presumably, the presence of other MT-severing enzymes like Spastin or Fidgetin can compensate for lower levels of p60 katanin. I concluded that the remaining p60 katanin protein in p60 +/- mice was sufficient to mantain general brain characteristics.

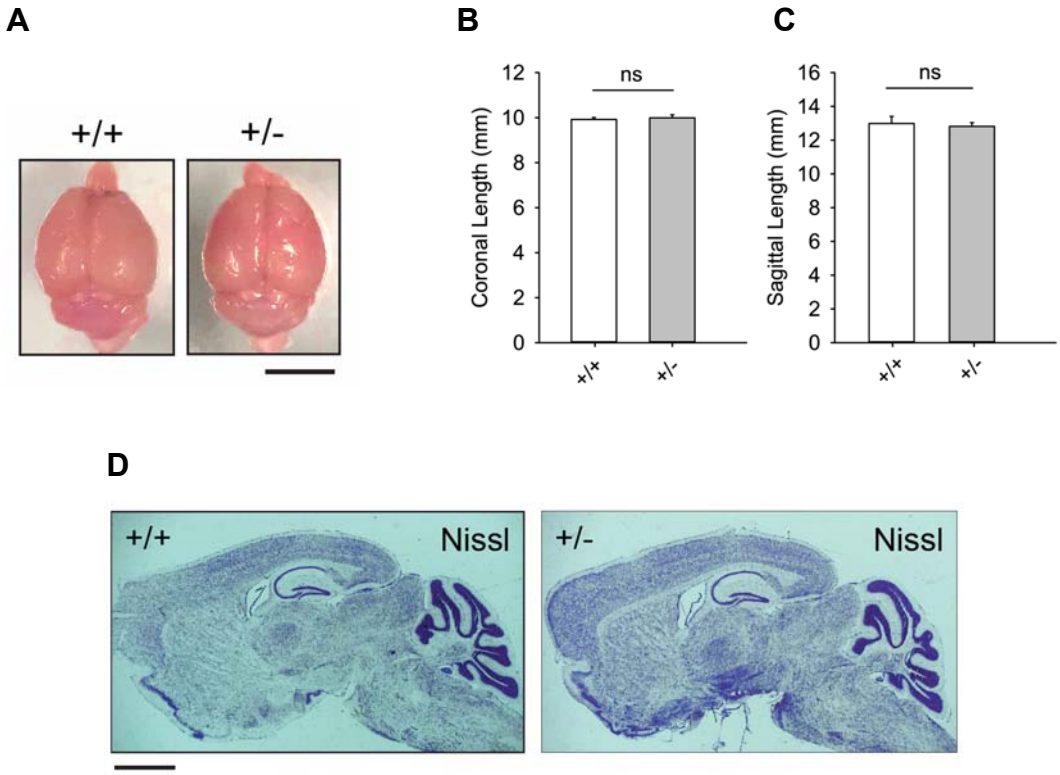

Figure 19. ***No gross morphological alterations in brains from p60 +/- mice.*** Sagittal and coronal measurements of brains from *p60+/+* and *p60+/-* animals show no significant difference (A to C). Data represented as mean +/- S.E.M. (+/+) n=3, (+/-) n=3, Independent sample T-test (Two-tailed). Nissl staining of brain sagittal sections (D).

5.1.5. Downregulation of katanin does not lead to increased apoptosis or neurodegeneration

Based on the embryonic lethality observed upon full depletion of p60 katanin and aiming to investigate developmental roles of p60 katanin in the brain, potential confounding processes like dysregulated apoptosis and early degeneration required investigation. PARP is a protein involved in the caspase cascade. It is known that caspases cleave PARP during programmed cell death so fragments of PARP are a sign of ongoing apoptosis and represent widely accepted markers for this process (Chaitanya G. V. et al., 2010). Quantification of cleaved PARP (cl-PARP) in relation to full length PARP showed no significant difference in western

blots (Fig. 20A and B), indicating physiological levels of apoptosis in both groups. Besides, sagittal brain slices were labeled with FluoroJade-C. Although the mechanism of FluoroJade-C labeling is still unknown, the scientific community accepts it as a reliable marker for neurite degeneration (Schmued L. C. et al., 1997). Notably, no increase in FluoroJade-C labeling was present in p60 +/- animals (Fig. 20C). Altogether, I concluded that exacerbated apoptotic processes and/or degeneration did not take place in p60 katanin +/- mice.

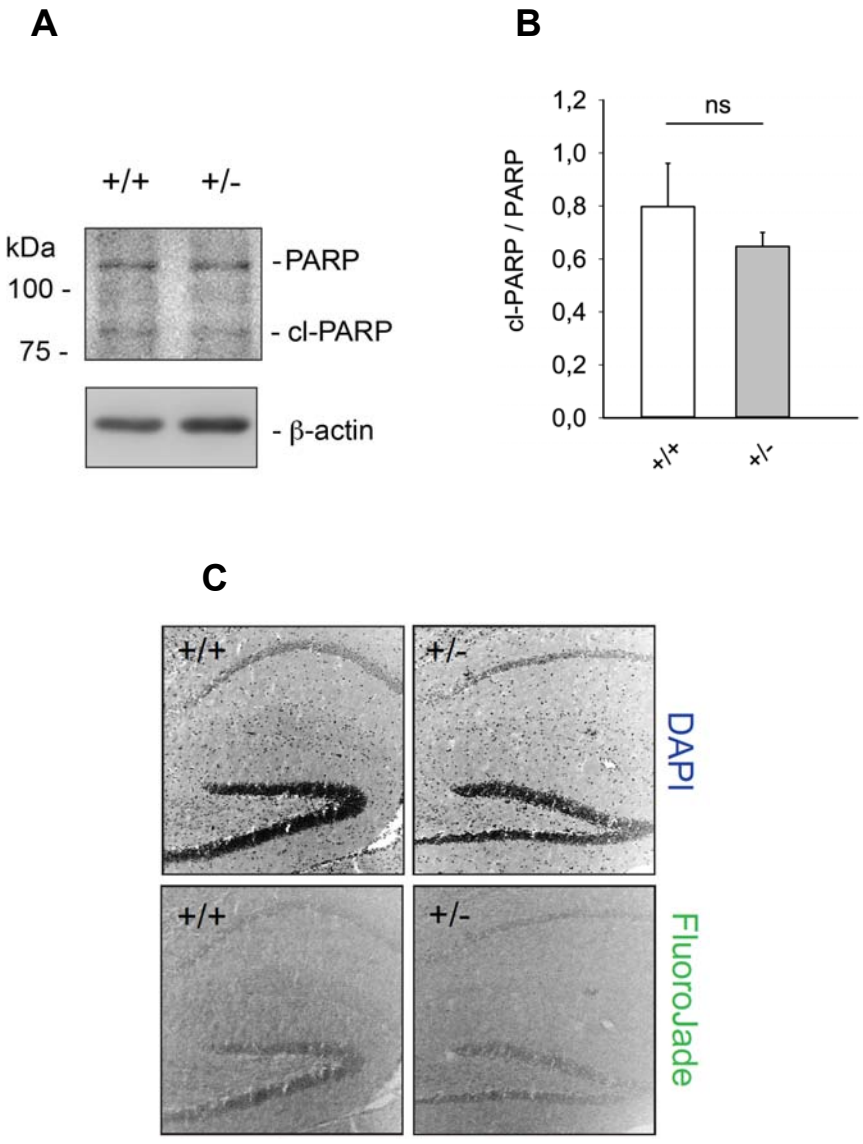

Figure 20. ***No evidence of increased apoptosis or degeneration in*** **p60 +/-** ***animals.*** Western Blot analysis of hippocampal lysates from 2-month old females shows no significant increase in the amount of PARP fragments (cl-PARP) (A and B). Data

represented as mean +/- S.E.M. (+/+) n=3, (+/-) n=3, Independent sample T-test (Two-tailed). The marker for neurite degeneration FluoroJadeC does not show any degeneration in the hippocampal region of sagittal brain sections (C).

5.1.6. Spastin, a MT-severing enzyme involved in Hereditary Spastic Paraplegia shows no altered expression upon P60 katanin downregulation

Hereditary Spastic Paraplegia (HSP) is an autosomal dominant disease characterized by loss of strength in lower and upper extremities and also intellectual disability (Klebe S. e al., 2015). Recent studies have shown that mutations in Spastin gene (*SPG4*) are associated with HSP (Charvin D. et al., 2003). Spastin is another MT-severing enzyme that belongs to the AAA-ATPase family (Roll-Mecak A. and Vale R.D., 2005) and has been shown to be influenced by tubulin polyglutamylation (Lacroix B. et al., 2010). Mutations in spastin are thought to be involved in the degeneration of the neuronal axon (Evans K.J. et al., 2005). Since katanin and spastin could have overlapping roles, compensatory effects by spastin could potentially be observed in p60 +/- model. In order to address this question I performed Western Blots from hippocampal tissue of 8-week old animals. The results showed no significant change in spastin protein levels (Fig. 21A and B). Although the basal enzymatic activity of spastin was not assessed, the presence of equal levels of spastin in p60 +/- mice when compared to p60 +/+ is a good indicator about the absence of potential compensations and suggests that spastin and p60 katanin functions are not redundant.

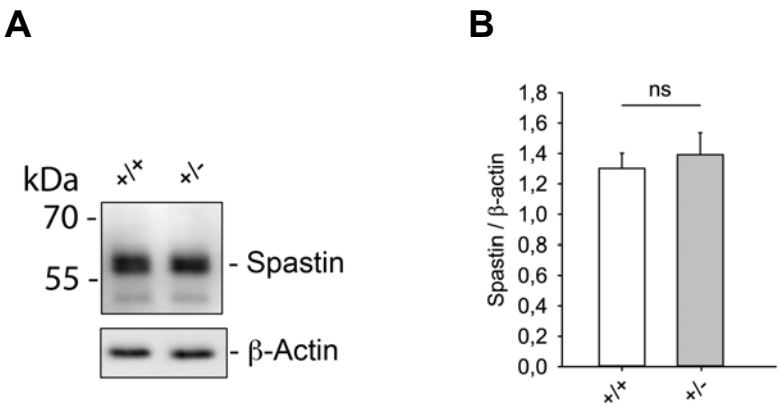

Figure 21. ***Spastin levels are not altered upon p60 downregulation.*** Western Blot analysis of hippocampal lysates from 2-month old females shows no altered expression of the MT-severing enzyme spastin (A and B). Data represented as mean +/- S.E.M. (+/+) n=3, (+/-) n=3, Independent sample T-test (Two-tailed).

5.1.7. General tubulin levels show no alteration in young adult p60+/- mice

A consequence of MT severing is the release of "second-hand" tubulin subunits that could be recycled and used for the formation of a new filament. Studies suggest that tubulin subunits modulate the translation of tubulin itself in a feedback loop (Zhou J. et al., 2002). P60 katanin downregulation and therefore a decrease of its severing activity could influence levels of free tubulin and as a consequence the translation of new monomers. In order to investigate this, Western Blots were performed from hippocampal lysates and protein levels of different tubulin isoforms were assessed. The results showed that a downregulation of p60 katanin does not affect general tubulin expression levels (Fig. 22A-F) and indicate that hypothetical changes in the amount of free tubulin monomers upon downregulation of p60 katanin do not alter significantly the overall tubulin concentration in the cell. At this point, it was interesting to test how tubulin was distributed in the cell and its impact on neuronal morphology.

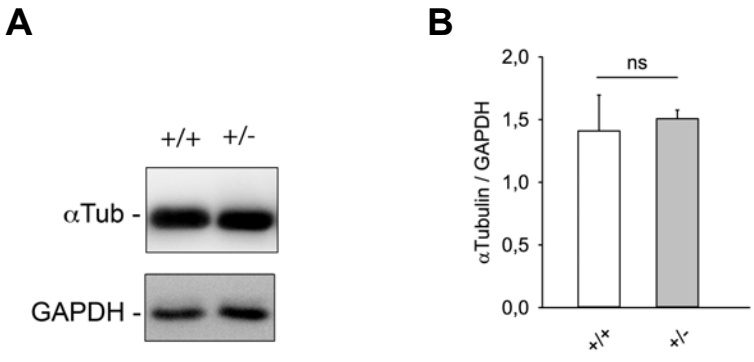

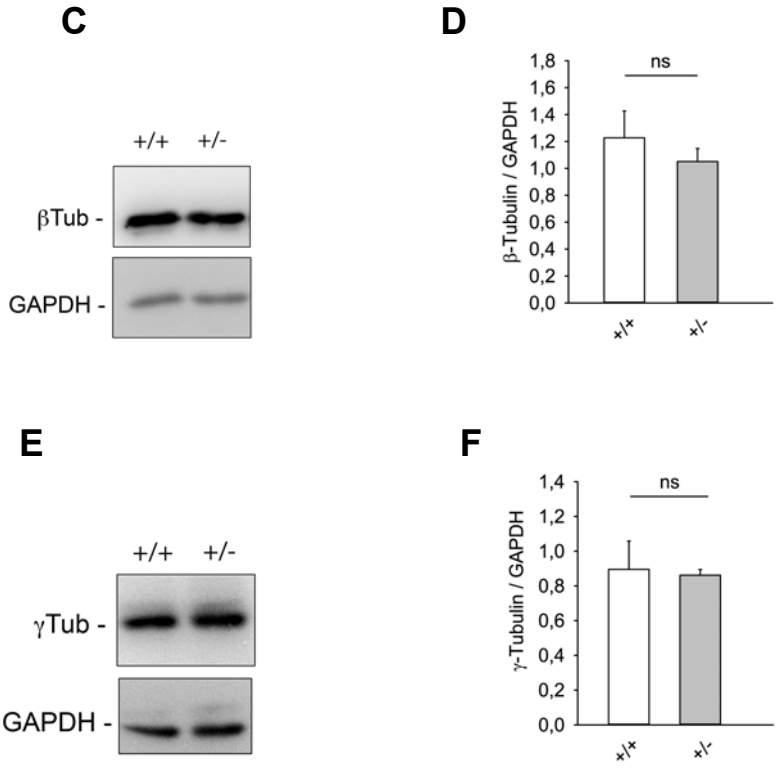

Figure 22. ***Tubulin levels are not affected upon p60 katanin downregulation.*** Lysates from the hippocampus of *p60 +/+ and +/-* mice were probed for alpha- (A and B) beta- (C and D) and gamma- (E and F) tubulin expression at 9 weeks of age. No significant changes were observed. For a-Tub (+/+) = 1.41±0.29; (+/-) = 1.51±0.07. For b-Tub (+/+) = 1.23±0.20; (+/-) = 1.05±0.10. For g-Tub (+/+) = 0.89±0.16; (+/-) = 0.86±0.03. Data represented as mean ± S.E.M. (+/+) n=3, (+/-) n=3, Independent samples T-test (Two-tailed).

5.1.8. p60 katanin downregulation leads to morphological abnormalities during neuronal development *in vitro*

Previous studies have reported that p60 katanin is involved in dendritic arborization (Mao C. –X. et al., 2014) and that its severing activity is influenced by Tubulin acetylation (Sudo H. and Baas P.W. 2010). Presumably, katanin severing

activity establishes the basis for the generation of new dendrites by generating new nucleation points in a time- and region-specific manner.

In order to test if a downregulation of p60 katanin affected dendritogenesis, primary hippocampal cultures from E.16 embryos from p60 +/+ and +/- mice were co-stained with Tubulin-βIII and acetylated α-Tubulin antibodies. In culture, p60 +/- cells indeed showed morphological changes when compared to +/+ (Fig. 23A), indicating that physiological levels of p60 katanin are needed for proper development. Specifically, defined dendrites were substituted by cell extensions resembling lamellipodia that resulted in increased cell surface (Fig. 23B). Since acetylation of α-Tubulin is thought to regulate p60 severing function (Sudo H. and Baas P.W. 2010), I checked if changes in morphology were correlated to differential modification of Tubulin filaments. However, results showed similar α-Tubulin acetylation in both groups (Fig. 23C). These results suggest that p60 is required for proper neuronal development and supports the idea that MT-severing is required at early stages of dendritogenesis.

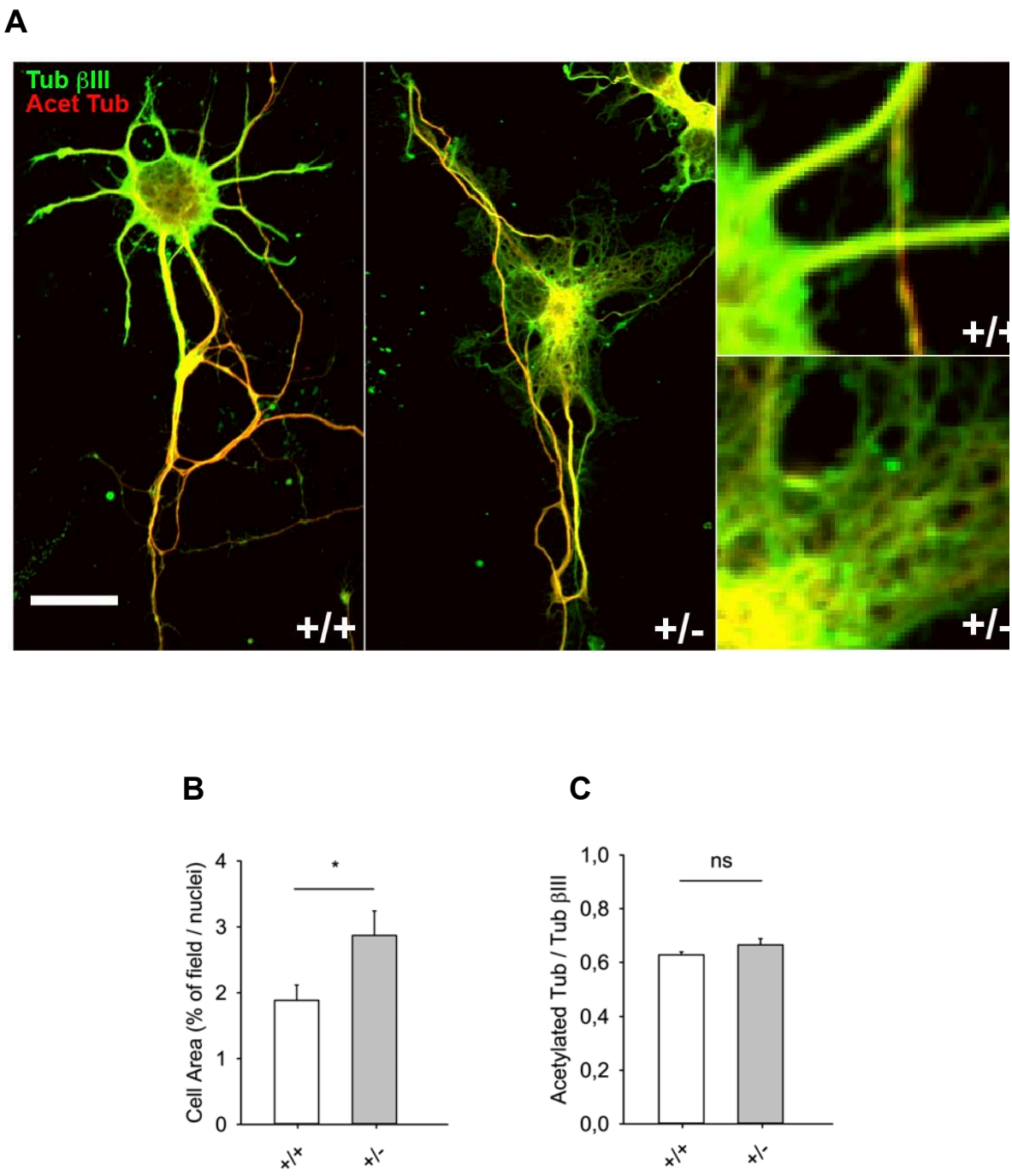

Figure 23. ***Developing hippocampal neurons show increased cell body area in vitro.*** Immunofluorescence analysis of hippocampal cultures at DIV6 show no imbalance between Tubulin-β-III and Acetylated α-Tubulin (A and B). However, p60 +/- neurons display increased cell body area (C). Data represented as mean ± S.E.M. $p<0,05$ *. For cell area (+/+) = 1.88±0.24; (+/-) = 2.87±0.37 (+/+) n=2, 18 cells, (+/-) n=3, 16 cells, Independent samples T-test (Two-tailed). Scale bar 20μM.

5.1.9. p60 katanin +/- animals show an accumulation of newborn cells in the VZ of the neocortex

Several studies have linked katanin and katanin-like proteins to cell migration (Zhang D. et al., 2011; Eom T. Y. et al., 2014). Moreover, Baas and Sharma have hypothesized that p60 activity might also happen at the +Tip of growing MT (Baas P. W. and Sharma V., 2011) influencing cellular motility.

In order to investigate the role of p60 katanin in the developing brain, I tested if neuronal migration during corticogenesis was affected in p60 +/- mice. During corticogenesis, neurons are born in the VZ and start their radial migration towards upper layers of the cortex. Since the goal was to assess long-range migration, we electroporated in utero E.15 embryos with a Venus fluorescent plasmid (Fig. 24A). The aim was to label progenitors that generate neurons in the VZ and migrate to layers I and II of the neocortex. Quantification showed an accumulation of cells in the VZ of p60 +/- animals, but no significant difference was observed in upper layers, although a decrease was expected to directly connect this effect to neuronal migration (Fig. 24B). Notably, the morphology of the pool of non-migrating cells was rounded and no leading or trailing processes, typically showed in migrating cells, could be observed (Fig. 24C).

In conclusion, an accumulation of newborn neurons in the VZ with no significant impact in upper layers was observed in p60 +/- mice. This result does not necessarily contradict previously published data about p60 katanin role in cellular migration (Zhang D. et al., 2011), since low levels of p60 katanin might be sufficient to sustain cell motility. It is worth mentioning that the lack of a bipolar phenotype in non-migrating cells which accumulate in the neurogenic niche leads to the hypothesis that lower levels of p60 katanin impair cell division rather than cell migration. In order to test this hypothesis, I decided to focus on the SGZ of the adult hippocampus, where adult neurogenesis takes place (Altman J. 1962; Altman J et al., 1965).

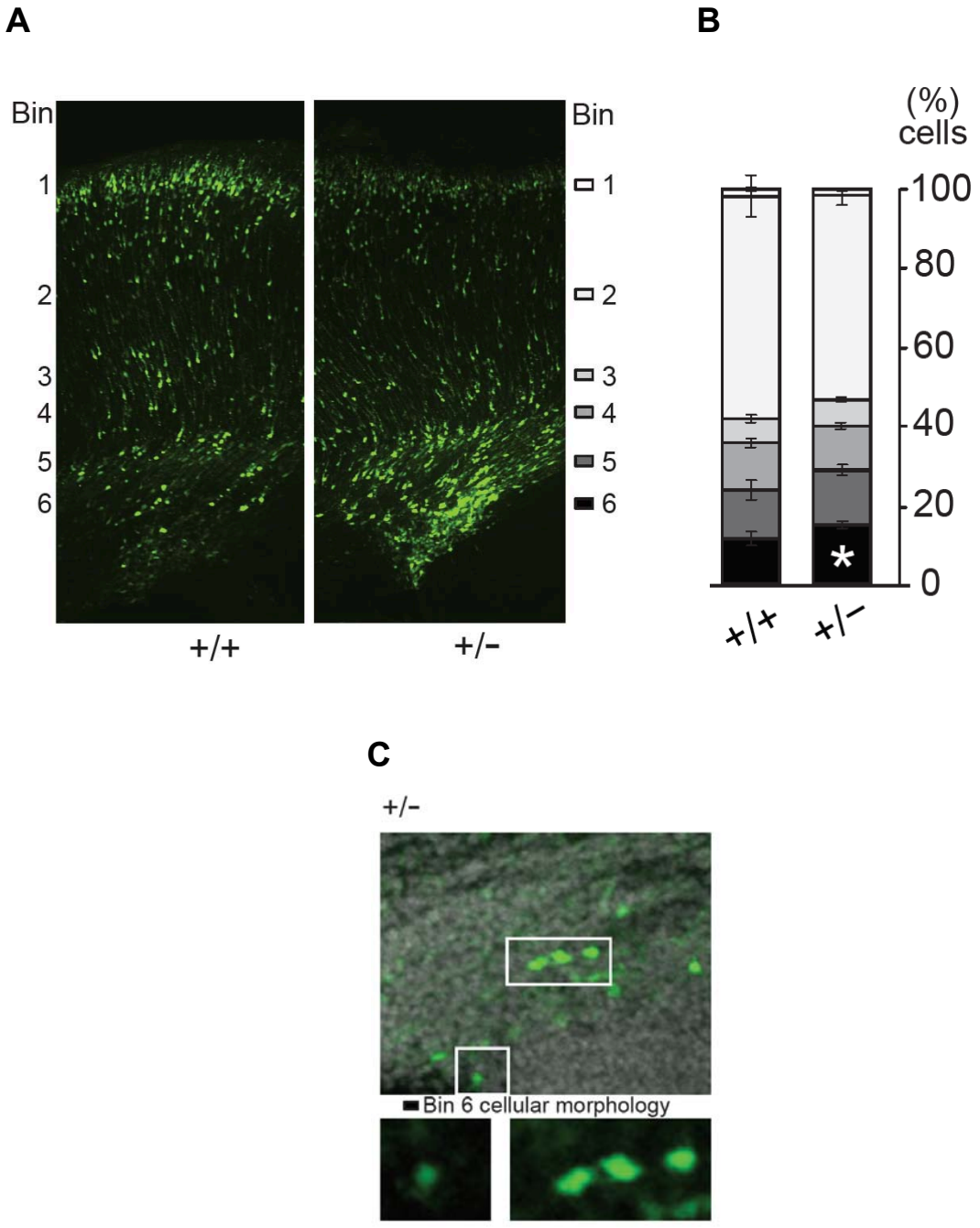

Figure 24. ***An accumulation of neurons is observed during corticogenesis in the VZ of p60 +/- mice.*** Confocal images of the cortex of in-utero electroporated embryos with pCAG-Venus in the ventricular region of the brain, 4 days later show a significant accumulation of neurons in the neurogenic niche of p60+/- mice indicated as layer 6 (A and B). Data represented as mean ± S.E.M. p<0,05 *. Non-parametric T-test (Two-tailed). For the LV (+/+) = 11.53%±1.81%; (+/-) = 15.64%±0.88% (+/+) n=4, 16 sections, (+/-) n=7, 26 sections. Morphology of non-migrating cells is rounded with no evident protrusions (C).

Brightness and contrast were modified for each image individually in order to properly observe Venus-expressing cells.

5.1.10. Expression of the neuronal marker NeuN is marginally decreased in the hippocampus of *p60+/-* mice

NeuN is a marker for post-mitotic neurons and its expression peaks when neurons are mature (Mullen R.J. et al., 1992; Lind D. et al., 2005). To have an indication about the expression of this marker and eventual correlation with changes in the number of neurons, western blots from hippocampal lysates of 9 weeks old animals were performed. The quantification showed a marginal but not significant decrease in NeuN expression in p60 heterozygous *knockout* mice (Fig. 25A and B). Besides, immunohistochemical stainings on sagittal sections from 2-month old animals showed a slight reduction of post-mitotic neurons when probed with NeuN antibody (Fig. 25C). These observations indicate that in heterozygouns p60 mice, a reduction of p60 might have a minimal effect on the number of post-mitotic neurons. The lack of dysregulated apoptotic events at the same age of the mice (Fig. 20), suggests that a slight reduction of mature neurons can be attributed to a slower neurogenesis.

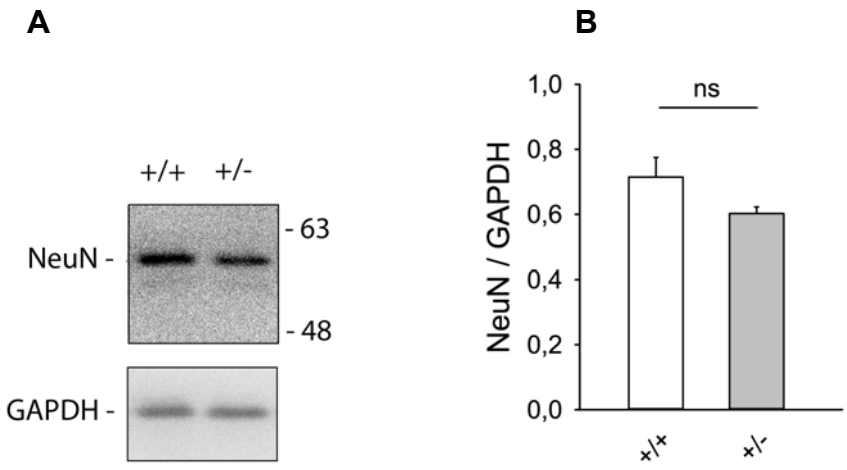

C

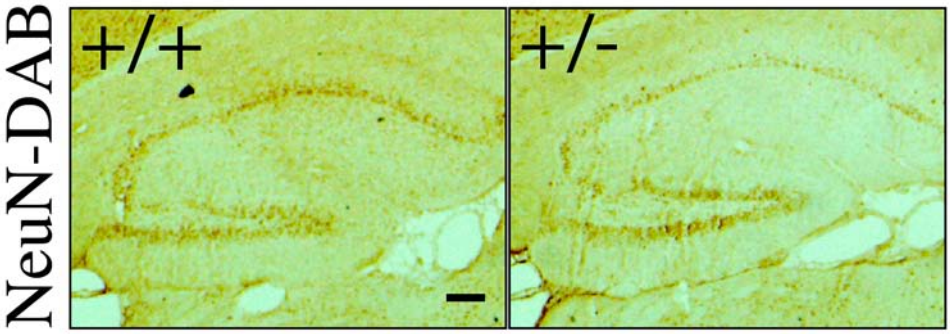

Figure 25. ***NeuN expression shows a marginal reduction upon p60 downregulation.*** Hippocampal lysates show only a tendency in reduction of the post-mitotic marker NeuN in western blots (A and B). N= (+/+)=3; (+/-)=3. NeuN (+/+) = 0.71±0.06; (+/-) = 0.60±0.02. Data represented as mean ± S.E.M. Independent samples T-test (Two-tailed). NeuN-DAB staining of free floating sagittal sections. Images taken from the hippocampal region (C). 500μM scale bar

5.1.11. P60 katanin +/- animals show an accumulation of newborn cells in the SGZ of the Dentate Gyrus

The involvement of p60 katanin in cell migration was previously tested and results showed an accumulation of cells in the neurogenic niche during corticogenesis (Fig. 24A and B). In the SGZ of the adult hippocampus, adult neurogenesis takes place (Altman J. 1962; Altman J et al., 1965). Previous results showed a mild decrease in NeuN expression that could indicate defects in neurogenesis in the adult DG. In order to test this hypothesis, I first investigated the positioning of newborn cells. Doublecortin (DCX) is a marker for IPCs and newborn migrating neuroblasts (Nacher J. et al., 2001; Zhang J. and Jiao J., 2015). In order to focus on these cellular populations, co-staining with NeuN and DCX was performed (Fig. 26A and B). The quantification of the number of cells that underwent migration and integrated in the granular layer of the DG shows that in p60 +/- animals, the number of DCX positive cells was not altered (Fig. 26C). However, the percentage of cells that stayed anchored to the SGZ was significantly increased in p60 +/- mice (Fig. 26D). This suggests that in the adult hippocampus, where new neurons

are generated before they undergo radial migration and become a functional part of the system, an accumulation of cells in the neurogenic niche was observed. This set of data mimics what was observed in the developing neocortex, where newborn cells accumulated in the VZ of p60 +/- embryos (Fig. 24). As stated before, DCX specifically labels both IPCs and neuroblasts (Nacher J. et al., 2001; Zhang J. and Jiao J., 2015) and in order to dissect whether differences in cell positioning are due to the role of p60 katanin in cell migration of newborn neurons or cell proliferation of IPCs , the identity of DCX+ cells that accumulate in the SGZ was invesigated.

A

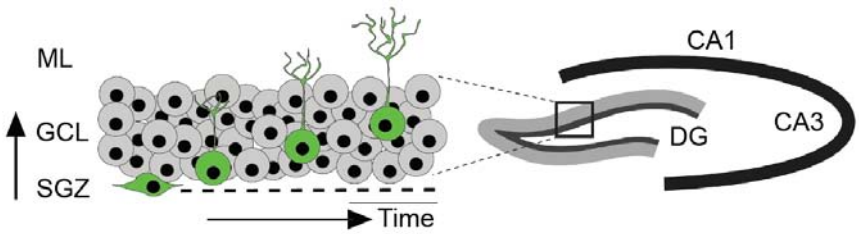

B

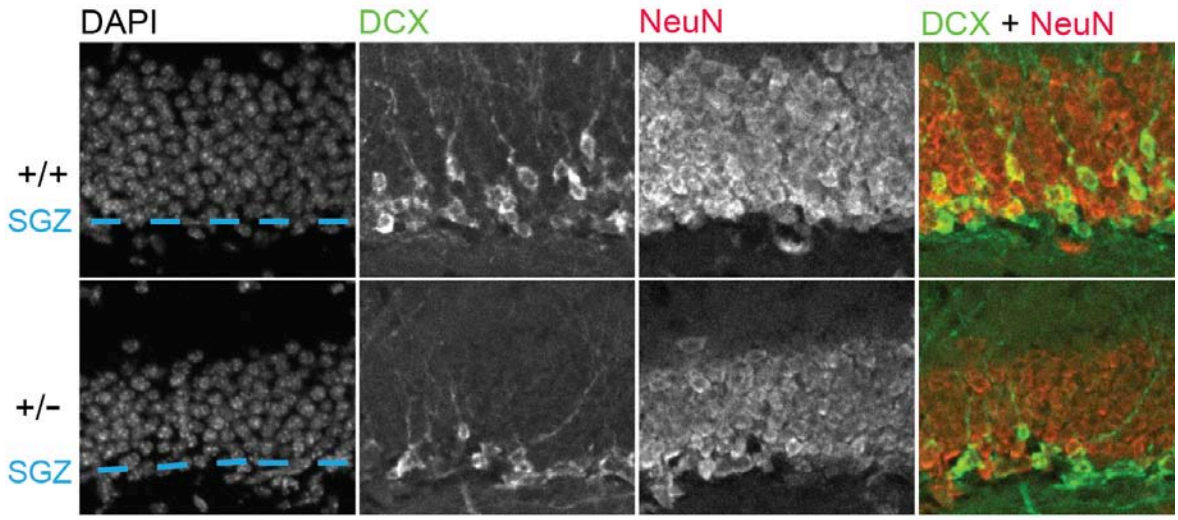

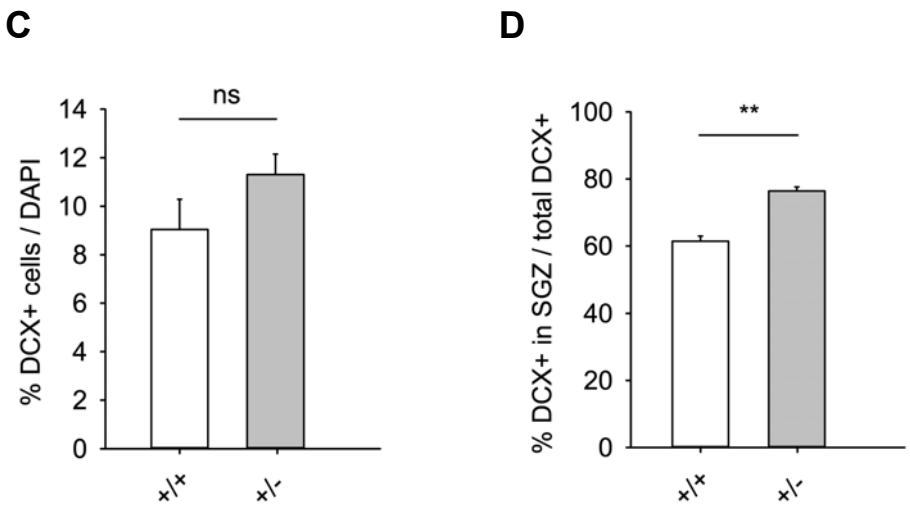

Figure 26 ***Doublecortin-positive cells accumulate in the subgranular zone of the DG.*** Sagittal sections of two months old animals were stained for DCX, NeuN and DAPI (A and B). The total number of DCX+ cells is not changed (+/+) = 9.04±1.243; (+/-) =11.31±0.842. (C) The position of DCX+ cells is significantly affected (+/+) = 61.4±1.51; (+/-) = 76.4±1.25. (+/+) n=3; (+/-) n=3. Data represented as mean percentage ± S.E.M. ** p<0,01. Independent samples T-Test (Two-tailed) (D). SGZ = Subgranular Zone.

5.1.12. p60 katanin affects cell proliferation during adult neurogenesis

It has been shown that katanin is targeted to the spindle pole and is involved in cytoskeletal rearrangement during cell division (McNally K.P. et al., 2000). For that, the regulatory subunit p80 plays an important role, allowing p60 to localize to the specific severing site (McNally K.P. et al., 2000). Studies have shown that upon katanin depletion, dividing cells are polynucleated and this is likely due to a block in a step of the cell cycle where MT dynamics are fundamental (Matsuo M. et al., 2013). By focusing on adult neurogenesis I hypothesized that impaired proliferation could be the cause of the accumulation of DCX+ cells in the SGZ of the DG. In order to address this, BrdU injections were performed intraperitoneally in p60 +/+ and +/- mice. BrdU is a thymidine analogue that stains DNA during synthesis (Miller M. W. et al., 1988). DNA polymerase incorporates BrdU in the newly synthesized helix and is recongnized by anti-BrdU antibodies for quantification. BrdU stainings of hippocampal slices from mice previously injected

with BrdU showed a strong decrease of dividing cells in the SGZ of the DG (Fig. 27A and B). This result reveals that reduced p60 expression levels delay neuronal proliferation in the SGZ of the hippocampus and suggests that the accumulation of DCX+ cells observed previously (Fig. X) is a result of impaired cell division. Altogether, these data supports p60 katanin function in cell division and attributes p60 to an important role in adult neurogenesis.

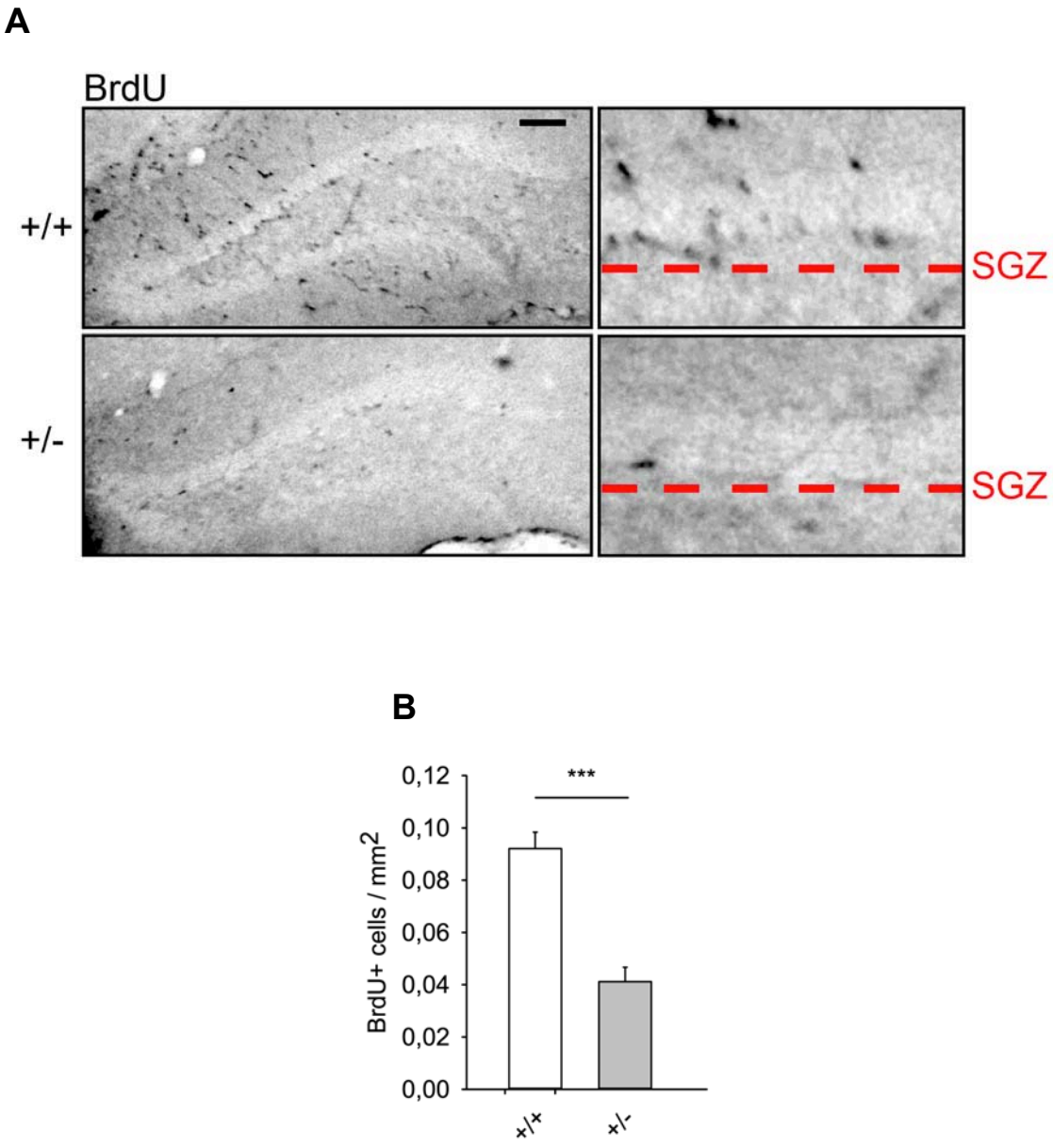

Figure 27. ***Decreased cell proliferation during adult neurogenesis in p60 +/- mice.*** Two months old mice were administered with BrdU intraperitoneally and 4 hours later were perfused under anesthesia for tissue processing (A). Immunohistochemical staining

of coronal sections shows a significant decrease in the number of cells that incorporated BrdU during the incubation time (B and C) (+/+) = 0.091±0.006; (+/-) = 0.041±0.005. (+/+) n=3, 28 sections, (+/-) n=3, 28 sections Data represented as mean ± S.E.M. ***p<0,001. Independent samples T-Test (Two-tailed). SGZ = Subgranular Zone. 100μM Scale Bar.

5.1.13. p60 katanin downregulation results in an increase in the progenitors pool in the SGZ

The previous findings showed a significant decrease in the number BrdU+ cells in the SGZ, indicating that either the number of progenitors that entered the S-phase of the cell cycle was smaller or cell division was delayed. If the cell cycle was delayed in p60 +/- animals, one possibility is that this could be reflected in the number of progenitors that reside in the neurogenic niche of the DG. In order to test this hypothesis, a combination of Sox2/GFAP antibodies was used to stain for SGZ neuronal precursor cells in the SGZ. The results showed a significant increase of Sox2/GFAP double positive cells in the SGZ, suggesting that a slower cell division in the progenitors population results in an increase of the progenitors pool itself (Fig. 28A and B). Such a phenomenon was also previously observed in a mouse model related to Amyloid Precursor Protein family members (Shariati S. A. M. et al., 2013) during embryonic corticogenesis, in which the authors claimed that APLP2 was required for differentiation. Altogether, these results suggest that upon p60 katanin downregulation, either less progenitors enter the S-phase of the cell cycle, or the resulting newborn cells struggle to divide. In summary, p60 katanin effect could be connected either to early phases of the cell cycle when centrosomes are duplicated, or to later phases when cell division occurs.

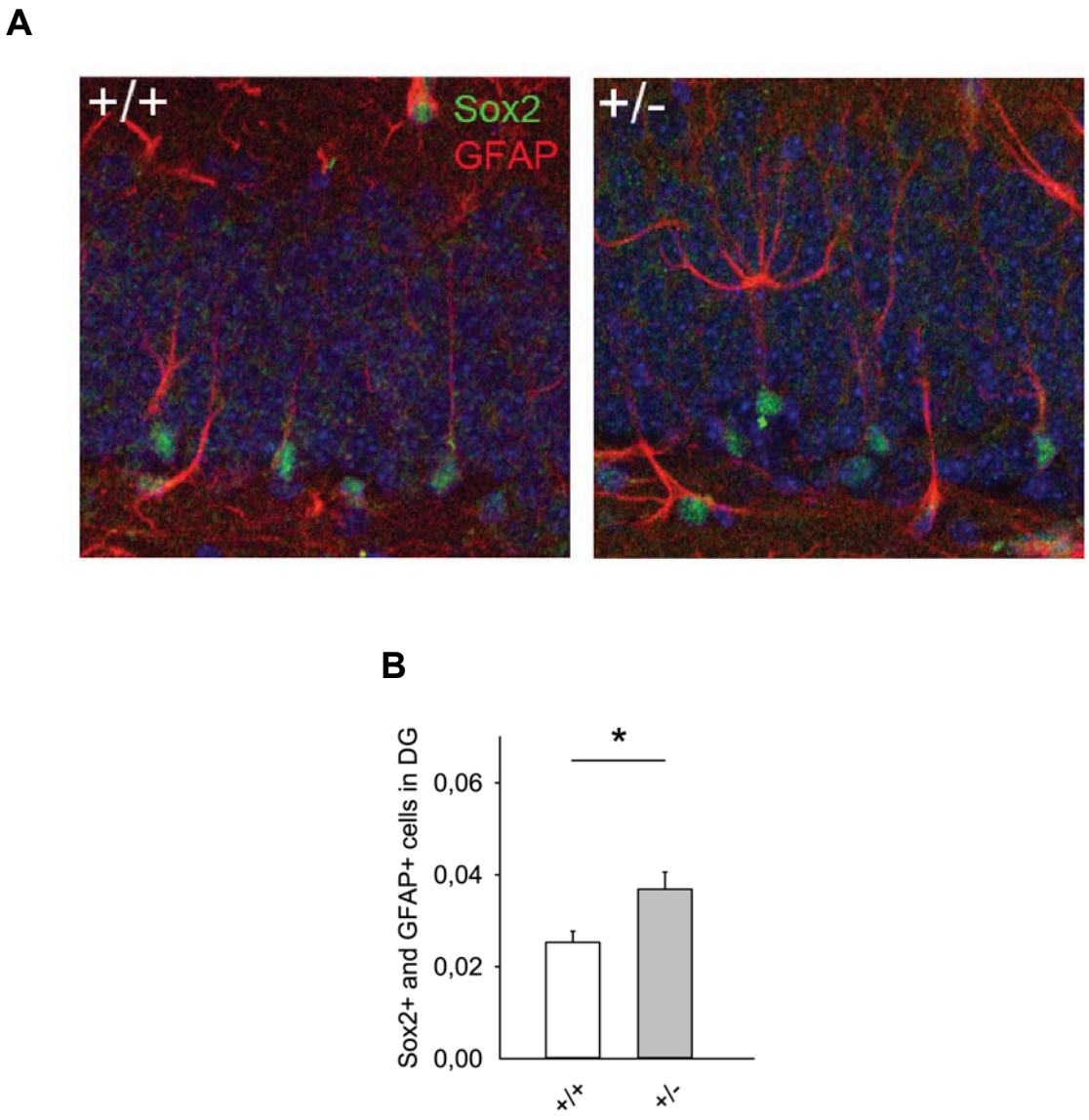

Figure 28 ***An accumulation of neuronal progenitors is observed in the SGZ of the DG in p60 heterozygous knockout mice.*** Neuronal progenitors were double stained with Sox2 and GFAP (A). A significant increase in the SGZ of neuronal progenitors is observed upon p60 katanin downregulation. (+/+) = 0.024±0.002; (+/-) = 0.037±0.004. (+/+) n=4, (+/-) n=3. Data represented as mean ± S.E.M. *p<0,05. Independent samples T-test (Two-tailed).

5.1.14. Dendritic arborization of granule cells of the DG is not altered in p60 +/- mice

Delayed cell proliferation and an accumulation of progenitors were observed in p60 +/- mice. P60 katanin was shown to be involved in dendritic arborization (Mao C. –X. et al., 2014) and previous results in this study showed impaired development of hippocampal neurons *in vitro* (Fig. 23A and B). Therefore, I tested if delayed proliferation in the adult DG affects the formation of the dendritic arbor and the integration of mature neurons into the DG network thereby compromising the function of the hippocampus. In order to test if neuronal morphology was affected in mature granule neurons, acute hippocampal slices were prepared from adult mice and labeled with DiI *ex vivo*. DiI is a lipophylic dye that spreads throughout the cell membrane thus highlighting the cell (Fig. 29A and B). By tracing the dendritic tree of mature neurons it was possible to analyze its complexity. Results showed that branching of the dendritic tree of mature granule cells was highly comparable between genotypes (Fig. 29C). These results, together with impaired neuronal development *in vitro,* show that MT-severing by katanin during early stages of neuronal maturation is required for proper axonal-dendritic formation, but dendritic branching is mainly delayed and not fully compromised. Finally, this data suggests that delayed adult neurogenesis does not fully impair adult granule neuron maturation. Although the capacity of newborn neurons to form active synapses within the hippocampal circuitry is worth investigating, the current data indicates that neurons that reach maturation are correctly incorporated in the DG.

A **B**

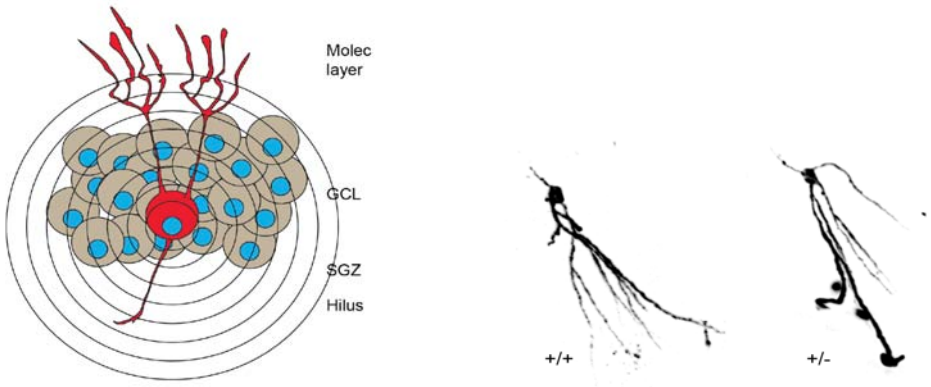

C

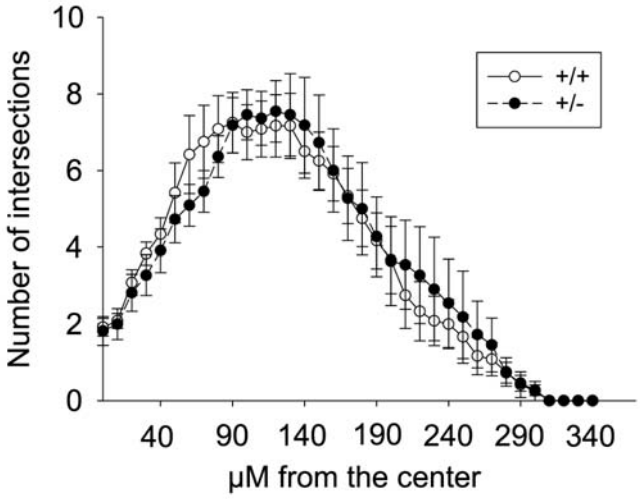

Figure 29. ***Mature DG neurons show no difference in dendritic branching.*** Sholl analysis in Granule cells in the DG (A and B) display a normal dendritic tree (C). (+/+) n=3, 12 cells; (+/-) n=3, 11 cells. Data represented as mean +/- S.E.M. Two-way (Gtype x 10μM bins) ANOVA. Repeated measures.

5.1.15. Heterozygous knockout of p60 katanin has minimal impact on locomotor activity and anxiety-related behavior

Based on the data showing a strong decrease but not complete ablation in the number of BrdU positive cells in p60 +/- mice, I tested whether these observations might correlate with changes in cognitive functions that are shown to depend on adult neurogenesis (Martinowich K and Schloesser R. J., 2016). Several paradigms were first used to test anxiety-like behavior in rodents, but no evident changes were observed in p60 +/- mice when compared to p60 +/+. This conclusion was based on the lack of significant difference between genotypes in the proportion of time spent in the open arms of the elevated-plus maze (EPM) (Fig. 30A and B), time spent in the lit compartment of the Light-dark Transition test (LDT) (Fig. 30F and G), or time in the center of the open field (OF) arena (Fig. 30C and E). Besides, locomotor habituation upon extended testing was comparable between p60 +/+ and p60 +/- mice (Fig. 30D). These results suggest that a

reduction in adult neurogenesis due to p60 katanin haploinsufficiency is not sufficient to alter anxiety-related functions or general activity. It was shown that under physiological conditions, newborn cells undergo selective apoptosis and only some become active units in the hippocampal circuitry (Dayer A.G. et al., 2003). Therefore, it is likely that remaining levels of adult neurogenesis are sufficient to mantain anxiety and activity levels at their physiological conditions. Also, the lack of impairments in these tests served as a control for the following cognitive tasks, where anxiety or locomotor impairments may influence appropriate performance. .

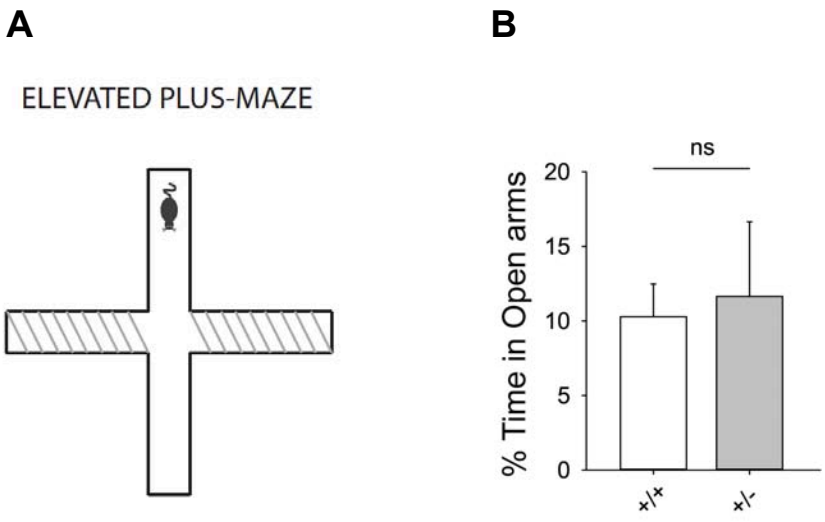

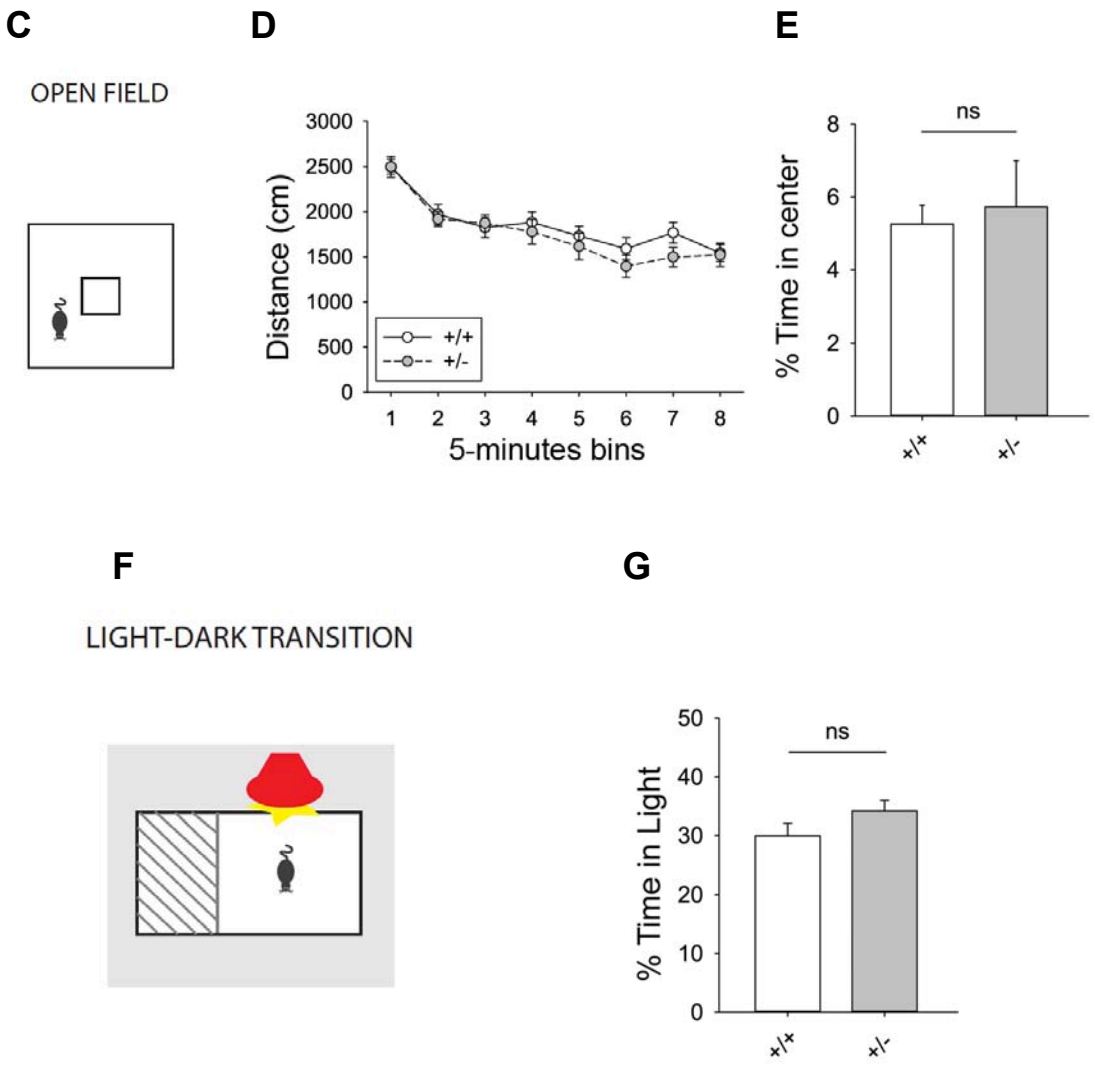

Figure 30. ***P60 katanin haploinsufficiency does not alter general activity or anxiety-related behavior.*** The percentage of time in the open arms during Elevated-plus maze (A and B), locomotor activity and the percentage of time in the center of the box during Open field (C-E) and the percentage of time in the light compartment of Light-dark box test (F and G) show no significant difference between *p60+/+* and *p60+/-* mice. Data represented as mean +/- S.E.M. Two-way (Genotype and Sex) ANOVA, and time-bins as repeated measures factor in Figure D.

5.1.16. Spontaneous alternation and Spatial place recognition are not affected in *p60 +/-* mice

It is known from previous literature that lesions of the hippocampus impair spontaneous alternation behavior (Stevens R. and Cowey A., 1973). Also, studies

have associated adult neurogenesis with working memory (Nilsson M. et al., 1999; Ouchi Y. et al., 2013), suggesting that newborn neurons play an important role in this process. Therefore, I examined whether delayed adult neurogenesis in p60 +/- mice may be associated with changes in working memory function by using the Y-maze spontaneous alternation task (Fig. 31A). This test is used to assess the rodent's preference for novelty and the capacity to alternate on successive arm entries (Hughes R. N., 2004). The results showed that p60 +/- males made significantly higher number of arm entries, but percentage of alternation was highly comparable between genotypes (Fig. 31B-C). These data indicated that working memory was not affected in p60 +/- mice but also served as a control for the Y-maze spatial place recognition task in which impared alternation might influence performance. I extended my analysis of p60 +/- mice to spatial place recognition by using a clear-walled symmetrical Y-maze with allocentric cues. On Trial 1 (acquisition), the mouse started from one arm and was allowed to explore and become familiar with allocentric cues of two arms, since the third arm was inaccessible for exploration. After a 10-minute session, the mouse was placed in a waiting cage for around 6 minutes, while the barrier was removed and the maze was rotated and carefully cleaned. On trial 2 (novelty preference), the mouse was re-introduced to the maze and allowed to explore the three arms (Fig. 31D). Results showed that during the acquisition trial, both genotypes spent a similar amount of time in the starting and the other open arm, which is necessary for appropriate performance in the following phase of the test. In the novelty preference phase of the experiment, p60 +/- mice were able to discriminate between novel and familiar locations, since they expressed significant preference for the novel location (previously inaccessible arm) (Fig. 31E). This data supported the natural preference for rodents for novel over familiar environments (Bannerman et al., 2008; Sanderson et al., 2007) and indicated that heterozygous p60 katanin knockout has little impact on spatial novelty preference.

A

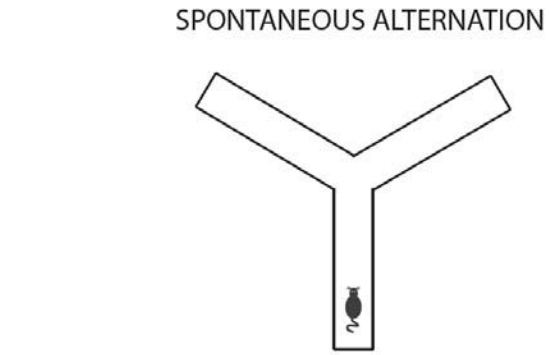
SPONTANEOUS ALTERNATION

B

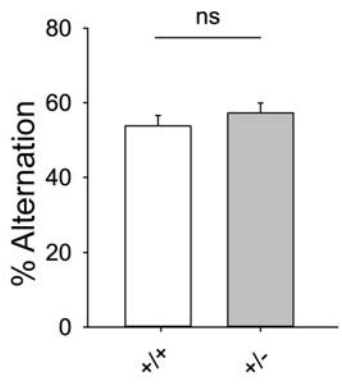
ns
80
60
40
20
0
% Alternation
+/+
+/-

C

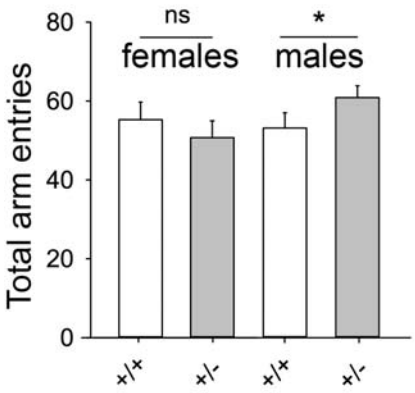
ns
*
females
males
80
60
40
20
0
Total arm entries
+/+
+/-
+/+
+/-

D

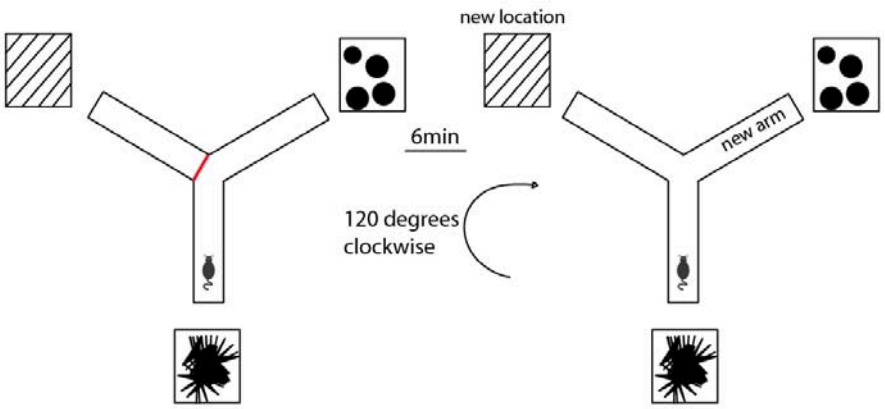
new location
6min
120 degrees
clockwise
new arm

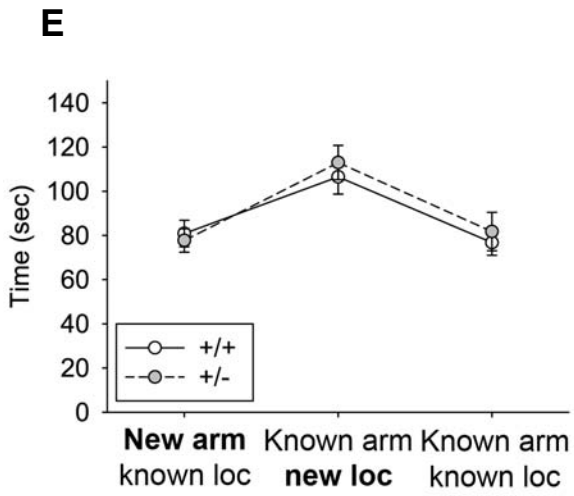

Figure 31 ***Heterozygous p60 katanin knockout does not alter spontaneous alternation behavior or spatial place recognition.*** The percentage alternation and total arm entries in the Y-maze continuous alternation task (A-C). Scheme of the Y-maze spatial recognition experiment (D). Both *p60+/+* and *p60+/-* mice spent more time in the arm located in the novel location (known arm, new loc) compared to previously explored arms (E). Data represented as mean +/- S.E.M. Two-way (Genotype and Sex) ANOVA, and Arms as repeated measures factor in Figure E.

5.1.17. A downregulation of p60 katanin does not affect cued fear conditioning

Previous studies have have linked adult neurogenesis to fear conditioning (Seo D.-O. et al., 2015; Glove L. R. et al., 2016), which is dependent on intact amygdala and hippocampus function (Marschner A. et al., 2008). In this respect, newborn neurons could be involved in this process by promoting the formation of new synaptic connections and facilitating the retrieval of fear memories. I therefore used auditory fear conditioning to test whether the decreased neurogenesis observed in p60 heterozygous *knockout* animals had an impact on the expression and extinction of fear memory (Fig. 32A and B).

During the context test performed 24 hours after conditioning, the freezing responses were similar for p60 +/+ and p60 +/- mice (Fig. 32C) indicating that long-term recent memory to contextual cues was intact despite p60 katanin downregulation. Exposure of the mice to the CS in the absence of the shock 48 hours after conditioning showed that fear retrieval in a neutral context (context B) was indistinguishable between the two genotypes (Fig. 32D). Likewise, continued exposure to the CS across 3 days (Fig. 32E and F) promoted successful and similar fear extinction levels for both genotypes (Fig. 32G). Finally, in a fear renewal protocol (Fig. 32E and F) performed in the traning context (context A) promoted recovery of freezing levels in a similar way for p60 +/+ and p60 +/- mice (Fig. 32H). This demonstrates that despite fear extinction, the previously acquired cued fear memory was retained in p60 +/- mice and taken together these findings indicate that lower levels of p60 katanin correlated with a decrease in adult neurogenesis, but are not sufficient to impair associative fear memory.

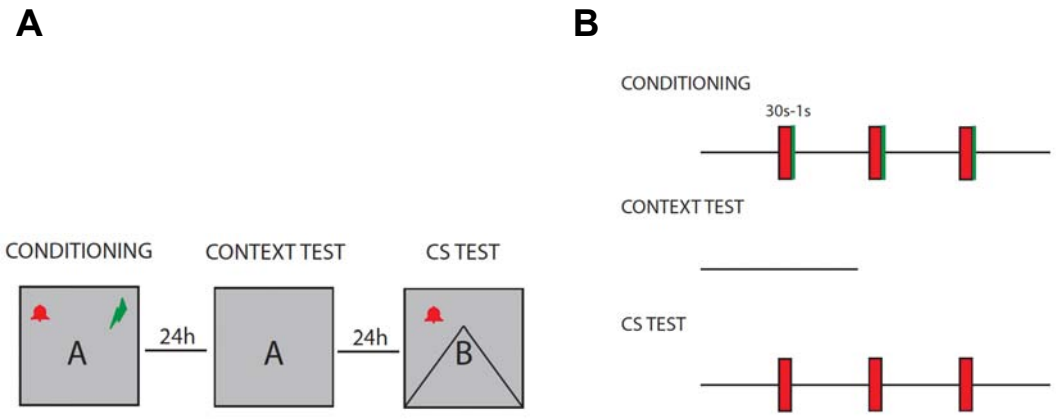

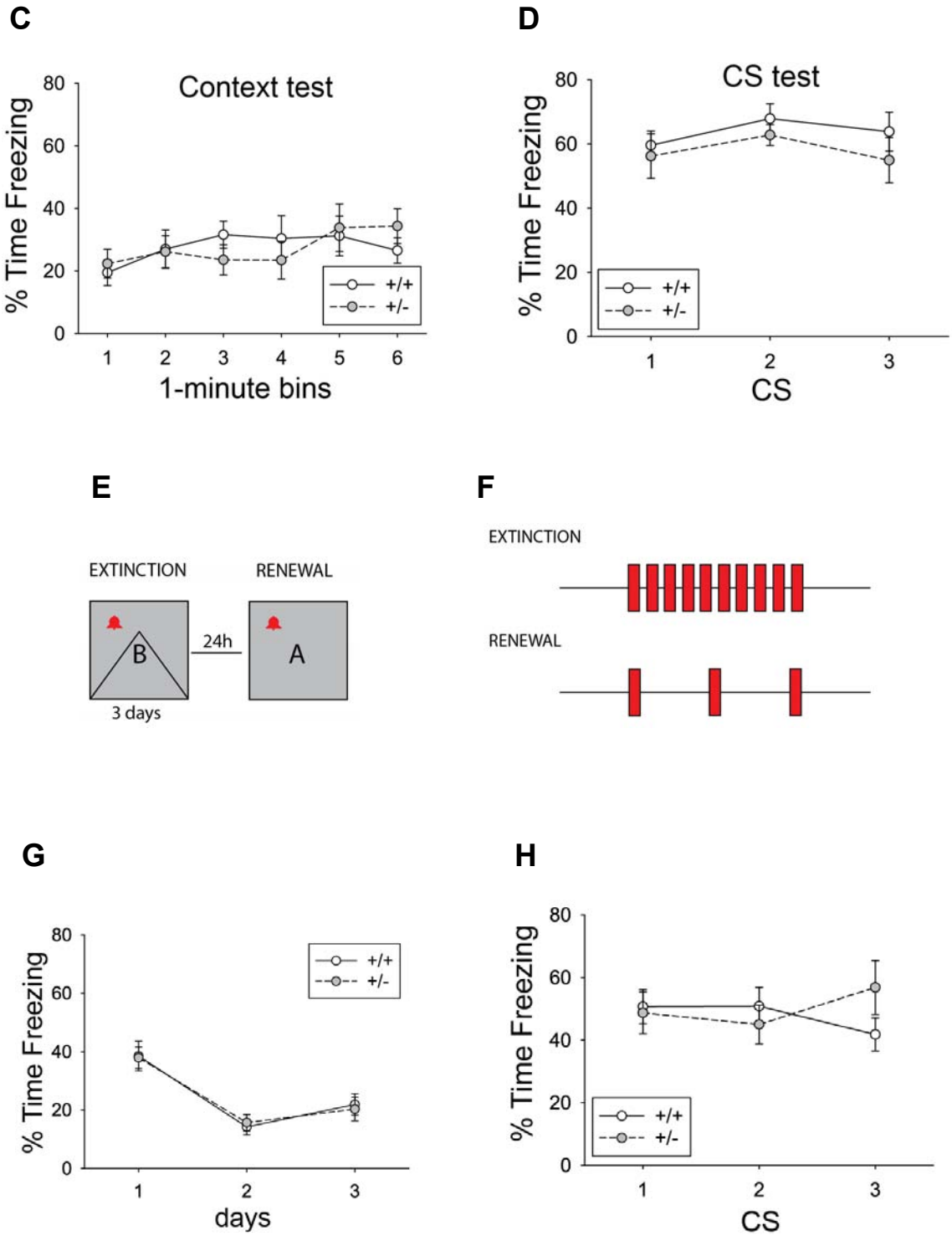

Figure 32 ***Cued fear conditioning is not affected in p60 +/- mice.*** Experimental protocol showing conditioning on day 1 in context A, a context test in context A on day 2 and a CS test in a neutral context B on day 3 (A). Red bars CS, Green bars US (B). No significant difference between genotypes in freezing levels was observed during context test (C) and CS test (D). No significant differences between genotypes across three days

of fear extinction (E, F and G) and in fear renewal when the mice were placed back in the original context A after fear extinction (E, F and H). Data represented as mean +/- S.E.M. Two-way (Genotype and Sex) ANOVA, with 1-min bins (C), CS trials (D and H) and Days (G) as repeated measures factors.

5.1.18. A downregulation of p60 katanin does not affect context discrimination in contextual fear conditioning

Context discrimination requires a functional hippocampus and it is thought that adult neurogenesis plays a major role in this process (Maren S et al., 1997; Saxe M.D. et al., 2006). To test whether a downregulation of p60 katanin could impact this process, contextual fear conditioning was performed and the ability of p60 +/+ and p60 +/- mice to learn and retrieve contextual memories was assessed. The mice were also tested for their capacity to distinguish between safe and aversive contexts (Fig. 33A). . The results showed a marginal decrease in learning the association of the shock to the context on Day 1 (Fig. 33B), but p60 +/- mice could distinguish safe and aversive contexts in similar ways as controls on Day 2 (Fig. 33C and D). These observations suggest that during acquisition, delayed neurogenesis in p60 +/- mice may consequently slow the rate of context-dependent learning, which requires rapid recruitment of newly generated neurons and formation of new synaptic connections. However, p60 katanin downregulation delays but does not impact the maturation and intergration of new neurons into the network, which may be sufficient to support context discrimination.

A

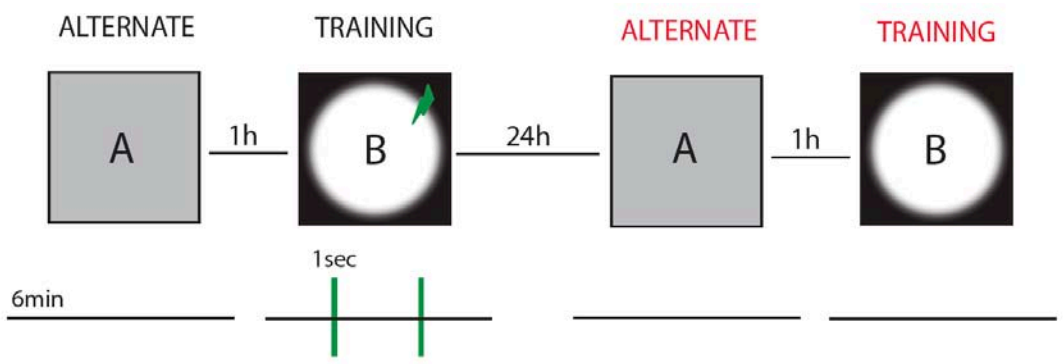

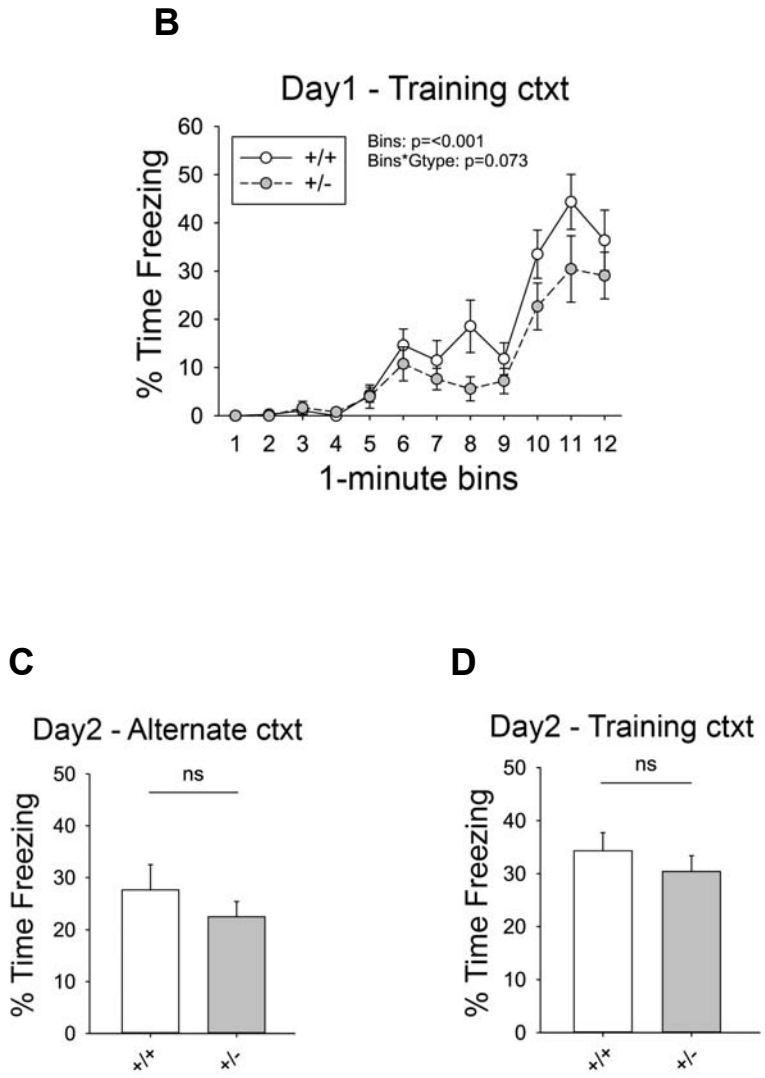

Figure 33 ***P60 katanin heterozygous knockout mice (+/-) show a marginal decrease in conditioned acquisition to contextual cues but normal context discrimination*** (A) Experimental protocol in which mice were first exposed to context A (alternate) and one hour later to a different context B (training) where they received two shocks (US). 24 hrs later, mice were returned first to context A and then context B (no shock) one hour later. On day 1 of training, p60 +/- mice showed a marginally significant decrease in conditioned aqusition (B). P60 +/- mice showed similar freezing responses as p60 +/+ control mice in context discrimination (safe versus aversive contexts) on day 2 (C and D). Data represented as mean +/- S.E.M. Two-way (Genotype and Sex) ANOVA, with 1-min bins (B) as repeated measures factors.

5.2. P60 katanin function in adult neurons

5.2.1. Expression of a dominant negative p60 katanin lacking ATPase function

In order to elucidate the role of p60 katanin in adult neurons, developmental effects present in p60 katanin heterozygous *knockout* animals had to be avoided. For cell biology experiments, I made use of plasmids kindly donated by prof. Francis J. McNally. The plasmids EGFP-p60-wt (p60-wt) and EGFP-p60-DEID (p60-DEID) were previously published by McNally's group (McNally K.P. et al., 2000). In p60-DEID, p60 katanin carries a mutation on its AAA-ATPase domain that inhibits ATP hydrolysis while bound to MTs, acting as a dominant negative on the wildtype endogenous katanin (McNally K.P. et al., 2000). Sequencing of p60-DEID confirmed the presence of the D308>Q and E309>Q mutations (Fig. 34A). To assess expression of the construct, I overexpressed p60-wt and p60-DEID in N2A cells (Fig. 34B). Notably, I observed cytoplasmatic localization of both constructs with enrichment in what appears to be the centrosome. Transfection in hippocampal neurons at different stages across our study was also performed.

A

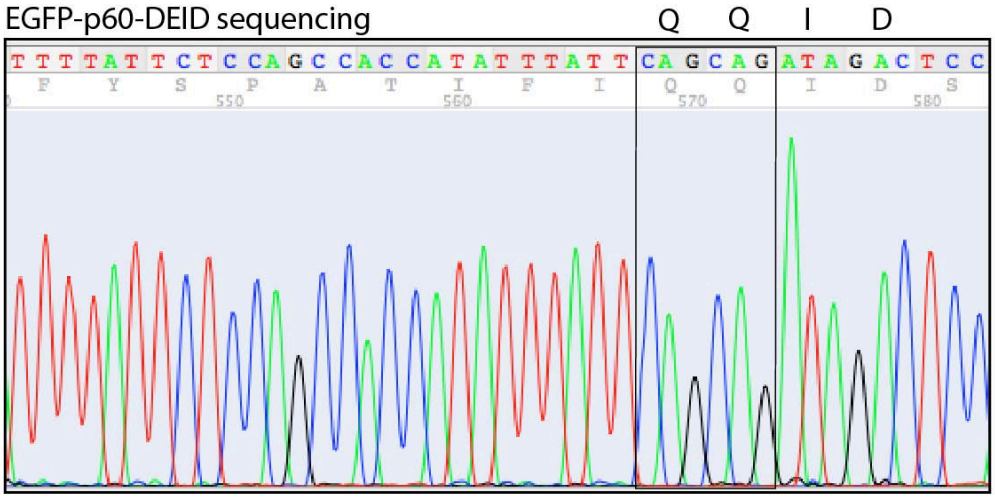

B

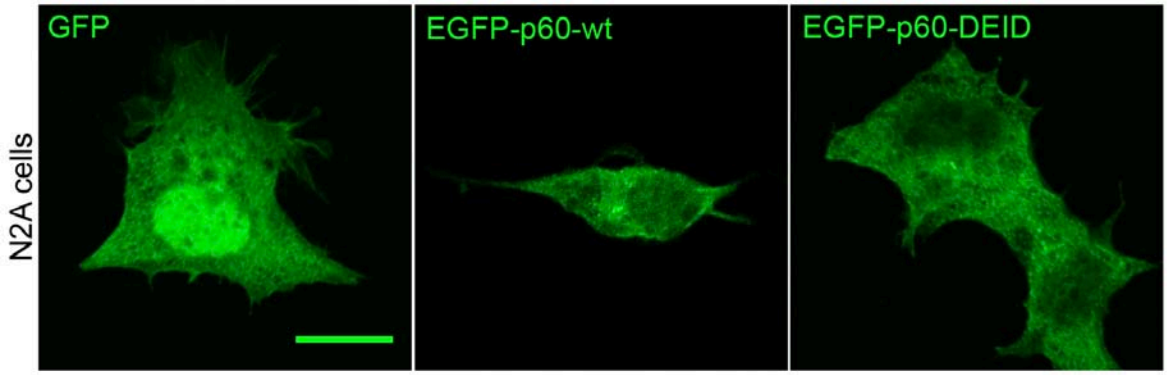

Figure 34 ***EGFP-P60-DEID clone is successfully transfected in cell lines.*** Sequencing analysis of EGFP-p60-DEID construct received from McNally F.J. shows substitution of D308>Q and E309>Q as described in McNally K. P. et al., 2000 (A). Qualitative fluorescence images in N2A cells demonstrated a correct expression of the clone kindly donated by McNally F.J. (B).

5.2.2. Dominant negative p60 katanin (p60 DEID) localizes to MTs

It was previously reported that the ATPase activity of the p60 subunit is the driving force for MT depolymerization but it is not required for MT binding (McNally F. J. and Vale R. D. 1993). I therefore to assessed whether p60-DEID localized to neuronal MTs. Results showed that p60-DEID overexpressing neurons show distribution of p60-DEID along MT filaments. Interestingly, katanin did not decorate the filaments entirely but appeared to have avidity for specific regions of the MT filaments (Fig. 35). It is likely that p60-DEID-positive regions on MTs are those that contain highly acetylated Tubulin (Sudo H. and Baas P.W. 2010), or represent Tau-free fragments of MTs (Qiang L. et al., 2006). Further testing in this direction is worthwhile in order to pursue this hypothesis because upstream regulation of p60 katanin is still under investigation. In this study however, I focused on the downstream effects upon inhibition of p60 katanin function, with particular attention to MT dynamics, cargo transport, and synaptic roles in mature neurons.

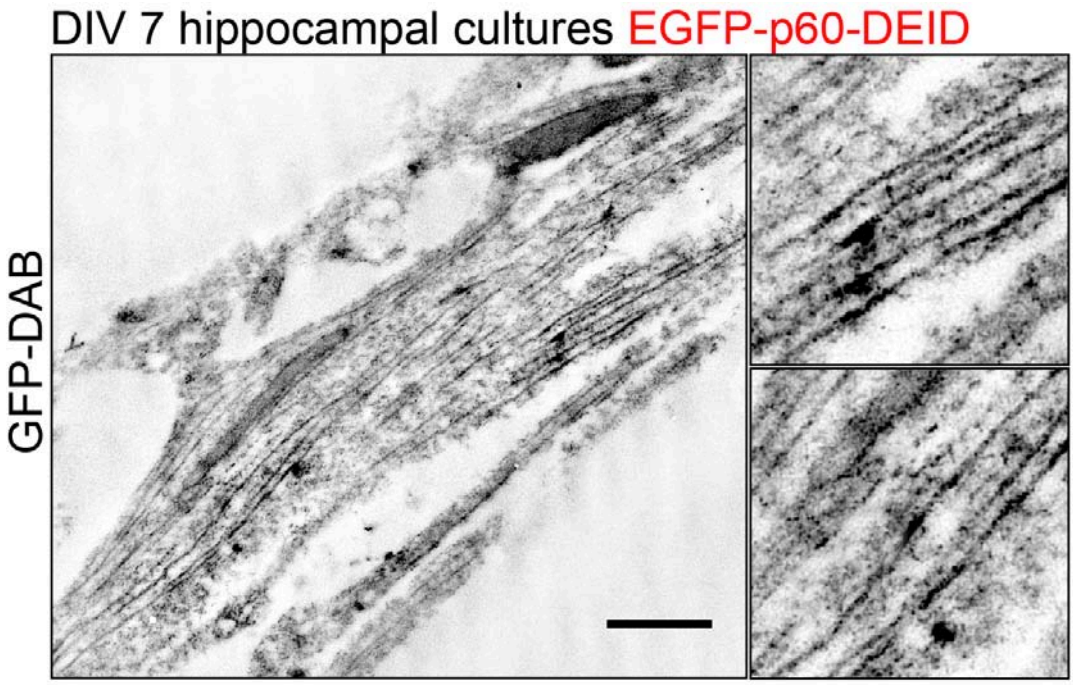

Figure 35 ***EGFP-p60-DEID decorates neuronal microtubules.*** Electron Microscopy micrographs of DIV7 primary hippocampal neurons overexpressing p60-DEID dominant negative for 24 hours and stained with α-GFP antibodies. 500nm ScaleBar

5.2.3. Dominant negative p60 katanin alters MT dynamics

Since the MT-severing activity of katanin has been reported to influence MT dynamics in *Arabidopsis thaliana* (Komis G. et al., 2017), the effects on MT dynamics after overexpression of p60-DEID in neurons *in vitro* was also tested. P60-DEID was overexpressed for 24 hours together with EB3-tomato. EB3 is a plus-end binding protein that enriches at the plus-end of growing microtubules (Su L. K. and Qi Y., 2001; Schuyler S. C. and Pellman D., 2001). During growth, an accumulation of EB3 at the +Tip of MTs results in a bright „comet“ that can be followed and traced (Gierke S. et al., 2010). When the filament stops growing, EB3 detaches and its fluorescence drops to background levels. Time-lapse microscopy was performed to test the speed of MT growth, which revealed that p60-DEID negatively affects MT dynamics and results in slower MT growth, consistent with a more stable MT structure (Fig. 36A and B).

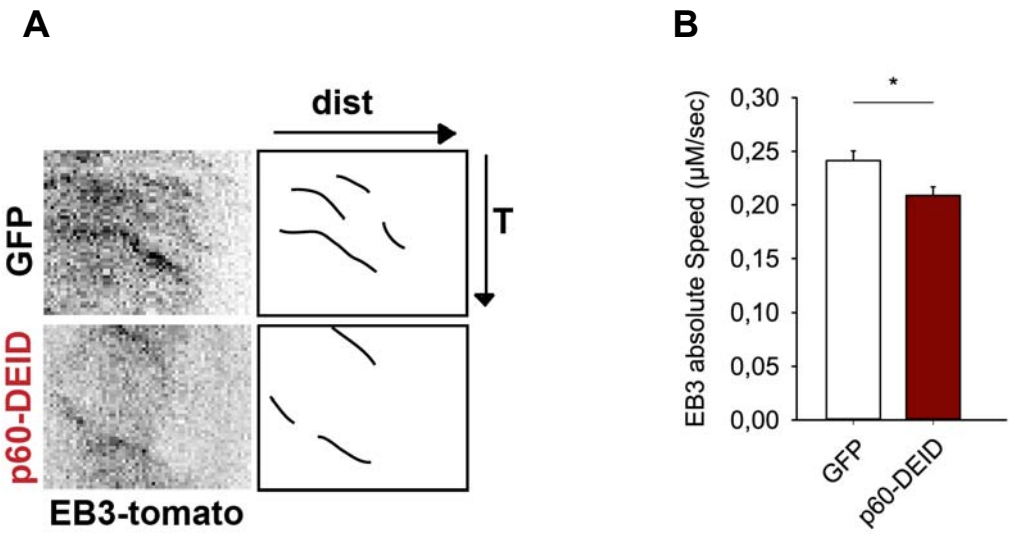

Figure 36 ***MT growth is affected upon p60 katanin inhibition.*** Kymograph showing distance and time of growing EB3 comets (A). Quantification shows a significant reduction in the absolute MT growing speed, consistent with an overall more stable MT network (+/+) = 0.241±0.009; (+/-) = 0.209±0.007. N=3. Data represented as mean ± S.E.M. * p<0,05. Independent samples T-test (Two-tailed). (B).

5.2.4. Dominant negative p60 katanin alters mitochondria displacement

Based on their properties and interaction partners, MTs can regulate intracellular transport (Franker M. A. M. and Hoogenraad C. C. 2013) and it was shown in this study that inhibition of p60 katanin function alters MT dynamics (Fig. 36). In order to test if altered MT dynamics may impact general cargo transport, mobile mitochondria in neurons were tracked using time-lapse microscopy. I made use of Mitotracker CMXRos, a dye that penetrates the plasma membrane and specifically labels mitochondria. Time-lapse imaging performed 48 hours after transfection revealed that the speed of mitochondria displacement in axons of young neurons was enhanced (Fig. 37A and B). This result indicates that the regulation of the MT cytoskeleton by p60 katanin is an important process for intracellular-cargo distribution. Here, I studied mitochondria as a general indicator of cargo

displacement, although different results for other neuronal cargoes cannot be excluded.

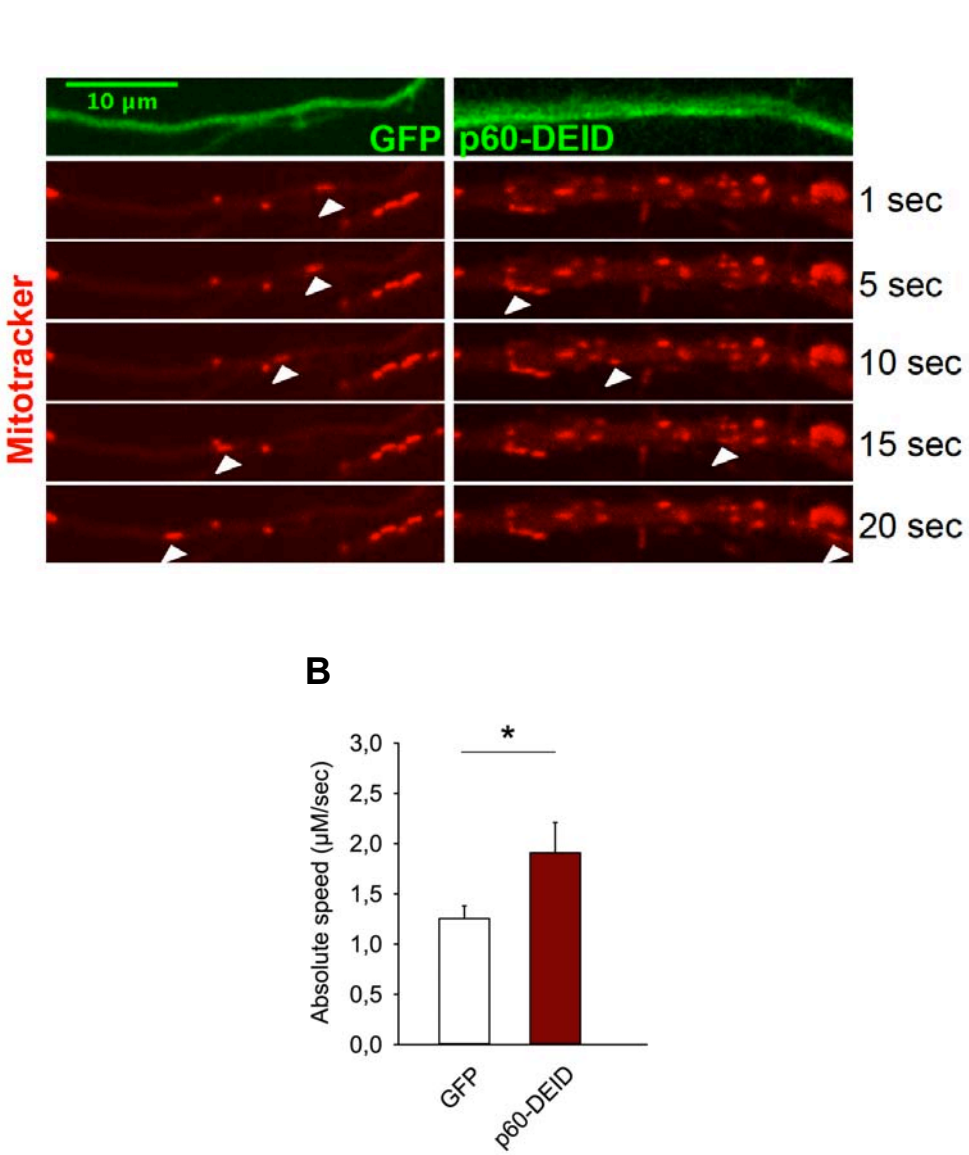

Figure 37 ***Mitochondrial displacement is significantly faster in p60-DEID overexpressing neurons.*** Mitotracker labeled mitochondria in young neurons shows a faster displacement in axons (A and B). Data represented as mean ± S.E.M. * p<0,05. Independent sample T-test (Two-tailed). (B).

5.2.5. Generation of time- and region-specific conditional knockout mice for p60 katanin

In the first part of this study, I showed that p60 katanin was involved in brain development and in the generation of new neurons in the SGZ of the adult dentate gyrus. In the second part, the relevance of p60 katanin in MT dynamics and cargo trasport was shown. However, functions of katanin in adult neurons and specifically at synaptic compartments of are currently unknown. MT-severing is a critical mechanism involved in many subcellular functions, including intracellular trafficking of cargoes and structural modifications of subcellular structures (De Brabander M. J., 1982; Franker M. A. M. and Hoogenrad C. C., 2013). In order to elucidate the role of p60 at synaptic compartments, previously generated floxed mice for exons 6 and 7 of the *Katna1* gene (Fig. 38A) were crossed with CRE-driver mice under the *CamKII-*α promoter (*CamKII-*α-CRE) (Tsien J. Z. et al., 1996). Characterization of these mice showed a high expression of CRE in the hippocampal CA1 region of *CamKII-*α-CRE animals, which peaks at post-natal day 21 (p21) (Tsien J. Z. et al., 1996). Taking this into account, p60 conditional knockout mice (CRE-katna1 fx/fx) were generated, overcoming developmental defects associated with constitutive depletion of p60 katanin. In order to validate this model, I tested if p60 katanin protein levels were reduced in the hippocampus of CRE-katna1 fx/fx mice. Western blot from hippocampal lysates showed a decrease but not complete ablation of p60 katanin (Fig. 38B). Since CRE expression was shown to occur mainly in CA1 pyramidal neurons (Tsien J. Z. et al., 1996), it is unlikely that total depletion of p60 katanin could be achieved in the entire hippocampus. As a result, p60 katanin depletion is diluted in biochemical experiments due localized CRE expression in a particular hippocampus area, including the mosaic expression pattern of CRE. This limits the use of CRE-katna1 fx/fx mice to electrophysiological experiments where network activity was assessed.

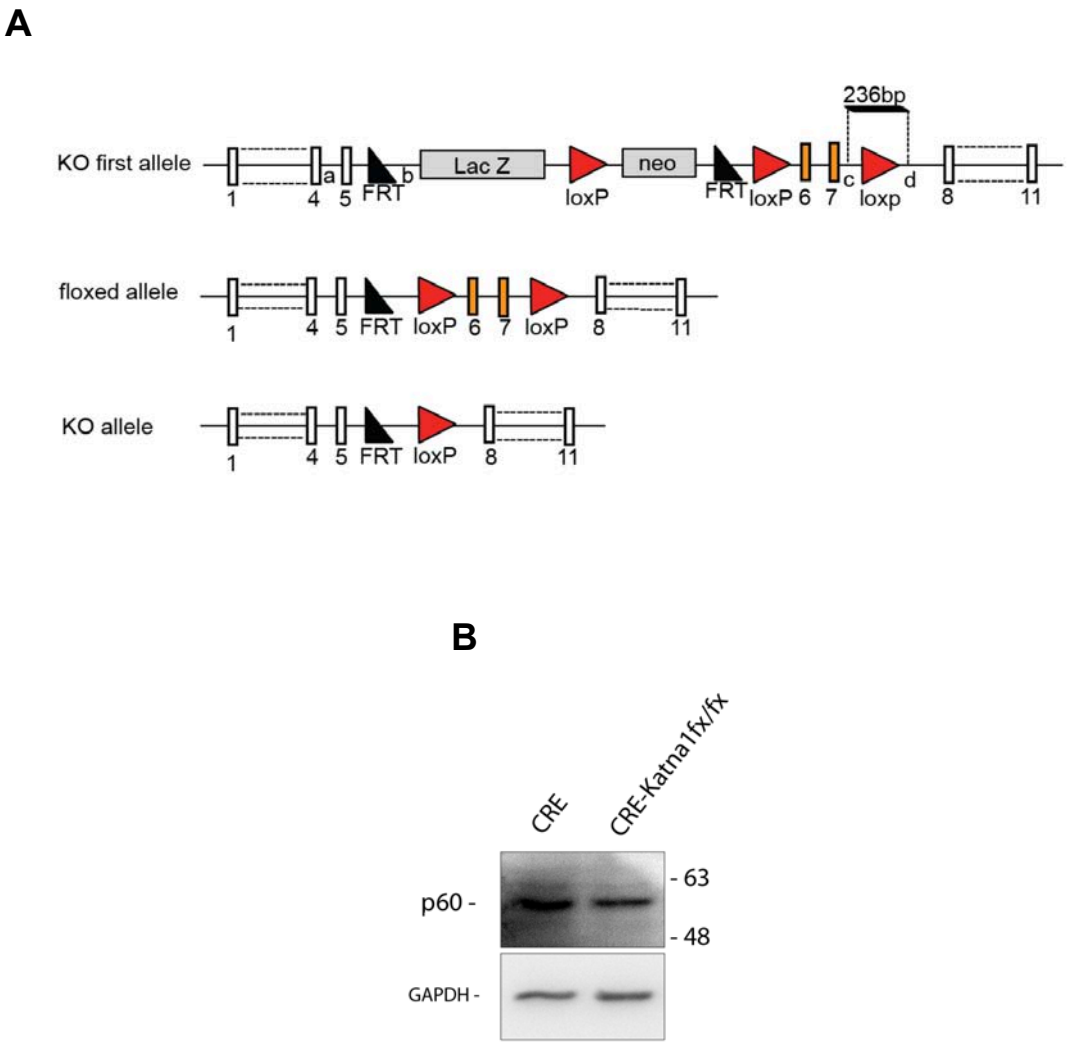

Figure 38 ***Generation and validation of CamKIIa-CRE-katna1fx (CRE-katna1 fx/fx) conditional knockout animals.*** The *knockout first* allele is shown including the main features. Floxed allele after flippase and KO allele after CRE recombinase are also shown. After CRE recombination, exons 6 and 7 from *katna1* gene are depleted. Binding sites for genotyping oligos are also represented. In the KO allele, binding sites for genotyping oligos are conserved (A). Western Blot showing a reduction of p60 katanin protein expression in the hippocampus of CRE-katna1 fx/fx mice (B).

5.2.6. Conditional knockout animals for p60 katanin show an increase in the early phase of Long-Term Potentiation at Schaffer collateral synapses

In an attempt to dissect p60 katanin function in the adult brain, I first tested if the capacity of p60-depleted neurons in showing Long-Term Potentiation (LTP) was

impaired. LTP is a form of synaptic plasticity that is associated with learning and memory (Lømo T., 1966; Bliss T. V. P. and Lømo T. 1973). LTP expression depends on kinase activity, protein synthesis and structural modifications, which results in stronger synaptic connections that persist across time (Lee Y. S. and Silva A. J., 2009; Lisman J. et al., 2018). To dissect p60 katanin functions at synaptic compartments, Field Potential recordings in the Schaffer collateral pathway of the CA1 region of the hippocampus were performed. Recordings showed a significant increase in the induction (initial minutes) of LTP but no significant changes in LTP expression for up to 180 minutes after stimulation (Fig. 39A and B). Notably, LTP induction depends on the amount of neurotransmitter released at the synaptic cleft by the pre-synaptic terminal (Schulz P. E. et al., 1994) and on the properties of the post-synaptic spine before the stimulation is delivered (Dong C. et al., 2008). Although it was not possible to exclude a pre-synaptic effect because of minor CRE expression in CA3, it is likely that changes in LTP induction were mainly due to differences in the post-synaptic compartment, were p60 katanin was mainly ablated. This result was the first evidence for a synaptic role of p60 katanin in synaptic plasticity.

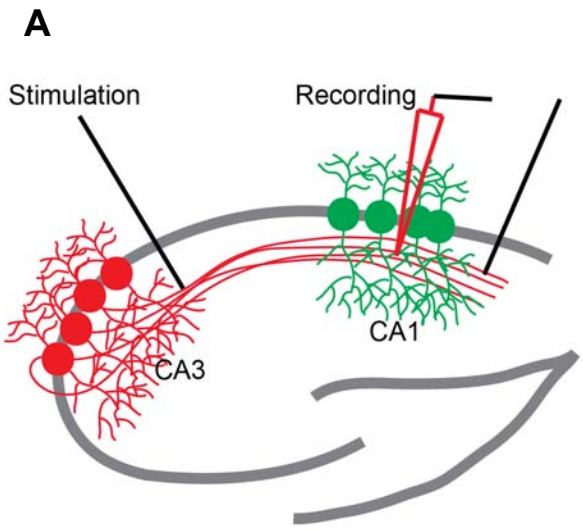

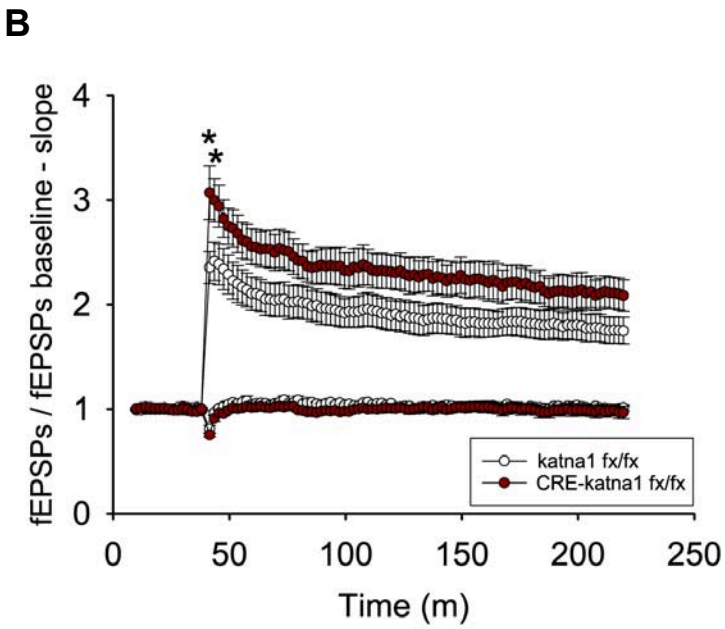

Figure 39 ***Conditional depletion of p60 katanin alters LTP induction at Schaffer collateral CA1-to-CA3 synapses.*** Schematic cartoon depicting stimulation and recording electrodes in Shaffer Collaterals of the hippocampus (A). LTP recordings were performed for 180 minutes upon Theta burst stimulation (TBs). Conditional knockout animals (CRE-katna1 fx/fx) showed an increase in the induction of LTP when compared to control animals (katna1 fx/fx) (A and B). Data represented as mean +/- S.E.M. * p<0,05.

5.2.7. P60-wt and endogenous p60 katanin shows localization to dendritic spines

The electrophysiological data suggested that p60 katanin is involved in synaptic plasticity, specifically during the induction of LTP. In the following experiments, I aimed to dissect the molecular mechanisms that underscore this effect. To achieve that, I first overexpressed p60-wt (McNally K.P. et al., 2000) in hippocampal neurons in combination with Phalloidin, a marker for filamentous actin and therefore dendritic spines. In neurons, p60-wt displayed a cytoplasmic localization as previously observed in N2A cells (Fig. 34B), but was also detected in dendritic spines (Fig. 40A).

In order to verify p60-wt localization in dendritic spines, I stained for endogenous katanin in adult hippocampal neurons in combination with Phalloidin. The presence

of katanin in F-actin-enriched dendritic spines was confirmed (Fig. 25B). Quantification of the percentage of spines containing p60 katanin showed that around 97% of spines were positive for katanin fluorescence (Fig. 40C). This data supports previous studies that showed that a high amount of katanin diffuses in the cytosol (McNally K.P. et al., 2000) and highlights the presence of katanin in specific sub-cellular compartments. The low affinity binding of katanin to MTs, sufficient for p60 to achieve its severing activity (McNally F. J. et al., 1996) may be one reason for cytoplasmic localization of katanin. However, I hypothesized that p60 katanin may have active functions in specific subcellular compartments, including dendritic spines. The following experiments were performed in order investigate possible p60 katanin roles in dendritic spines.

A

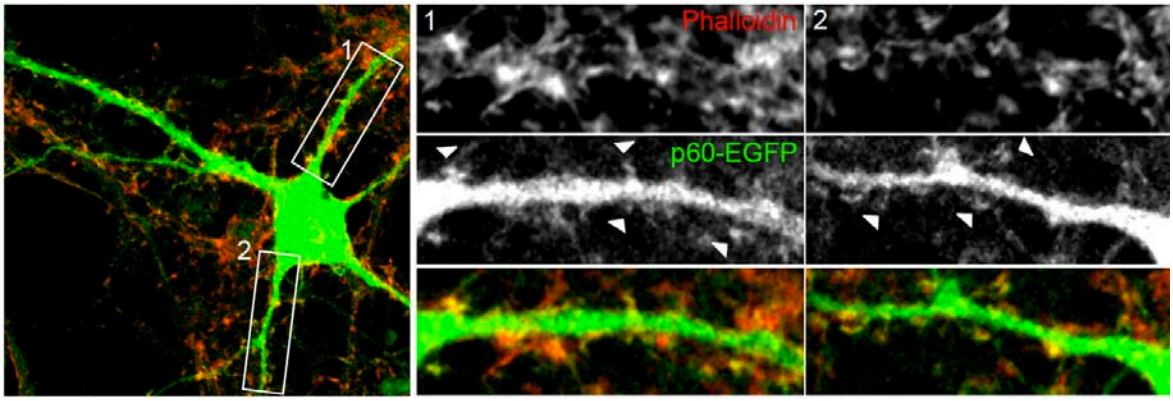

B

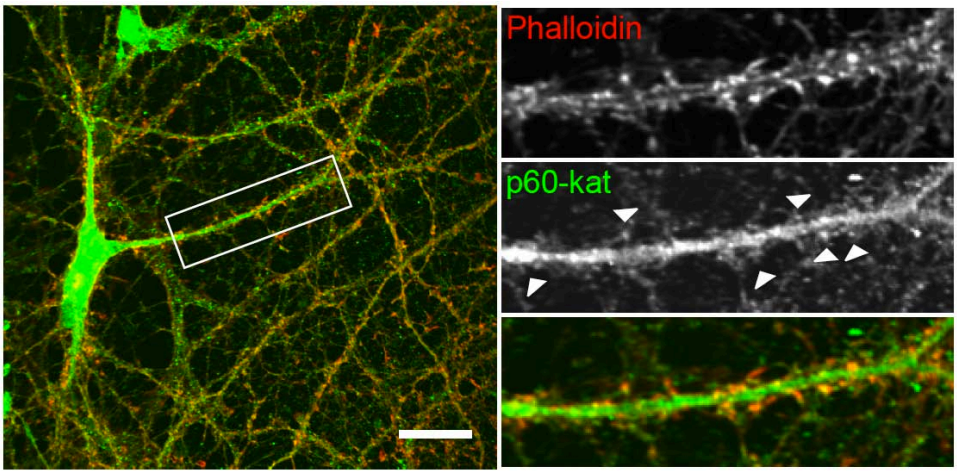

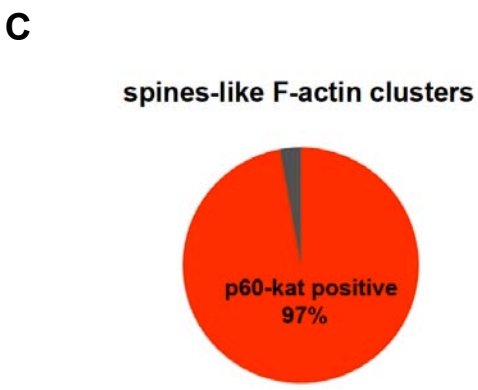

Figure 40 ***Overexpressed p60-wt and endogenous katanin are present in dendritic spines of hippocampal neurons.*** Fluorescence images of hippocampal neurons expressing p60-wt in combination with Rhodamine/Phalloidin staining to label dendritic spines (A). Hippocampal neurons were co-stained with Phalloidin as a marker for dendritic spines and p60 katanin antibody to observe endogenous localization (B). Quantification showed that nearly all the spines showed diffused p60 katanin staining (C).

5.2.8. Plus-tips of growing MTs are significantly decreased in dendritic spines of hippocampal neurons upon inhibition of p60 katanin function

Dendritic spines are cellular protrusions that receive inputs from pre-synaptic terminals at excitatory synapses (Hering H. and Sheng M., 2001). Growing MTs were shown to be ocasionally invade dendritic spines during synaptic plasticity (Jaworski J et al., 2009). However, the way MTs invade dendritic spines and how this process is regulated is not fully known.

In previous experiments, I showed that the speed of MT-growth is decreased upon inhibition of p60 katanin-mediated severing activity (Fig. 36). The presence of p60 katanin in dendritic spines led to the hypothesis that MT-severing might contribute to MT-invasion of dendritic spines. To test this hypothesis, I performed immunostainings for endogenous EB3 in DIV12 hippocampal cultures transfected for 48 hours with p60-DEID or control-GFP and td-Tomato as a volume marker (Fig. 41A). Quantification of the percentage of spines that were positive for EB3 showed a significant reduction of EB3-positive spines in neurons transfected with

p60-DEID (Fig. 41B), suggesting that p60 katanin promotes MT spine invasion under physiological conditions.

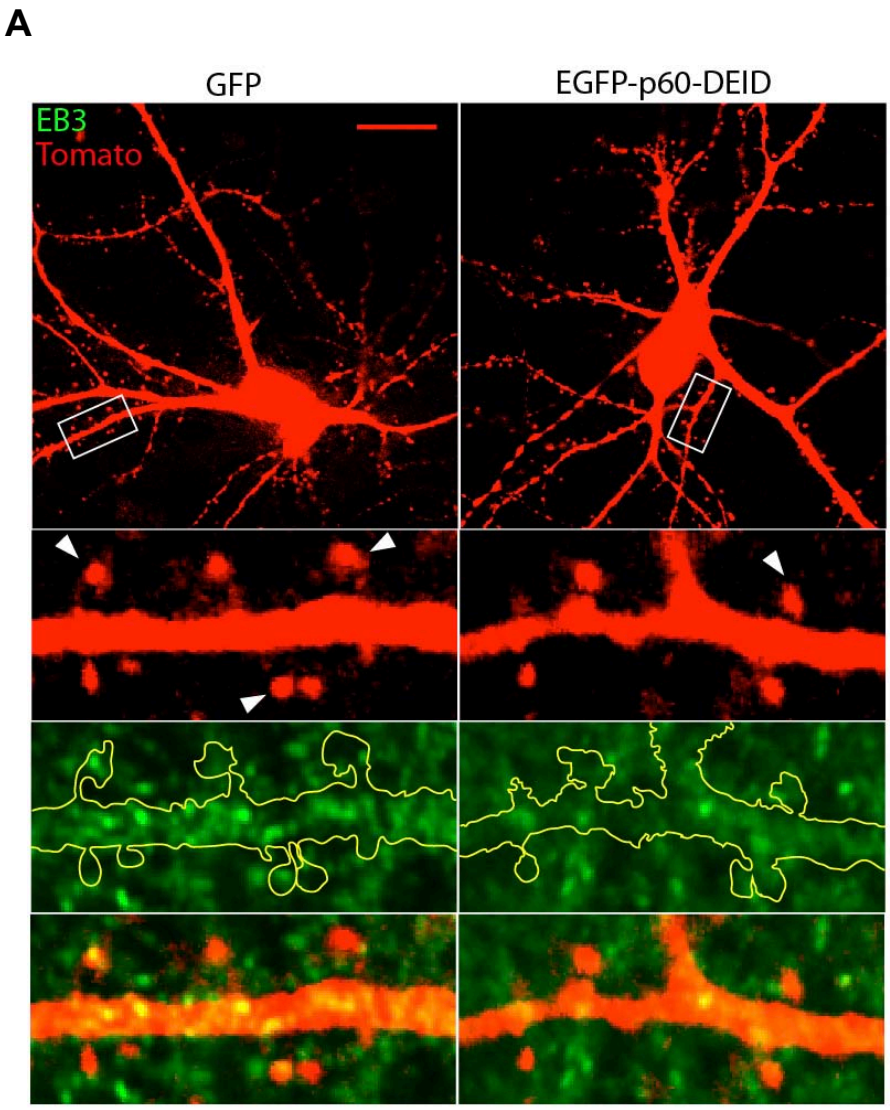

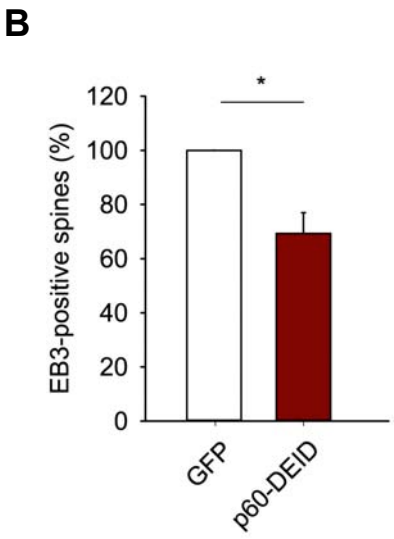

Figure 41 ***Inhibition of katanin decreases the number of MT-plusTips in dendritic spines.*** DIV12 hippocampal neurons transfected with EGFP-p60-DEID and GFP as a control, plus Tomato as a volume marker, were stained with EB3 antibody (A). Quantification shows a significant decrease of EB3 puncta in dendritic spines upon inhibition of p60 katanin function, suggesting that MT severing by katanin enhances MT entry in dendritic spines (B). N= 3 indipendent experiments, 1604 spines total, (GFP) 43 cells, (p60-DEID) 26 cells. (GFP)= 100%, (p60-DEID)= 80.94%, 54,91%, 72.21%. Data represented as mean +/- S.E.M. * p<0,05. Independent sample T-test (Two-tailed). 20mM Scale bar.

5.2.9. Spine area and number are not altered upon p60 katanin inhibition

It was previously shown that MT cytoskeleton is involved in spine formation (Gu J. et al., 2008; Gu J. and Zheng J. Q. 2009). In order to elucidate the impact of p60 katanin inhibition on spine morphology and number, hippocampal neurons were transfected with p60-DEID (Fig. 42A). Interestingly, neurons overexpressing p60-DEID showed comparable number of dendritic spines and spine size was not altered when compared to GFP transfected neurons (Fig. 42B and C). These results indicate that a decrease in MT +Tip invasion of dendritic spines due to transient overexpression of p60-DEID has minimal impact on spine morphology

under basal conditions. So far in this study, MT-severing activity of katanin was shown to be involved in processes like cell division or cell migration where massive morphological changes occur; or in intracellular transport where the MT network is required for proper distribution of different cargoes in the cell. Both scenarios are known to depend on dynamic MTs. Since the data presented here was obtained in neurons in their steady state, is likely that a more pronounced impact of p60 inhibition could be observed under conditions that require extensive re-organization of the cytoskeleton in spines.

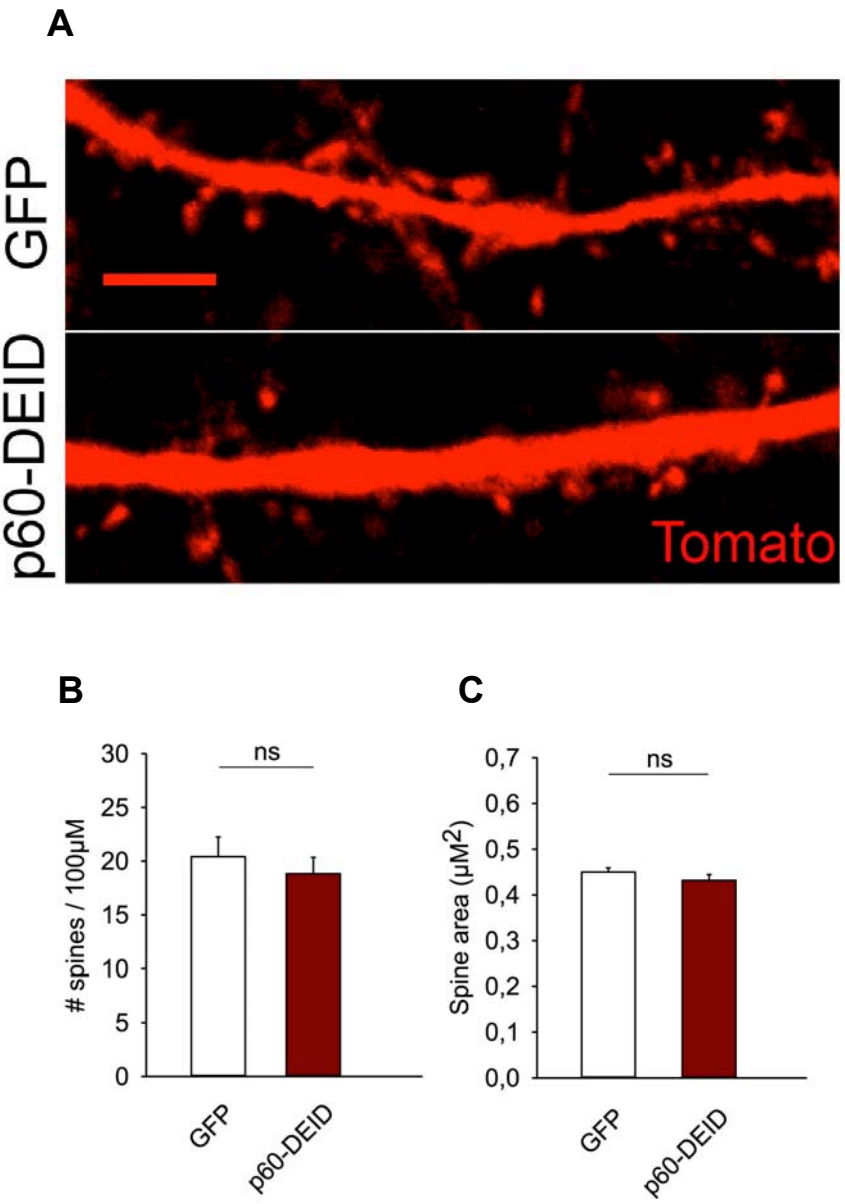

Figure 42 ***Inhibition of p60 katanin does not alter dendritic spine area and number.*** Representative image showing td-Tomato volume marker (A). Quantification of the number and the area of dendritic spines show no significant changes upon p60-DEID overexpression (B and C). Data represented as means ± S.E.M. Independent sample T-test. Scale Bar 5µM.

5.2.10. Katanin p60 is involved in structural plasticity

Synaptic plasticity involves modifications of previously formed synapses or the formation of new connections and these changes are related to learning and memory (Bailey A. H. and Kandel E. R., 1993). It was shown that LTP promotes spine growth (Yang Y. et al., 2008). Dynamic MTs are known to enter dendritic spines (Gu J. and Zheng J. Q., 2009) and some have hypothesized that these events are connected to post-synaptic re-arrangements during plasticity (Hoogenraad C. C. and Akhmanova A. 2010). In order to assess the role of p60 katanin on spine remodeling during neuronal activity, local stimulation of dendritic spines using 2-photon glutamate uncaging was performed. The goal was to determine whether a decreased MT-invasion observed in p60-DEID transfected neurons had an impact on spine structural plasticity. The experiment showed that GFP control transfected neurons grow significantly upon glutamate uncaging, while p60-DEID overexpressing neurons fail to undergo structural changes (Fig. 43A and B). At first glance, this data appears to contradict the observation of enhanced induction during LTP (Fig. 39). However the binding of p60-DEID to MTs may also block access to tubulin for katanin-like proteins, leading to a stronger dominant negative effect when compared to CRE-katna1 fx/fx mice. These results underline the importance of MT-entry in dendritic spines and directly connect p60 katanin to synaptic plasticity. Notably, substantial rearrangements of the actin cytoskeleton are known to take place in the post-synaptic compartments when spines undergo structural modifications (Lin B. et al., 2005). Therefore, these results support the idea that dynamic interactions between the actin and the MT cytoskeletons play a key role during plasticity.

A

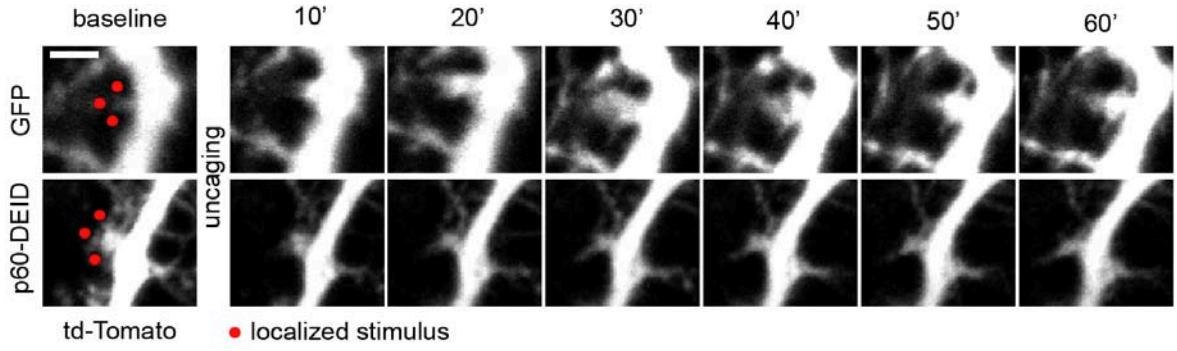

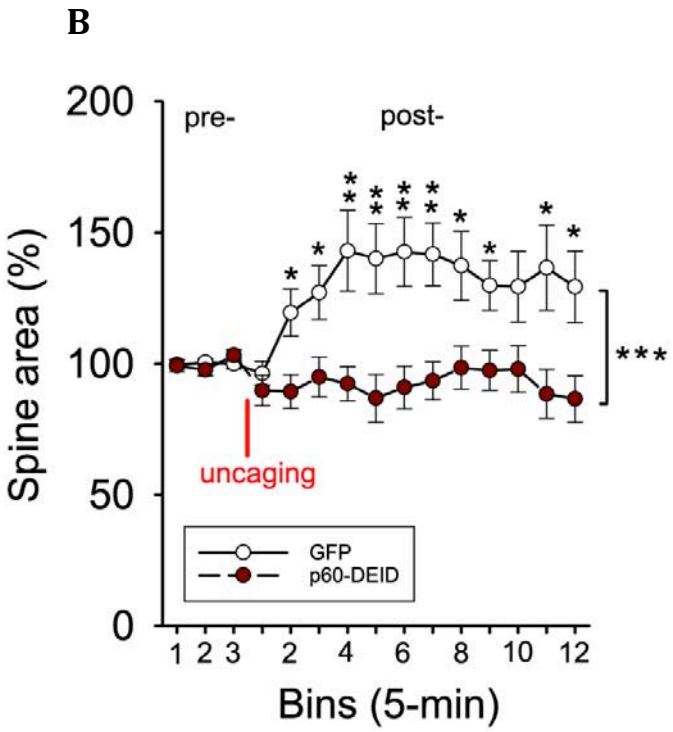

Figure 43 ***P60-DEID overexpressing neurons show altered structural plasticity upon glutamate uncaging.*** Local stimulation of dendritic spines with 2-photon glutamate uncaging (A). Quantification shows a baseline of three time points before uncaging and twelve time points (five minutes each) after stimulation. GFP-overexpressing neurons displayed a significant growth after uncaging, while P60-DEID neurons do not show spine growth. *** p<0,001. Two-way (condition x 5-min bins) ANOVA. Repeated measures. * p<0,05, ** p<0.01. Independent samples T-test (Two-tailed) (B). 5μM Scale bar.

5.3. Katanin p60 in the context of disease

5.3.1. Katanin expression in Tau transgenic animals

Tau is a MAP that binds microtubules (Weingarten M.D. et al., 1975). It has been hypothesized that upon MT binding, Tau protects MTs from depolymerization by

MT-severing enzymes like katanin (Qiang L. et al., 2006). Besides, since many years Tau was connected to different kinds of neurodegenerative diseases like Alzheimer's disease (AD) (Goedert M. et al., 1988), Frontotemporal Dementia (FTD) (Hutton M. et al., 1998), and Pick disease (Pickering-Brown S. et al., 2001). In disease conditions, Tau appears to be hyperphosphorylated and aggregates in the form of tangles (Goedert M. et al., 1988; Biernat J. et al., 1992). One key mutation in Tau is P301L. This mutation was first characterized in FTD patients (Hutton M. et al., 1998) and has been shown to affect tau properties on MT (Rizzu P. et al., 1999) and leads to cognitive impairments in mice (Ramsden M. et al., 2005). I assessed if under pathological conditions, p60 katanin could be differentially regulated. I used lysates (kindly donated by Prof. Mandelkow E.) from transgenic mice expressing human Tau that harbours the P301L mutation (rTg(tau_{P301L})4510 mice) and performed western blot analysis of p60 katanin expression. Interestingly, p60 katanin was significantly downregulated in Tau transgenic animals (Fig. 44A and B).

A

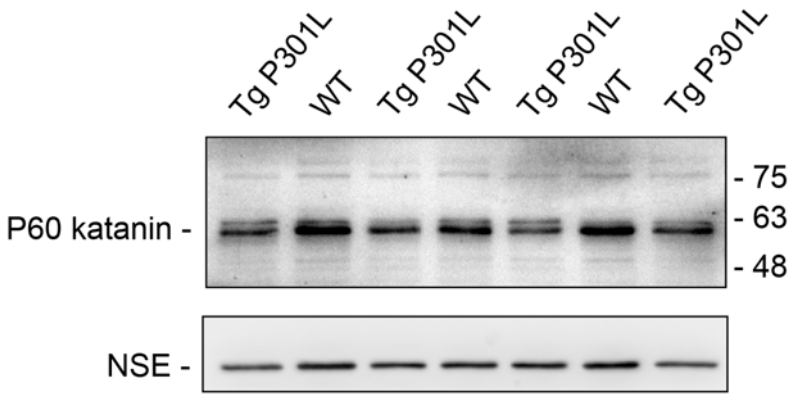

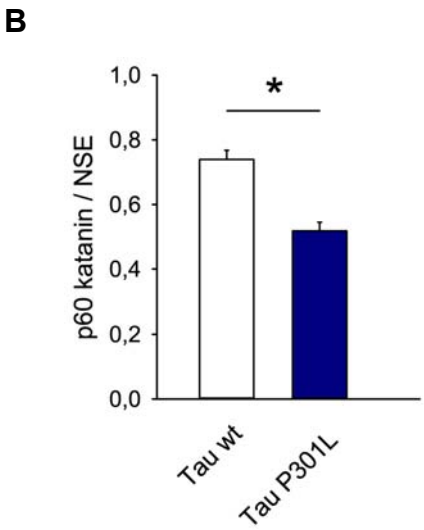

Figure 44 ***Tau transgenic animals show a decrease on p60 katanin expression.*** Hippocampal lysates from 11 months animals show a significant decrease in p60 katanin expression (A and B). N= (wt) =3; (P301L) =4. (wt)= 0.74±0.03, (P301L)= 0.52±0.03. Data represented as means ± S.E.M. p<0,05 *. Independent sample T-Test (Two-tailed).

6. Discussion

The first aim of this study was to investigate the roles of the catalytic subunit of katanin, p60, during embryonic development and adult neurogenesis. For that, I made use of an animal model that was constitutively depleted of the catalytic subunit of katanin, p60. Since full constitutive ablation of p60 led to embryonic lethality, heterozygous knockout mice were used. Focus was primarily on embryonic corticogenesis and adult neurogenesis.

P60 katanin is also expressed in the adult brain (Yu W. et al., 2014) but little is known about its function. Therefore the second aim was to elucidate the roles of p60 katanin in mature neurons. In order to address this, p60 katanin floxed animals were crossed to a time- and region-specific CRE recombinase-driver line to dissect the role of MT-severing by p60 katanin in the adult brain. This, together with the use of a dominant negative ATPase-deficient construct, allowed the dissociation of p60 katanin roles in development from its functions in the adult brain. The following sections provide a detailed discussion about the key findings presented in this study.

6.1. P60 katanin is fundamental for embryonic survival

Following the generation of a constitutive *knockout* mouse for the catalytic subunit of katanin, I could not obtain homozygous *knockout* pups. Although tissue from full *knockout* embryos was isolated, the fetuses were already dead and partially digested and this is presumably due to katanin function in cell division. During cell division, mitotic or meiotic spindles are formed (Inoue' S. and Sato H. 1967). Stable MTs have been shown to be severed by mitotic extracts from Xenopus (Vale R.D. 1991), suggesting that in these preparations, key components for MT-severing were present. Besides, p60 katanin depletion leads to polynucleated cells, indicating that the cell cycle is blocked (Matsuo M. et al., 2013). Katanin localizes to the spindle pole and mediates cytoskeletal rearrangements during cell division (McNally K. P. et al., 2000) and shortening of the spindle during mitosis and meiosis (McNally K. et al., 2006). Indeed, during anaphase, the length of the spindle is important for sister chromatide separation (Liang F. et al., 2013). Last

but important is the fact that mice carrying a missense mutation in the regulatory subunit of katanin, p80, produce a significantly smaller number of spermatocytes, supporting the role of katanin in proliferation (O'Donnell L. et al., 2012), while a full depletion of p80 katanin causes embryonic lethality in mice (Hu W. F. et al., 2014). Based on these evidences, I connected the lack of p60 homozygous *knockouts* in my study to a fundamental role of katanin during embryonic cell division.

6.2. P60 katanin is required for proper neuronal development

In this work, during neuritogenesis *in vitro,* neurons from p60 +/- mice displayed an array of non-canonical morphological features. These consisted of lamellipodia-like structures instead of well-defined dendrites and blobs possibly formed by bundles of un-severed MTs, plus a wrapped disposition of the axon. These findings demonstrated that neuronal development *in vitro* was impaired in p60 heterozygous *knockout* neurons.

The morphology of neurons is a key factor in the context of their electrical properties and subsequent connectivity. It was shown that neurons are rounded during initial stages of development and then start forming axon and dendrites (Dotti C.G. et al., 1988). During this process, the re-organization of the MT cytoskeleton plays a fundamental role. One critical player in orchestrating the MT architecture is the centrosome (Mazia D. 1984; reviewed by Kuijpers M. and Hoogenraad C.C. 2011). MT minus-ends are attached to the centrosome while their plus-ends point away from it (Nguyen M. M. et al., 2011). De Anda and colleagues have shown that the localization of the centrosome determines the position of the future axon (De Anda F.C. et al., 2005), and centrosomal motility is also required for axonal formation in cortical neurons (De Anda F.C. et al., 2010). A well-established function of katanin is to sever MTs in an ATP-dependent manner (McNally F.J. and Vale R.D. 1993). Katanin has been shown to target the centrosome in early studies by Hartman and colleagues (Hartman J.J. et al., 1998) and severing of MTs by katanin has been reported to occur also at the minus-end of MTs (Jiang K., et al., 2017). Importantly, local stabilization of the MT cytoskeleton is required in the neurite that eventually becomes the future axon (Witte H. et al., 2008).

Although not addressed in the present study, it is possible that upon downregulation of p60 katanin, MT-severing at the centrosome is impaired during early stages of neuronal development. As a consequence, the dynamics of the entire MT network are impaired, thus altering the characteristics of different sub-populations of MTs and having an impact on overall morphology during development.

6.3. Katanin p60 downregulation leads to an accumulation of cells in the progenitor niche during corticogenesis and adult neurogenesis

Previous studies have linked katanin to cell migration (Zhang D. et al., 2011; Eom T. Y. et al., 2014). The regulatory subunit of katanin (p80) was shown to be involved in neuronal migration (Jin M. et al., 2017) and mutations in KATNB1, the gene that encodes for p80, have been linked to microlissencephaly (Hu W. F. et al., 2014). Interestingly, some of these mutations alter the WD40 domain of p80 katanin, which targets the severing-complex to the centrosome (Hartman J. J. et al., 1998). It was demonstrated that p60 katanin is expressed in RGCs or newly generated neurons in the developing cortex (Yu W. et al., 2005) and MT-severing activity of p60 at the +Tip of MTs indicates that p60 is involved in cell migration (Baas P. W. and Sharma V., 2011; Toyo-Oka K. et al., 2005).

In this study, *in utero* electroporation of embryos showed that venus-tagged cells accumulated in the VZ during neocortex formation. This approach was chosen in order to label progenitors that migrate radially to upper layers of the neocortex. At first glance, the accumulation of cells in the progenitor niche upon p60 downregulation suggested a neuronal migration deficit. However, a detailed analysis showed no significant decrease in cell number in upper layers of the neocortex. Instead, non-migrating cells displayed a rounded form and no processes were observed. In order to migrate, neurons develop a long leading process that extends through the neocortex and a trailing process (Nadarajah B. et al., 2003). The lack of such a bipolar phenotype in non-migrating cells that accumulate in the VZ during corticogenesis indicates that p60 downregulation impairs cell division rather than cell migration. This closely mimics the phenotypes observed in other animal models (Shariati S.A.M. et al., 2013) in which APLP2, a

member of the Amyloid Precursor Protein family, was shown to regulate differentiation.

To test this hypothesis, I stained for DCX+ migrating cells in the DG of young adult animals. In this region, adult neurogenesis occurs (Kaplan M. S. and Hinds J. W. 1977), with newborn cells shown to undergo short radial migration before they get fully integrated in the DG circuitry (reviewed by Benarroch E.E. 2013). This experiment showed that an accumulation of DCX positive cells (i.e. IPCs and migrating neuroblasts) was also present during adult neurogenesis. In this respect, the phenotype observed in the adult hippocampus phenocopied the effect observed in the neocortex of the developing brain (Fig. XY). It is worth noting that one cannot fully exclude the role of katanin in neuronal migration, since a downregulation of p60 katanin in p60 heterozygous *knockouts* could show only dose-dependent phenotypes. That is, a conditional full depletion of p60 katanin specifically during corticogenesis might lead to a more severe phenotype. Migration therefore, can still be directly regulated by katanin, but this phenomenon was not evident upon p60 haploinsufficiency. It is likely therefore, that the phenotypes observed in the context of p60 katanin haploinsufficiency were mainly due to defects in cell proliferation rather than cell motility.

6.4. P60 katanin regulates neuronal proliferation in the adult hippocampus

Moreover, it was previously demonstrated that p80 katanin targets the katanin severing complex to the spindle poles (McNally K. P. et al., 2000) and to the centrosome (Hartman J. J. et al., 1998) during cell division. Mutations in the WD40 domain of p80 lead to brain malformations (Hu W. F. et al., 2014).

The evidence provided here supports a role for p60 katanin and therefore MT-severing in cell division during development as well as at the level of adult neurogenesis. Based on the phenotype showing an accumulation of DCX+ cells in the SGZ, I hypothesized that the non-migrating cells reflected instead an effect in cell division in the SGZ of adult mice. Upon BrdU injections, I showed that in the DG of p60 heterozygous *knockout* mice cell proliferation is severely delayed and this results in an accumulation of precursor cells. The importance of the cellular

cytoskeleton during cell division has been described by others (Nakaseko Y. and Yanagida M., 2001; Akhshi T. K. et al., 2014) and MTs have been shown to orchestrate this process (Lodish H. et al., 2000). It is known that MTs display a typical array during different phases of the cell cycle and it is therefore possible to distinguish astral MTs, kinetochore MTs and interpolar MTs (reviewed by Forth S. and Kapoor T. M. 2017). Among the most important structures during cell division are the centrosomes, which are involved in organizing and polarizing the dividing cell (Kellogg D. R. et al., 1994). When a cell enters the cell cycle, the centrioles that form the centrosome duplicate and as a result, the two daughter cells will contain a single centrosome each (Nano M. and Basto R., 2017). Centrosomes are involved in the nucleation of MTs that generate the mitotic spindle (Nano M. and Basto R., 2017) and were hypothesized to release MTs from the minus-ends when mitosis concludes (Kellogg D. R. et al., 1994). It has been proposed that defects in centrosomal positioning and replication delays or arrests the cell cycle (Nano M. and Basto R., 2017). In this respect, katanin is involved in the process of releasing MTs from the centrosomal formation in neurons (Ahmad F.J. et al., 1999) and in cell division (Toyo-Oka K. et al., 2005). Therefore, loss of p60 katanin may delay the exit of cells from the cell cycle.

Alternatively, a reduction in the number of cells incorporating BrdU may imply fewer cells entering the S-phase of the cell cycle, or a delay in the transition between G1 and S-phases. Thus, it is worthwhile to understand the possible role of p60 katanin in phases of the cell cycle that precede DNA synthesis. Before DNA replication, centrosomes duplicate (Mardin B. R. and Schiebel E., 2012) and defects in centrosome duplication have been linked to disease, including G1/S cell cycle arrest during cell division (Nigg E. A. and Raff J. W., 2009). Centrosomes are formed by barred-shaped centrioles and pericentriolar material, with centrioles shown to display a complex MT structure formed by 9 triplets of MTs (Mardin B. R. and Schiebel E., 2012; Nigg E. A. and Raff J. W., 2009). Interestingly, highly acetylated and polyglutamylated MTs in the centrosome appear to be rather stable (Gönczy P., 2012) and although the regulation of the centriolar length is still unclear, studies in drosophila suggest that MT-depolymerizing proteins are required (Delgehyr N. et al., 2012). It appears likely therefore, that p60 katanin regulates steps prior to or immediately after centrosome duplication, since its association with the centrosome during cell division has been described previously

(Ahmad F.J. et al., 1999). Altogether, reduced adult neurogenesis in animals lacking a single katanin allele underscore the importance of MT severing during cell division. Importantly, this study connects p60 katanin specifically to adult neurogenesis.

6.5. Granule neurons in the adult hippocampus display a normal dendritic arborization

Because of their passive electrical properties, dendrites are important for receiving and transmitting a given input from a pre-synaptic terminal (Gulledge A. T. et al., 2005). Besides, dendrites express a variety of voltage-gated ion channels that allow them to actively participate in the propagation of synaptic inputs (Magee J. C. and Johnston D., 1995). It is therefore fundamental that neurons develop an effective dendritic tree that allows them to be properly wired in the network.

In my study, *ex vivo* Sholl analysis of adult granule neurons in the DG showed that dendritic branching is not affected when p60 katanin is downregulated. In p60 +/- mice, developmental defects observed *in vitro* were not seen *in vivo.* This is maybe due to differences between the two approaches but also likely that katanin-like proteins and spastin, which are involved in neurite formation may compensate for downregulation of p60 katanin *in vivo*. Indeed, spastin has been linked to dendritic branching by other groups (Jinushi-Nakao S. et al., 2007; Ye B. et al., 2011). In the p60 katanin heterozygous *knockout* mouse model, I showed that although spastin protein levels are not upregulated, I cannot exclude that the enzymatic activity of other MT-severing enzymes is not enhanced. Tests to confirm this hypothesis were not performed in this study, but it is a reasonable way for p60 +/- cells to compensate for defects in the context of dendritogenesis. Also, it has been suggested that only half of the newborn neurons in the DG reach maturity and integrate into the hippocampal circuitry (Dayer A. G. et al., 2003). The observation that neurons in the DG showed no dendritic arborization defects suggests that delayed proliferation in the hippocampus of p60 +/- young adult mice does not affect maturation and final integration of granule neurons.

6.6. P60 katanin downregulation has minimal impact on behavior

As a resultThe downregulation of p60 is likely to have katanin had minimal impact on adult behavioral function. The outcome from the set of experiments conducted in this study indicated that despite showing reduced production of newborn neurons, p60 +/- animals were able to perform normally across several cognitive and non-cognitive domains. Previous data has linked adult hippocampal neurogenesis with spatial navigation and contextual fear conditioning (Dupret D. et al., 2008; Wojtowicz J. M. et al., 2008). Others have shown that impaired adult neurogenesis affects spatial memory in the object location test and the Morris water maze task (Goodman T. et al., 2010). Finally, newborn neurons in the DG are proposed to reduce interference between old and new memories in a process called pattern separation (Sahay et al., 2011; Aimone J. B. et al., 2014). However, several studies claim that adult neurogenesis is either redundant, or that the ablation of this process could be positive in terms of enhancing learning and memory (Shors T. J. et al., 2002; Bartolomucci A. et al., 2002; Leuner B. et al., 2006; Saxe M. D. et al., 2007; Sharfman H. E. and Hen R., 2007; Barker J. M. et al., 2011; Groves J. O. et al., 2013). The role of newborn neurons in hippocampal circuitry and ultimately in mammalian behavior is therefore still under debate. It appears that experimental conditions or type of manipulation influence the interpretation of the role of adult neurogenesis. Final conclusions in the field are still controversial and in some cases also criticized (Lazic S. E., 2010). The observation that around half of the newborn cells undergo apoptosis and only the remaining ones reach maturation (Dayer A. G. et al., 2003), supports the idea that the impaired neurogenesis in p60 +/- animals might not be sufficient to observe a strong behavioral effect. In this study, I showed that a reduction in adult neurogenesis in the SGZ correlates with delayed associative learning in contextual fear conditioning (Fig. 33). However, no impairments were observed during auditory fear conditioning (Fig. 32). Auditory fear conditioning depends on an intact amygdala function (Park S. et al., 2016). A discrete CS (tone) and a paired foot shock (US) enter in rapid association since the tone acts as the best predictor for the aversive event. On the other hand, contextual fear conditioning relies on plasticity in the amygdala and the hippocampus (Antoniadis E. A. and McDonald

R. J., 2000). In this respect, the hippocampus represents multiple elements in the context in a unified manner (Rudy J. W., 2009). It is therefore likely that adult generated neurons are recruited and encode the unification of different contextual cues (tactile, visual and olfactory). In this respect, a slower neurogenesis in p60 +/- mice may lead to a slower association of the aversive event due to ambiguity about which of the contextual cues predict better the incoming aversive event. Alternatively, a delayed adult neurogenesis in p60 +/- mice may slower context-dependent learning, which requires recruitment of newborn neurons and the formation of new synapses. Since a proper maturation of DG neurons was also observed in p60 +/- mice (Fig. 29), it is not surprising that discrimination between safe and aversive contexts was normal 24 hours later, indicating that learning is not fully compromised, but rather delayed. This evidence indicates that testing the mice in rather similar contexts (increased ambiguity) would lead to a more severe phenotype.

6.7. ATPase-deficient p60 katanin mutant alters MT growth speed and cargo transport

MTs are very dynamic structures that polymerize and depolymerize based on their properties in a process known as dynamic instability (Mitchison T. and Kischner M., 1984), which involves shrinking and growth events and the transition among these two states (Gierke S. et al., 2010). Factors that determine the remodeling of MT filaments can be categorized as either MT-promoting or MT-destabilizing (Horio T. and Murata T., 2014). In this study, I assessed whether inhibition of p60 katanin function could alter MT dynamics in neurons. I made use of the p60-DEID construct in which p60 katanin lacks ATPase activity (McNally K.P. et al., 2000). First, the observation that p60-DEID binds to MTs confirmed previous findings that the ATPase activity of katanin drives MT-depolymerization but is not required for binding. Second, by tracking the +Tip binding protein EB3 with time-lapse microscopy, I showed that dominant negative katanin overexpression decreases the absolute growth speed of MTs in neurons. This data supports a recent study in *Arabidopsis thaliana* showing that MT-severing by katanin influences MT dynamics (Komis G. et al., 2017). Furthermore, I conclude that p60-DEID overexpression

leads to an overall less dynamic MT network, in agreement with data from others that have used the MT-stabilizing agent taxol (Marx A. et al., 2013).
P60-DEID overexpressing neurons showed a faster mitochondrial displacement. Mitochondria are organelles important for a variety of cellular processes such as ATP production, metabolism and cell survival (Course M. M. and Wang X., 2016). Their transport in the cell is mediated by kinesin-1 and dynein motors, depending on their directionality (Pilling A. D., 2006). In this study, mitochondria were used as a general candidate to understand how a less dynamic MT network could affect intracellular transport, although the consequences of an impaired mitochondrial transport at the cellular level were not tested. However, mitochondria transport changes in p60-DEID overexpressing neurons can be due to several reasons. First, more stable MT tracks (Ryan S. D. et al., 2012). Second, an indirect effect mediated by MAPs, which modify the processivity of MT-based motors (Kanaan N. M. et al., 2011; Rodriguez-Martin T. et al., 2013). Third, more stable MTs may lead to increased tubulin PTMs that are known to interfere with MT-based transport (Sirajuddin M. et al., 2014). It is worth mentioning that in all possible scenarios p60 katanin might be affecting intracellular transport in an indirect way, by directly modifying MT-tracks stability.

6.8. P60 katanin is present in post-synaptic compartments and its conditional depletion in the hippocampus affects LTP induction

During this study, I showed that p60 katanin displays cytoplasmic localization in neurons in agreement with previous findings (McNally K.P. et al., 2000). Interestingly, I also observed the presence of p60 katanin in dendritic spines, suggesting that p60 may play an active role in synaptic transmission. In order to overcome developmental defects associated with a constitutive knockout of p60 katanin and focus on the roles of p60 in the adult brain, p60 katanin floxed mice were crossed with a CRE-driver line under the CamKII-a promoter (Tsien J. Z. et al., 1996). In the CRE-driver mice, CRE expression mainly occurs in the CA1 region of the hippocampus and peaks in the third post-natal week (Tsien J. Z. et al., 1996). Therefore, this approach allows for a time- and region-specific depletion of p60 katanin. However, the mosaic pattern showed by CRE expression limited the study to electrophysiological experiments. Focus was on CA3-to-CA1 Schaffer

collateral LTP because p60 katanin could be involved in synaptic changes that underline the strengthening of synapses upon stimulation (Alger B. E. and Teyler T. J., 1976). In this experiment, induction of LTP was positively affected in p60 conditional knockout mice while later phases were comparable to controls. LTP can be divided in different phases (Huang E. P., 1998). Early phases of LTP (E-LTP) are thought to involve the activity of protein kinases (Huang E. P., 1998) which lasts 4 to 6 hours (Frey S. et al., 2001), while late phases of LTP (L-LTP) are known to require protein synthesis (Frey U. et al., 1988). The phenotype observed in p60 conditionally depleted animals might be due to several possibilities. Evidence indicates that stabilization of proteins in the post-synaptic compartment upon proteasome inhibition leads to an increase in the induction of LTP (Dong C. et al., 2008). Therefore, the depletion of p60 katanin in the CA1 region of the hippocampus could lead to a stable post-synaptic compartment at the steady state prior to stimulation, making the spines more prone to be excited. Alternatively, the minimal CRE expression in the CA3 region of the T29.1 CRE driver line (Tsien J. Z. et al., 1996) used to deplete p60 katanin, may lead to alterations in the pre-synaptic pool of synaptic vesicles and influence neurotransmitter release (Schulz P. E. et al., 1994).

6.9. Hypothesis of p60 katanin function in dendritic spines

I showed that p60 katanin influences MT dynamics, is present in dendritic spines of adult hippocampal neurons, and contributes to synaptic plasticity. Together, these findings allowed me to hypothesize an important role for MT-severing in synaptic plasticity. It has been shown that MTs enter spines and this contributes to dendritic spine growth (Jaworski J. et a., 2009). Katanin MT-severing activity can take place either at the +Tip (Baas P. W. and Sharma V. 2011); or at the minus-end of MTs (Jiang K. et al., 2017). Here, I hypothesized that under physiological conditions, p60 katanin regulates MT-entryy into dendritic spines via two possible scenarios. On one hand, katanin can be a MT-blocking agent that inhibits MT-entering into spines by severing at the +Tip of growing MTs. On the other hand, p60 katanin may be a MT-invasion promoting agent by either promoting organized MT growth or generating new nucleation points at the dendritic shaft that facilitates

MT growth into the spines (Fig. 45). To test these hypotheses, the katanin p60-DEID construct (McNally K.P. et al., 2000) was used.

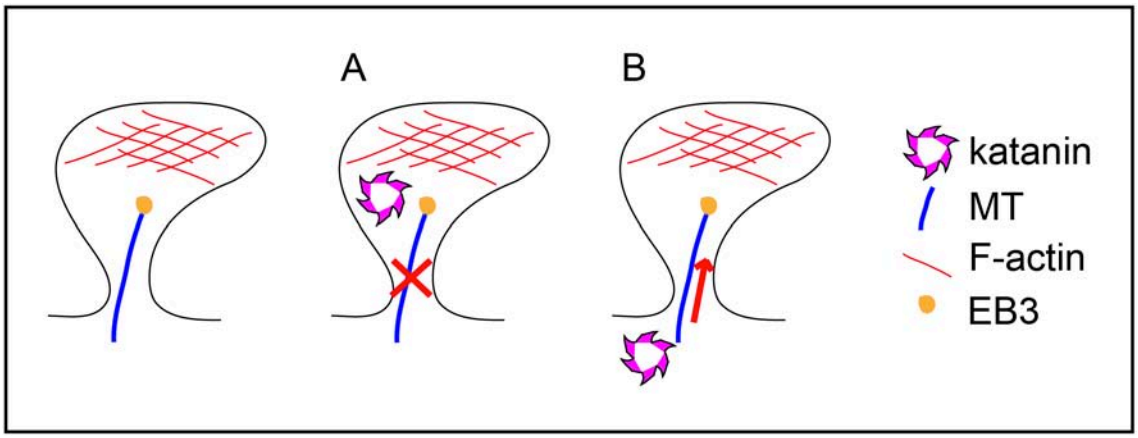

Figure 45 ***Model for hypothetical function of katanin in dendritic spines.*** Currently, it is unclear how MTs invade spines and the possible functions of this process in synaptic function. Here, I propose two possible scenarios in which MT-severing plays key roles in either blocking or promoting MT invasion of spines. In summary, katanin might block the entrance of MTs (A) or, increase the chance of MT invasion in dendritic spines by generating new nucleation points (B). In my work, I tested these hypotheses. MT = microtubules; EB3 = end-binding protein 3; F-actin = filamentous actin.

6.10. Inhibition of p60 katanin function decreases EB3 puncta in dendritic spines

I showed that the growing speed of MTs is affected in dendrites of developing neurons upon overexpression of a p60-DEID construct that lacks the possibility to hydrolyze ATP (McNally K.P. et al., 2000). Furthermore, data showing the presence of p60 katanin in dendritic spines, together with an effect in LTP induction upon p60 depletion led me to hypothesize that p60 katanin could also play an active function in post-synaptic compartments. Based on a previous study showing that MTs invade dendritic spines (Jaworski J. et al., 2009), I hypothesized that p60 katanin could either inhibit or promote MT entry into spines (Figure 1, above).

EB3 is a MT +Tip binding protein that is widely used for tracking growing MT filaments (Akhmanova A. and Steinmetz M. O., 2008). In this study, I stained for

endogenous EB3 and checked for the presence of growing MTs in dendritic spines. Results showed a significant decrease of EB3 puncta in dendritic spines of hippocampal neurons overexpressing p60-DEID although no changes in spine number or size were observed under basal conditions.

The fact that a MT severing enzyme promotes MT entry into a given subcellular compartment could be, at a first glance, controversial. Studies performed in Drosophila have shown that p60 katanin removes tubulin subunits from MT plus-ends (Diaz-Valencia J. D. et al., 2011; Zhang D. et al., 2011; Baas P. W. and Sharma V., 2011). In their review, Baas and Sharma proposed that cutting MTs at their +Tips is a way to keep the MT network organized. On the other hand, it has been proposed that p60 katanin can also sever MTs at their minus-ends (Jiang K. et al., 2017) and it is targeted to the centrosome (Hartman J.J. et al., 1998). Katanin therefore is not only a severing protein that disassembles MT filaments but also does it in a regulated manner promoting order in the network. The results obtained with this experiment allowed me to conclude that MT-severing by p60 katanin provides order in the network and allows MTs to target specific locations in the cell.

Dendritic spines might require MTs for their formation (Gu J. et al., 2008) but results upon p60-DEID overexpression showed no changes in spine number under basal conditions. It is important to note that in the study by Gu J. and colleagues, the authors applied either nocodazole or taxol to manipulate the MT network. In this study, a single MT-severing enzyme, p60 katanin, was inhibited, so the effect might not be as strong as in Gu J. and colleagues study (2008). These data suggest that p60-katanin positively regulates MT-entering in dendritic spines of adult hippocampal neurons.

6.11. Inhibition of p60 katanin function impairs structural plasticity

In the previous set of experiments, I showed that the presence of p60 katanin in dendritic spines contributes to spine invasion by MTs. Despite a reduction in the number of EB3 comets in spines of p60-DEID overexpressing neurons, spine number or area was not impaired. For that, glutamate uncaging in order to stimulate individual spines was performed and the results showed that upon uncaging, a significant increase in the spine area was achieved in GFP expressing

neurons, while no morphological changes were observed when p60 katanin function was inhibited by the presence of p60-DEID.

It was shown previously that p60 katanin localizes to the growth cone of growing axons (Yu W. et al., 2005), a dynamic structure that depends on actin and the MT cytoskeleton rearrangement (Dent E. W. et al., 2011). The presence of katanin in this subcellular compartment as well as its function during cell division (McNally K. P. et al., 2000), suggests that katanin-mediated MT-severing is involved in processes that require vast cytoskeleton rearrangement.

Dendritic spines are protrusions that form the post-synaptic compartment of excitatory synapses (Nimchisky E. A. et al., 2002). It was shown that dendritic spines undergo structural modifications upon LTP (Lin H. et al., 2004) and these modifications occur before new AMPA receptors are incorporated at the synapse (Kopec C. D. et al., 2006). Remodeling of the actin cytoskeleton was shown to play an important role in LTP (Krucker T. et al., 2000) and it was suggested that F-actin drives MT-invasion of dendritic spines via drebrin, a protein that connects both cytoskeletal structures (Merriam E. B. et al., 2013). Other studies have shown that MT-invasion of dendritic spines is required for actin dynamics, spine maintenance and LTP (Jaworski J. et al., 2009). In agreement with these findings, deficient spine growth in neurons overexpressing p60-DEID upon glutamate uncaging, suggests that MT invasion in dendritic spines is required for structural plasticity. Besides, I directly connect MT-severing activity by katanin as a modulatory mechanism in this process.

6.12. P60 katanin in the context of disease

6.12.1. P60 katanin expression is reduced in Tau P301L transgenic mice

Tau is a MAP that has been shown to bind MTs (Weingarten M.D. et al., 1975) and stabilizes them (Drubin D. G. and Kirschner M. W., 1986). Interplay between katanin and Tau has been described. Qiang and colleagues together with other groups showed that MTs are protected by Tau from severing by katanin (Qiang L. et al., 2006; Sudo H. and Baas P. W., 2011). Here, I showed that the expression

levels of the catalytic subunit of katanin, p60, are significantly decreased in transgenic mice expressing the mutated form of human Tau (Ramsdem M. et al., 2005). TAU P301L mutation is linked to frontotemporal dementia (FTD) (Hutton M. et al., 1998) and promotes the formation of paired helical filaments (PHFs) (Barghorn S. et al., 2000) found in tauopathies. This is interesting because the phenotypes observed in these animals might not only be directly related to Tau, but also to defects in the MT network caused by reduced expression of p60 katanin. It is likely that in the context of altered Tau binding to MTs, katanin may have easier access to a more susceptible MT network (Matamoros A. J. and Baas P. W., 2016). Therefore, the data in this study opens a new branch of investigation for the role of katanin in the aging brain. Possible questions worth addressing are whether the actual severing activity of p60 is also reduced, or whether the regulatory subunit, p80, is also affected. As mentioned previously, this is the first of a set of experiments that is worth addressing in the context of neuropathies. I believe that a detailed understanding of upstream regulators of katanin function can modulate its activity under pathological conditions.

6.13. Conclusions and future directions

In summary, the findings presented in the first part of this thesis provide relevant information regarding p60 katanin function during embryonic brain development and adult neurogenesis as an orchestrator of the cell cycle. In the second set of data, the role of p60 katanin in adult neurons as a modulator of structural plasticity via its MT-severing function was shown. Taken together, these data shed light on the importance of a tight regulation of MT-dynamics by p60 katanin during these processes. Besides, understanding the molecular basis of neuronal degeneration by examining possible implications of p60 katanin dysfunction in neuropathology require further investigation.

7. References

1. Ahmad, F. J., Yu, W., McNally, F. J. & Baas, P. W. An essential role for katanin in severing microtubules in the neuron. *J. Cell Biol.* **145,** 305–315 (2000).
2. Aimone, J. B., Wiles, J. & Gage, F. H. Potential role for adult neurogenesis in the encoding of time in new memories. *Nat Neurosci* **9,** 723–727 (2006).
3. Aimone, J. B. *et al.* Regulation and Function of Adult Neurogenesis: From Genes to Cognition. *Physiol. Rev.* **94,** 991–1026 (2014).
4. Akella, J. S. *et al.* MEC-17 is an alpha-tubulin acetyltransferase. *Nature* **467,** 218–222 (2010).
5. Akhmanova, A. & Steinmetz, M. O. Tracking the ends: A dynamic protein network controls the fate of microtubule tips. *Nature Reviews Molecular Cell Biology* **9,** 309–322 (2008).
6. Akhshi, T. K., Wernike, D. & Piekny, A. Microtubules and actin crosstalk in cell migration and division. *Cytoskeleton* **71,** 1–23 (2014).
7. Alberts, B. *et al.* Molecular Cell Biology, 4. edition. *Biochem. Mol. Biol. Educ.* **Chapter 19,** (2002).
8. Alger, B. E. & Teyler, T. J. Long-term and short-term plasticity in the CA1, CA3, and dentate regions of the rat hippocampal slice. *Brain Res.* **110,** 463–480 (1976).
9. Altman, J. Are New Neurons Formed in the Brains of Adult Mammals? *Science (80-.).* **135,** 1127–1128 (1962).
10. Altman, J. & Das, G. D. Post-natal origin of microneurones in the rat brain. *Nature* **207,** 953–956 (1965).
11. Amaral, D. G. & Witter, M. P. The three-dimensional organization of the hippocampal formation: A review of anatomical data. *Neuroscience* **31,** 571–591 (1989).
12. Amos, L. A. & Schlieper, D. Microtubules and maps. *Advances in Protein Chemistry* **71,** 257–298 (2005).
13. Angelastro, J. M. & Purich, D. L. Apparently irreversible GTP hydrolysis attends tubulin self-assembly. *Eur. J. Biochem.* **191,** 507–511 (1990).
14. Antoniadis, E. A. & McDonald, R. J. Amygdala, hippocampus and discriminative fear conditioning to context. *Behav. Brain Res.* **108,** 1–19 (2000).
15. Apple, D. M., Fonseca, R. S. & Kokovay, E. The role of adult neurogenesis in psychiatric and cognitive disorders. *Brain Research* **1655,** 270–276 (2017).
16. Arruda-Carvalho, M., Sakaguchi, M., Akers, K. G., Josselyn, S. A. & Frankland, P. W. Posttraining Ablation of Adult-Generated Neurons Degrades Previously Acquired Memories. *J. Neurosci.* **31,** 15113–15127 (2011).
17. Baas, P. W. & Sharma, V. Cell migration: Katanin gives microtubules a trim. *Curr. Biol.* **21,** (2011).
18. Bailey, C. H. & Kandel, E. R. Structural Changes Accompanying Memory Storage. *Annu. Rev. Physiol.* **55,** 397–426 (1993).
19. Bär, J., Kobler, O., Van Bommel, B. & Mikhaylova, M. Periodic F-actin structures shape the neck of dendritic spines. *Sci. Rep.* **6,** (2016).
20. Barghorn, S. *et al.* Structure, microtubule interactions, and paired helical filament aggregation by tau mutants of frontotemporal dementias. *Biochemistry* **39,** 11714–11721 (2000).
21. Barker, J. M., Boonstra, R. & Wojtowicz, J. M. From pattern to purpose: How comparative studies contribute to understanding the function of adult neurogenesis. *Eur. J. Neurosci.* **34,** 963–977 (2011).

22. Bartolomucci, A., De Biurrun, G., Czéh, B., Van Kampen, M. & Fuchs, E. Selective enhancement of spatial learning under chronic psychosocial stress. *Eur. J. Neurosci.* **15,** 1863–1866 (2002).
23. Benarroch, E. E. Adult neurogenesis in the dentate gyrus: General concepts and potential implications. *Neurology* **81,** 1443–1452 (2013).
24. Bennett, M. V. Gap junctions as electrical synapses. *J. Neurocytol.* **26,** 349–66 (1997).
25. Biernat1, J. *et al.* The switch of tau protein to an Alzheimer-like state includes the phosphorylation of two serine-proline motifs upstream of the microtubule binding region. *EMBO J.* **1,** 593–1 (1992).
26. Bliss, T. V. P. & Lømo, T. Long-lasting potentiation of synaptic transmission in the dentate area of the anaesthetized rabbit following stimulation of the perforant path. *J. Physiol.* **232,** 331–356 (1973).
27. Blitzer, R. D. *et al.* Gating of CaMKII by cAMP-regulated protein phosphatase activity during LTP. *Science (80-.).* **280,** 1940–1943 (1998).
28. Boldrini, M. *et al.* Human Hippocampal Neurogenesis Persists throughout Aging. *Cell Stem Cell* **22,** 589–599.e5 (2018).
29. Bonnet, C. *et al.* Differential Binding Regulation of Microtubule-associated Proteins MAP1A, MAP1B, and MAP2 by Tubulin Polyglutamylation. *J. Biol. Chem.* **276,** 12839–12848 (2001).
30. Bradke, F. & Dotti, C. C. The role of local actin instability in axon formation. *Science (80-.).* **283,** 1931–1934 (1999).
31. Braun, S. M. G. & Jessberger, S. Adult neurogenesis: mechanisms and functional significance. *Development* **141,** 1983–1986 (2014).
32. Breunig, J. J. *et al.* Primary cilia regulate hippocampal neurogenesis by mediating sonic hedgehog signaling. *Proc. Natl. Acad. Sci.* **105,** 13127–13132 (2008).
33. Breunig, J. J., Silbereis, J., Vaccarino, F. M., Sestan, N. & Rakic, P. Notch regulates cell fate and dendrite morphology of newborn neurons in the postnatal dentate gyrus. *Proc. Natl. Acad. Sci. U. S. A.* **104,** 20558–63 (2007).
34. Briscoe, J., Pierani, A., Jessell, T. M. & Ericson, J. A homeodomain protein code specifies progenitor cell identity and neuronal fate in the ventral neural tube. *Cell* **101,** 435–445 (2000).
35. Chaitanya, G. V., Alexander, J. S. & Babu, P. P. PARP-1 cleavage fragments: Signatures of cell-death proteases in neurodegeneration. *Cell Communication and Signaling* **8,** (2010).
36. Chakraborti, S., Natarajan, K., Curiel, J., Janke, C. & Liu, J. The emerging role of the tubulin code: From the tubulin molecule to neuronal function and disease. *Cytoskeleton* **73,** 521–550 (2016).
37. Charvin, D. *et al.* Mutations of SPG4 are responsible for a loss of function of spastin, an abundant neuronal protein localized in the nucleus. *Hum. Mol. Genet.* **12,** 71–78 (2003).
38. Chung, W. S., Allen, N. J. & Eroglu, C. Astrocytes control synapse formation, function, and elimination. *Cold Spring Harb. Perspect. Biol.* **7,** (2015).
39. Citri, A. & Malenka, R. C. Synaptic plasticity: multiple forms, functions, and mechanisms. *Neuropsychopharmacology* **33,** 18–41 (2008).
40. Clark, P. J. *et al.* Genetic influences on exercise-induced adult hippocampal neurogenesis across 12 divergent mouse strains. *Genes, Brain Behav.* **10,** 345–353 (2011).
41. Colón-Ramos, D. A. Chapter 2 Synapse Formation in Developing Neural Circuits. *Current Topics in Developmental Biology* **87,** 53–79 (2009).
42. Conde, C. & Cáceres, A. Microtubule assembly, organization and dynamics in axons and dendrites. *Nature Reviews Neuroscience* **10,** 319–332 (2009).
43. Course, M. M. & Wang, X. Transporting mitochondria in neurons. *F1000Research* **5,** 1735 (2016).

44. Cowen, M. & Kandel, E. in *Synapses* 767 (2001). at <https://books.google.com/books?id=FO5efrKGVQoC&pgis=1>
45. Craig, A. M. & Banker, G. Neuronal Polarity. *Annu. Rev. Neurosci.* **17,** 267–310 (1994).
46. Crawley, J. & Goodwin, F. K. Preliminary report of a simple animal behavior model for the anxiolytic effects of benzodiazepines. *Pharmacol. Biochem. Behav.* **13,** 167–170 (1980).
47. Dayer, A. G., Ford, A. A., Cleaver, K. M., Yassaee, M. & Cameron, H. A. Short-term and long-term survival of new neurons in the rat dentate gyrus. *J. Comp. Neurol.* **460,** 563–572 (2003).
48. de Anda, F. C., Meletis, K., Ge, X., Rei, D. & Tsai, L.-H. Centrosome Motility Is Essential for Initial Axon Formation in the Neocortex. *J. Neurosci.* **30,** 10391–10406 (2010).
49. De Anda, F. C. *et al.* Centrosome localization determines neuronal polarity. *Nature* **436,** 704–708 (2005).
50. De Brabander, M. J. Microtubules, central elements of cellular organization. *Endeavour* **6,** 124–134 (1982).
51. Dehay, C. & Kennedy, H. Cell-cycle control and cortical development. *Nature Reviews Neuroscience* **8,** 438–450 (2007).
52. Delgehyr, N. *et al.* Klp10A, a microtubule-depolymerizing kinesin-13, cooperates with CP110 to control drosophila centriole length. *Curr. Biol.* **22,** 502–509 (2012).
53. Dent, E. W., Gupton, S. L. & Gertler, F. B. The growth cone cytoskeleton in Axon outgrowth and guidance. *Cold Spring Harb. Perspect. Biol.* **3,** 1–39 (2011).
54. Desai, A. & Mitchison, T. J. MICROTUBULE POLYMERIZATION DYNAMICS. *Annu. Rev. Cell Dev. Biol.* **13,** 83–117 (1997).
55. Díaz-Valencia, J. D. *et al.* Drosophila katanin-60 depolymerizes and severs at microtubule defects. *Biophys. J.* **100,** 2440–2449 (2011).
56. Dixit, R., Ross, J. L., Goldman, Y. E. & Holzbaur, E. L. F. Differential regulation of dynein and kinesin motor proteins by tau. *Science (80-.).* **319,** 1086–1089 (2008).
57. Doetsch, F., García-Verdugo, A. & Alvarez-Buylla, J. Cellular Composition and Three-Dimensional Organization of the Subventricular Germinal Zone in the Adult Mammalian Brain. *J. Neurosci.* **17(13),** 5046–61 (1997).
58. Dong, C., Upadhya, S. C., Ding, L., Smith, T. K. & Hegde, A. N. Proteasome inhibition enhances the induction and impairs the maintenance of late-phase long-term potentiation. *Learn. Mem.* **15,** 335–347 (2008).
59. Dotti, C. G., Sullivan, C. a & Banker, G. a. The establishment of polarity by hippocampal neurons in culture. *J. Neurosci.* **8,** 1454–1468 (1988).
60. Drew, M. R., Denny, C. A. & Hen, R. Arrest of adult hippocampal neurogenesis in mice impairs single- but not multiple-trial contextual fear conditioning. *Behav. Neurosci.* **124,** 446–454 (2010).
61. Drubin, D. G. & Kirschner, M. W. Tau protein function in living cells. *J. Cell Biol.* **103,** 2739–46 (1986).
62. Dupret, D. *et al.* Spatial relational memory requires hippocampal adult neurogenesis. *PLoS One* **3,** (2008).
63. Echelard, Y. *et al.* Sonic hedgehog, a member of a family of putative signaling molecules, is implicated in the regulation of CNS polarity. *Cell* **75,** 1417–1430 (1993).
64. Ellis, P. *et al.* SOX2, a persistent marker for multipotential neural stem cells derived from embryonic stem cells, the embryo or the adult. *Dev. Neurosci.* **26,** 148–165 (2004).
65. Eom, T. Y. *et al.* Differential regulation of microtubule severing by APC underlies distinct patterns of projection neuron and interneuron migration. *Dev. Cell* **31,** 677–689 (2014).
66. Ericson, J. *et al.* Pax6 controls progenitor cell identity and neuronal fate in response to graded Shh signaling. *Cell* **90,** 169–180 (1997).

67. Eriksson, P. S. *et al.* Neurogenesis in the adult human hippocampus. *Nat Med* **4,** 1313–1317 (1998).
68. Evans, K. J., Gomes, E. R., Reisenweber, S. M., Gundersen, G. G. & Lauring, B. P. Linking axonal degeneration to microtubule remodeling by Spastin-mediated microtubule severing. *J. Cell Biol.* **168,** 599–606 (2005).
69. Ferraro, F. F., Lo Celso, C. & Scadden, D. D. Adult stem cells and their niches. *Adv. Exp. Med. Biol.* **695,** 155–168 (2010).
70. Fletcher, D. A. & Mullins, R. D. Cell mechanics and the cytoskeleton. *Nature* **463,** 485–492 (2010).
71. Forth, S. & Kapoor, T. M. The mechanics of microtubule networks in cell division. *Journal of Cell Biology* **216,** 1525–1531 (2017).
72. Franker, M. A. M. & Hoogenraad, C. C. Microtubule-based transport - basic mechanisms, traffic rules and role in neurological pathogenesis. *J. Cell Sci.* **126,** 2319–2329 (2013).
73. Frey, S., Bergado-Rosado, J., Seidenbecher, T., Pape, H.-C. C. & Frey, J. U. Reinforcement of Early Long-Term Potentiation (Early-LTP) in Dentate Gyrus by Stimulation of the Basolateral Amygdala: Heterosynaptic Induction Mechanisms of Late-LTP. *J. Neurosci.* **21,** 3697–3703 (2001).
74. Frey, U., Krug, M., Reymann, K. G. & Matthies, H. Anisomycin, an inhibitor of protein synthesis, blocks late phases of LTP phenomena in the hippocampal CA1 region in vitro. *Brain Res.* **452,** 57–65 (1988).
75. Gadadhar, S., Bodakuntla, S., Natarajan, K. & Janke, C. The tubulin code at a glance. *J. Cell Sci.* **130,** 1347–1353 (2017).
76. Gage, F. H. Mammalian Neural Stem Cells. *Science (80-.).* **287,** 1433–1438 (2000).
77. Gal, J. S. Molecular and Morphological Heterogeneity of Neural Precursors in the Mouse Neocortical Proliferative Zones. *J. Neurosci.* **26,** 1045–1056 (2006).
78. Galvani, L. De viribus electricitatis in motu muscularis commentarius. *Bononiensi Sci. Artium Inst. atque Acad. Comment.* **7,** 363–418 (1791).
79. Ghetti, B. *et al.* Invited review: Frontotemporal dementia caused by microtubule-associated protein tau gene (MAPT) mutations: A chameleon for neuropathology and neuroimaging. *Neuropathology and Applied Neurobiology* **41,** 24–46 (2015).
80. Ghosh, D. K., Dasgupta, D. & Guha, A. Models, Regulations, and Functions of Microtubule Severing by Katanin. *ISRN Mol. Biol.* **2012,** 1–14 (2012).
81. Gierke, S., Kumar, P. & Wittmann, T. *Analysis of Microtubule Polymerization Dynamics in Live Cells*. *Methods in Cell Biology* **97,** (2010).
82. Gilbert SF. in *The Epidermis and the Origin of Cutaneous Structures* (2000).
83. Goedert, M., Wischik, C. M., Crowther, R. A., Walker, J. E. & Klug, A. Cloning and sequencing of the cDNA encoding a core protein of the paired helical filament of Alzheimer disease: identification as the microtubule-associated protein tau. *Proc. Natl. Acad. Sci.* **85,** 4051–4055 (1988).
84. Goldmann, W. H. Intermediate filaments and cellular mechanics. *Cell Biology International* (2018). doi:10.1002/cbin.10879
85. Gonçalves, J. T., Schafer, S. T. & Gage, F. H. Adult Neurogenesis in the Hippocampus: From Stem Cells to Behavior. *Cell* **167,** 897–914 (2016).
86. Gönczy, P. Towards a molecular architecture of centriole assembly. *Nature Reviews Molecular Cell Biology* **13,** 425–435 (2012).
87. Gong, C.-X. & Iqbal, K. Hyperphosphorylation of microtubule-associated protein tau: a promising therapeutic target for Alzheimer disease. *Curr. Med. Chem.* **15,** 2321–8 (2008).
88. Goodman, T. *et al.* Young hippocampal neurons are critical for recent and remote spatial memory in adult mice. *Neuroscience* **171,** 769–778 (2010).
89. Groves, J. O. *et al.* Ablating Adult Neurogenesis in the Rat Has No Effect on Spatial Processing: Evidence from a Novel Pharmacogenetic Model. *PLoS Genet.* **9,** e1003718 (2013).

90. Grundke-Iqbal, I. *et al.* Microtubule-associated protein tau. A component of Alzheimer paired helical filaments. *J. Biol. Chem.* **261,** 6084–9 (1986).
91. Grundke-Iqbal, I. *et al.* Abnormal phosphorylation of the microtubule-associated protein (tau) in Alzheimer cytoskeletal pathology. *Alzheimer Dis. Assoc. Disord.* **1,** 202 (1987).
92. Grüneberg, H. Two new mutant genes in the house mouse. *J. Genet.* **45,** 22–28 (1943).
93. Gu, J. & Zheng, J. Q. Microtubules in Dendritic Spine Development and Plasticity. *Open Neurosci. J.* **3,** 128–133 (2009).
94. Gulledge, A. T., Kampa, B. M. & Stuart, G. J. Synaptic integration in dendritic trees. *Journal of Neurobiology* **64,** 75–90 (2005).
95. Hall, A. C., Mira, H., Wagner, J. & Arenas, E. Region-specific effects of glia on neuronal induction and differentiation with a focus on dopaminergic neurons. *Glia* **43,** 47–51 (2003).
96. Halpain, S. Actin and the agile spine: How and why do dendritic spines dance? *Trends in Neurosciences* **23,** 141–146 (2000).
97. Handley, S. L. & Mithani, S. Effects of alpha-adrenoceptor agonists and antagonists in a maze-exploration model of 'fear'-motivated behaviour. *Naunyn. Schmiedebergs. Arch. Pharmacol.* **327,** 1–5 (1984).
98. Hartman, J. J. *et al.* Katanin, a microtubule-severing protein, is a novel AAA ATPase that targets to the centrosome using a WD40-containing subunit. *Cell* **93,** 277–287 (1998).
99. Hartman, J. J. & Vale, R. D. Microtubule disassembly by ATP-dependent oligomerization of the AAA enzyme katanin. *Science (80-.).* **286,** 782–785 (1999).
100. Hazan, J. *et al.* Spastin, a new AAA protein, is altered in the most frequent form of autosomal dominant spastic paraplegia. *Nat. Genet.* **23,** 296–303 (1999).
101. Hering, H. & Sheng, M. Dentritic spines: structure, dynamics and regulation. *Nat. Rev. Neurosci.* **2,** 880–888 (2001).
102. Hoogenraad, C. C. & Akhmanova, A. Dendritic spine plasticity: New regulatory roles of dynamic microtubules. *Neuroscientist* **16,** 650–661 (2010).
103. Horio, T. & Murata, T. The role of dynamic instability in microtubule organization. *Front. Plant Sci.* **5,** (2014).
104. Hotulainen, P. & Hoogenraad, C. C. Actin in dendritic spines: Connecting dynamics to function. *Journal of Cell Biology* **189,** 619–629 (2010).
105. Hu, W. F. *et al.* Katanin p80 regulates human cortical development by limiting centriole and cilia number. *Neuron* **84,** 1240–1257 (2014).
106. Huang, E. P. Synaptic plasticity: Going through phases with LTP. *Curr. Biol.* **8,** R350–R352 (1998).
107. Hubbert, C. *et al.* HDAC6 is a microtubule-associated deacetylase. *Nature* **417,** 455–458 (2002).
108. Hughes, R. N. The value of spontaneous alternation behavior (SAB) as a test of retention in pharmacological investigations of memory. *Neuroscience and Biobehavioral Reviews* **28,** 497–505 (2004).
109. Hutton, M. *et al.* Association of missense and 5'-splice-site mutations in tau with the inherited dementia FTDP-17. *Nature* **393,** 702–704 (1998).
110. Inoue, S. Cell Motility by Labile Association of Molecules: The nature of mitotic spindle fibers and their role in chromosome movement. *J. Gen. Physiol.* **50,** 259–292 (1967).
111. Jaworski, J. *et al.* Dynamic Microtubules Regulate Dendritic Spine Morphology and Synaptic Plasticity. *Neuron* **61,** 85–100 (2009).
112. Jiang, K. *et al.* Microtubule minus-end regulation at spindle poles by an ASPM-katanin complex. *Nat. Cell Biol.* **19,** 480–492 (2017).
113. Jin, M. *et al.* Katanin p80, NuMA and cytoplasmic dynein cooperate to control microtubule dynamics. *Sci. Rep.* **7,** 1–16 (2017).

114. Jinushi-Nakao, S. *et al.* Knot/Collier and Cut Control Different Aspects of Dendrite Cytoskeleton and Synergize to Define Final Arbor Shape. *Neuron* **56,** 963–978 (2007).
115. Jonas, P. & Lisman, J. Structure, function, and plasticity of hippocampal dentate gyrus microcircuits. *Front. Neural Circuits* **8,** (2014).
116. Kadavath, H. *et al.* Tau stabilizes microtubules by binding at the interface between tubulin heterodimers. *Proc. Natl. Acad. Sci.* **112,** 7501–7506 (2015).
117. Kaltschmidt, J. a & Brand, A. H. Asymmetric cell division: microtubule dynamics and spindle asymmetry. *J. Cell Sci.* **115,** 2257–2264 (2002).
118. Kanaan, N. M. *et al.* Pathogenic Forms of Tau Inhibit Kinesin-Dependent Axonal Transport through a Mechanism Involving Activation of Axonal Phosphotransferases. *J. Neurosci.* **31,** 9858–9868 (2011).
119. Kaplan, M. S. & Hinds, J. W. Neurogenesis in the adult rat: electron microscopic analysis of light radioautographs. *Science* **197,** 1092–4 (1977).
120. Kellogg, D. R., Moritz, M. & Alberts, B. M. The Centrosome and Cellular Organization. *Annu. Rev. Biochem.* **63,** 639–674 (1994).
121. Kheirbek, M. A., Klemenhagen, K. C., Sahay, A. & Hen, R. Neurogenesis and generalization: A new approach to stratify and treat anxiety disorders. *Nature Neuroscience* **15,** 1613–1620 (2012).
122. Klebe, S., Stevanin, G. & Depienne, C. Clinical and genetic heterogeneity in hereditary spastic paraplegias: From SPG1 to SPG72 and still counting. *Revue Neurologique* **171,** 505–530 (2015).
123. Knoblich, J. A. Asymmetric cell division: Recent developments and their implications for tumour biology. *Nature Reviews Molecular Cell Biology* **11,** 849–860 (2010).
124. Knoth, R. *et al.* Murine features of neurogenesis in the human hippocampus across the lifespan from 0 to 100 years. *PLoS One* **5,** (2010).
125. Köhler, C. A projection from the deep layers of the entorhinal area to the hippocampal formation in the rat brain. *Neurosci. Lett.* **56,** 13–19 (1985).
126. Komis, G. *et al.* Katanin Effects on Dynamics of Cortical Microtubules and Mitotic Arrays in Arabidopsis thaliana Revealed by Advanced Live-Cell Imaging. *Front. Plant Sci.* **8,** (2017).
127. Kopec, C. D. Glutamate Receptor Exocytosis and Spine Enlargement during Chemically Induced Long-Term Potentiation. *J. Neurosci.* **26,** 2000–2009 (2006).
128. Korn, E. D., Carlier, M. F. & Pantaloni, D. Actin polymerization and ATP hydrolysis. *Science* **238,** 638–644 (1987).
129. Kuhn, H. G., Dickinson-Anson, H. & Gage, F. H. Neurogenesis in the dentate gyrus of the adult rat: age-related decrease of neuronal progenitor proliferation. *J Neurosci* **16,** 2027–2033 (1996).
130. Kuijpers, M. & Hoogenraad, C. C. Centrosomes, microtubules and neuronal development. *Molecular and Cellular Neuroscience* **48,** 349–358 (2011).
131. Lacroix, B. *et al.* Tubulin polyglutamylation stimulates spastin-mediated microtubule severing. *J. Cell Biol.* **189,** 945–954 (2010).
132. Lagace, D. C. *et al.* Adult hippocampal neurogenesis is functionally important for stress-induced social avoidance. *Proc. Natl. Acad. Sci.* **107,** 4436–4441 (2010).
133. Lancaster, M. A. & Knoblich, J. A. Spindle orientation in mammalian cerebral cortical development. *Current Opinion in Neurobiology* **22,** 737–746 (2012).
134. Lavdas, a a, Grigoriou, M., Pachnis, V. & Parnavelas, J. G. The medial ganglionic eminence gives rise to a population of early neurons in the developing cerebral cortex. *J. Neurosci.* **19,** 7881–7888 (1999).
135. Lazic, S. E. Relating hippocampal neurogenesis to behavior: The dangers of ignoring confounding variables. *Neurobiology of Aging* **31,** 2169–2171 (2010).
136. Lee, Y. S. & Silva, A. J. The molecular and cellular biology of enhanced cognition. *Nature Reviews Neuroscience* **10,** 126–140 (2009).

137. Lendahl, U., Zimmerman, L. B. & McKay, R. D. CNS stem cells express a new class of intermediate filament protein. *Cell* **60,** 585–595 (1990).
138. Leuner, B., Gould, E. & Shors, T. J. Is there a link between adult neurogenesis and learning? *Hippocampus* **16,** 216–224 (2006).
139. Levitan, I. B. & K., L. K. The Neuron. Cell and molecular biology. Second edition. *Oxfor Univ. Press* (1997). at <http://linkinghub.elsevier.com/retrieve/pii/S089106180300019X>
140. Levitt, P., Cooper, M. L. & Rakic, P. Coexistence of neuronal and glial precursor cells in the cerebral ventricular zone of the fetal monkey: an ultrastructural immunoperoxidase analysis. *J. Neurosci.* **1,** 27–39 (1981).
141. Liang, F., Richmond, D. & Wang, Y. Coordination of Chromatid Separation and Spindle Elongation by Antagonistic Activities of Mitotic and S-Phase CDKs. *PLoS Genet.* **9,** (2013).
142. Lim, D. A. & Alvarez-Buylla, A. The adult ventricular–subventricular zone (V-SVZ) and olfactory bulb (OB) neurogenesis. *Cold Spring Harb. Perspect. Biol.* **8,** (2016).
143. Lin, B. Theta Stimulation Polymerizes Actin in Dendritic Spines of Hippocampus. *J. Neurosci.* **25,** 2062–2069 (2005).
144. Lin, H., Huganir, R. & Liao, D. Temporal dynamics of NMDA receptor-induced changes in spine morphology and AMPA receptor recruitment to spines. *Biochem. Biophys. Res. Commun.* **316,** 501–511 (2004).
145. Lin, Y.-C. & Koleske, A. J. Mechanisms of Synapse and Dendrite Maintenance and Their Disruption in Psychiatric and Neurodegenerative Disorders. *Annu. Rev. Neurosci.* **33,** 349–378 (2010).
146. Lind, D., Franken, S., Kappler, J., Jankowski, J. & Schilling, K. Characterization of the neuronal marker NeuN as a multiply phosphorylated antigen with discrete subcellular localization. *J. Neurosci. Res.* **79,** 295–302 (2005).
147. Lisman, J., Cooper, K., Sehgal, M. & Silva, A. J. Memory formation depends on both synapse-specific modifications of synaptic strength and cell-specific increases in excitability. *Nature Neuroscience* **21,** 309–314 (2018).
148. Liu, H. & Song, N. Molecular Mechanism of Adult Neurogenesis and its Association with Human Brain Diseases. *J. Cent. Nerv. Syst. Dis.* **8,** JCNSD.S32204 (2016).
149. Lodish, H., Berk, A. & Zipursky, S. Cell Biology. 4th edition. *Section 17.9, Receptor-Mediated Endocytosis and the Sorting of Internalized Proteins* (2000).
150. Lodish, H. *et al. Molecular Cell Biology. 4th edition*. *New York: W. H. Freeman* (2000). doi:10.1017/CBO9781107415324.004
151. Lois, C. & Alvarez-Buylla, a. Proliferating subventricular zone cells in the adult mammalian forebrain can differentiate into neurons and glia. *Proc. Natl. Acad. Sci. U. S. A.* **90,** 2074–2077 (1993).
152. Lois, C. & Alvarez-Buylla, A. Long-distance neuronal migration in the adult mammalian brain. *Science (80-.).* **264,** 1145–1148 (1994).
153. Lømo, T. Frequency potentiation of excitatory synaptic activity in the dentate area of the hippocampal formation. *Acta Physiol. Scand* **227,** 128 (1966).
154. Lucassen, P. J. *et al.* Regulation of adult neurogenesis by stress, sleep disruption, exercise and inflammation: Implications for depression and antidepressant action. *European Neuropsychopharmacology* **20,** 1–17 (2010).
155. Ludueña, R. F. Multiple forms of tubulin: different gene products and covalent modifications. *Int. Rev. Cytol.* **178,** 207–275 (1998).
156. Luptovčiak, I., Komis, G., Takáč, T., Ovečka, M. & Šamaj, J. Katanin: A Sword Cutting Microtubules for Cellular, Developmental, and Physiological Purposes. *Front. Plant Sci.* **8,** (2017).
157. Luskin, M. B. & Shatz, C. J. Studies of the earliest generated cells of the cat's visual cortex: cogeneration of subplate and marginal zones. *J. Neurosci.* **5,** 1062–1075 (1985).
158. Magee, J. C. & Johnston, D. Synaptic activation of voltage-gated channels in the dendrites of hippocampal pyramidal neurons. *Science (80-.).* **268,** 301–304 (1995).

159. Mak, G. K. & Weiss, S. Paternal recognition of adult offspring mediated by newly generated CNS neurons. *Nat. Neurosci.* **13,** 753–758 (2010).
160. Malatesta, P., Hartfuss, E. & Götz, M. Isolation of radial glial cells by fluorescent-activated cell sorting reveals a neuronal lineage. *Development* **127,** 5253–5263 (2000).
161. Mao, C.-X. *et al.* Microtubule-severing protein Katanin regulates neuromuscular junction development and dendritic elaboration in Drosophila. *Development* **141,** 1064–1074 (2014).
162. Mardin, B. R. & Schiebel, E. Breaking the ties that bind: New advances in centrosome biology. *Journal of Cell Biology* **197,** 11–18 (2012).
163. Maren, S., Aharonov, G. & Fanselow, M. S. Neurotoxic lesions of the dorsal hippocampus and Pavlovian fear conditioning in rats. *Behav. Brain Res.* **88,** 261–274 (1997).
164. Marin-Padilla, M. Dual origin of the mammalian neocortex and evolution of the cortical plate. *Anat. Embryol. (Berl).* **152,** 109–126 (1978).
165. Marschner, A., Kalisch, R., Vervliet, B., Vansteenwegen, D. & Buchel, C. Dissociable Roles for the Hippocampus and the Amygdala in Human Cued versus Context Fear Conditioning. *J. Neurosci.* **28,** 9030–9036 (2008).
166. Martí, E. *et al.* Distribution of Sonic hedgehog peptides in the developing chick and mouse embryo. *Development* **121,** 2537–47 (1995).
167. Martinez-Canabal, A., Akers, K. G., Josselyn, S. A. & Frankland, P. W. Age-dependent effects of hippocampal neurogenesis suppression on spatial learning. *Hippocampus* **23,** 66–74 (2013).
168. Martinowich, K. & Schloesser, R. J. in *Genes, Environment and Alzheimer's Disease* 51–94 (2016). doi:10.1016/B978-0-12-802851-3.00003-6
169. Marx, A. *et al.* Xenopus cytoplasmic linker-associated protein 1 (XCLASP1) promotes axon elongation and advance of pioneer microtubules. *Mol. Biol. Cell* **24,** 1544–1558 (2013).
170. Matamoros, A. J. & Baas, P. W. Microtubules in health and degenerative disease of the nervous system. *Brain Res. Bull.* **126,** 217–225 (2016).
171. Matsuo, M. *et al.* Katanin p60 contributes to microtubule instability around the midbody and facilitates cytokinesis in rat cells. *PLoS One* **8,** (2013).
172. Mazia, D. Centrosomes and mitotic poles. *Exp. Cell Res.* **153,** 1–15 (1984).
173. McNally, F. J., Okawa, K., Iwamatsu, a & Vale, R. D. Katanin, the microtubule-severing ATPase, is concentrated at centrosomes. *J. Cell Sci.* **109 (Pt 3,** 561–567 (1996).
174. McNally, F. J. & Thomas, S. Katanin is responsible for the M-phase microtubule-severing activity in Xenopus eggs. *Mol. Biol. Cell* **9,** 1847–1861 (1998).
175. McNally, F. J. Mechanisms of spindle positioning. *Journal of Cell Biology* **200,** 131–140 (2013).
176. McNally, F. J. & Vale, R. D. Identification of katanin, an ATPase that severs and disassembles stable microtubules. *Cell* **75,** 419–429 (1993).
177. McNally, K. P., Bazirgan, O. a & McNally, F. J. Two domains of p80 katanin regulate microtubule severing and spindle pole targeting by p60 katanin. *J. Cell Sci.* **113 (Pt 9,** 1623–1633 (2000).
178. McNally, K., Audhya, A., Oegema, K. & McNally, F. J. Katanin controls mitotic and meiotic spindle length. *J. Cell Biol.* **175,** 881–891 (2006).
179. Merkle, F. T., Mirzadeh, Z. & Alvarez-Buylla, A. Mosaic organization of neural stem cells in the adult brain. *Science* **317,** 381–4 (2007).
180. Merriam, E. B. *et al.* Synaptic Regulation of Microtubule Dynamics in Dendritic Spines by Calcium, F-Actin, and Drebrin. *J. Neurosci.* **33,** 16471–16482 (2013).
181. Meyer, G., Schaaps, J. P., Moreau, L. & Goffinet, a M. Embryonic and early fetal development of the human neocortex. *J. Neurosci.* **20,** 1858–1868 (2000).

182. Miller, M. W. & Nowakowski, R. S. Use of bromodeoxyuridine-immunohistochemistry to examine the proliferation, migration and time of origin of cells in the central nervous system. *Brain Res.* **457,** 44–52 (1988).
183. Mitchison, T. & Kirschner, M. Dynamic instability of microtubule growth. *Nature* **312,** 237–242 (1984).
184. Miyata, T. Asymmetric production of surface-dividing and non-surface-dividing cortical progenitor cells. *Development* **131,** 3133–3145 (2004).
185. Molnár, Z. *et al.* Comparative aspects of cerebral cortical development. *Eur. J. Neurosci.* **23,** 921–34 (2006).
186. Monteiro, B. M. M., Moreira, F. A., Massensini, A. R., Moraes, M. F. D. & Pereira, G. S. Enriched environment increases neurogenesis and improves social memory persistence in socially isolated adult mice. *Hippocampus* **24,** 239–248 (2014).
187. Moser, E. I., Moser, M.-B. & McNaughton, B. L. Spatial representation in the hippocampal formation: a history. *Nat. Neurosci.* **20,** 1448–1464 (2017).
188. Mullen, R. J., Buck, C. R. & Smith, A. M. NeuN, a neuronal specific nuclear protein in vertebrates. *Development* **116,** 201–211 (1992).
189. Nacher, J., Crespo, C. & McEwen, B. S. Doublecortin expression in the adult rat telencephalon. *Eur. J. Neurosci.* **14,** 629–644 (2002).
190. Nadarajah, B., Alifragis, P., Wong, R. O. L. & Parnavelas, J. G. Neuronal Migration in the Developing Cerebral Cortex: Observations Based on Real-time Imaging. *Cereb. Cortex* **13,** 607–611 (2003).
191. Nagy, J. I., Pereda, A. E. & Rash, J. E. On the occurrence and enigmatic functions of mixed (chemical plus electrical) synapses in the mammalian CNS. *Neuroscience Letters* (2017). doi:10.1016/j.neulet.2017.09.021
192. Nakaseko, Y. & Yanagida, M. Cytoskeleton in the cell cycle. *Nature* **412,** 291–292 (2001).
193. Nano, M. & Basto, R. in *Advances in Experimental Medicine and Biology* **1002,** 19–45 (2017).
194. Nguyen, M. M., Stone, M. C. & Rolls, M. M. Microtubules are organized independently of the centrosome in Drosophila neurons. *Neural Dev.* **6,** (2011).
195. Nicklas, R. B., Kubai, D. F. & Hays, T. S. Spindle microtubules and their mechanical associations after micromanipulation in anaphase. *J. Cell Biol.* **95,** 91–104 (1982).
196. Nigg, E. A. & Raff, J. W. Centrioles, Centrosomes, and Cilia in Health and Disease. *Cell* **139,** 663–678 (2009).
197. Nilsson, M., Perfilieva, E., Johansson, U., Orwar, O. & Eriksson, P. S. Enriched environment increases neurogenesis in the adult rat dentate gyrus and improves spatial memory. *J. Neurobiol.* **39,** 569–578 (1999).
198. Nimchinsky, E. A., Sabatini, B. L. & Svoboda, K. Structure and Function of Dendritic Spines. *Annu. Rev. Physiol.* **64,** 313–353 (2002).
199. Noctor, S. C., Martinez-Cerdeño, V., Ivic, L. & Kriegstein, A. R. Cortical neurons arise in symmetric and asymmetric division zones and migrate through specific phases. *Nat. Neurosci.* **7,** 136–144 (2004).
200. O'Donnell, L. *et al.* An essential role for Katanin p80 and microtubule severing in male gamete production. *PLoS Genet.* **8,** (2012).
201. O'Keefe, J. & Dostrovsky, J. The hippocampus as a spatial map. Preliminary evidence from unit activity in the freely-moving rat. *Brain Res.* **34,** 171–175 (1971).
202. O'Keefe, J. & Nadel, L. *The Hippocampus as a Cognitive Map*. *Clarendon Press. Oxford* (1978).
203. O'Keefe, J. Place units in the hippocampus of the freely moving rat. *Exp. Neurol.* **51,** 78–109 (1976).
204. Okabe, S. Molecular anatomy of the postsynaptic density. *Molecular and Cellular Neuroscience* **34,** 503–518 (2007).
205. Okamoto, K. I., Nagai, T., Miyawaki, A. & Hayashi, Y. Rapid and persistent modulation of actin dynamics regulates postsynaptic reorganization underlying bidirectional plasticity. *Nat. Neurosci.* **7,** 1104–1112 (2004).

206. Ouchi, Y. *et al.* Reduced Adult Hippocampal Neurogenesis and Working Memory Deficits in the Dgcr8-Deficient Mouse Model of 22q11.2 Deletion-Associated Schizophrenia Can Be Rescued by IGF2. *J. Neurosci.* **33,** 9408–9419 (2013).
207. Pang, T., Atefy, R. & Sheen, V. Malformations of Cortical Development. *Neurologist* **14,** 181–191 (2008).
208. Paridaen, J. T. & Huttner, W. B. Neurogenesis during development of the vertebrate central nervous system. *EMBO Reports* **15,** 351–364 (2014).
209. Park, S. *et al.* Sound tuning of amygdala plasticity in auditory fear conditioning. *Sci. Rep.* **6,** (2016).
210. Paton, J. A. & Nottebohm, F. N. Neurons generated in the adult brain are recruited into functional circuits. *Science (80-.).* **225,** 1046–1048 (1984).
211. Patten, I. & Placzek, M. The role of Sonic hedgehog in neural tube patterning. *Cell. Mol. Life Sci.* **57,** 1695–1708 (2000).
212. Pearson, C. G. & Bloom, K. Dynamic microtubules lead the way for spindle positioning. *Nature Reviews Molecular Cell Biology* **5,** 481–492 (2004).
213. Perera, T. D., Park, S. & Nemirovskaya, Y. Cognitive role of neurogenesis in depression and antidepressant treatment. *Neuroscientist* **14,** 326–338 (2008).
214. Petzoldt, A. G. & Sigrist, S. J. Synaptogenesis. *Curr. Biol.* **24,** R1076–80 (2014).
215. Pfaffl, M. W. A new mathematical model for relative quantification in real-time RT-PCR. *Nucleic Acids Res* **29,** 16–21 (2001).
216. Pfaffl, M. W., Horgan, G. W. & Dempfle, L. Relative expression software tool (REST) for group-wise comparison and statistical analysis of relative expression results in real-time PCR. *Nucleic Acids Res.* **30,** e36 (2002).
217. Philippidou, P. & Dasen, J. S. Hox Genes: Choreographers in Neural Development, Architects of Circuit Organization. *Neuron* **80,** 12–34 (2013).
218. Piccolino, M. Luigi Galvani and animal electricity: Two centuries after the foundation of electrophysiology. *Trends Neurosci.* **20,** 443–448 (1997).
219. Pickering-Brown, S. *et al.* Pick's disease is associated with mutations in the tau gene. *Ann. Neurol.* **48,** 859–867 (2000).
220. Pierre, M. & Nunez, J. Multisite phosphorylation of tau proteins from rat brain. *Biochem. Biophys. Res. Commun.* **115,** 212–9 (1983).
221. Pilling, A. D. Kinesin-1 and Dynein Are the Primary Motors for Fast Transport of Mitochondria in Drosophila Motor Axons. *Mol. Biol. Cell* **17,** 2057–2068 (2006).
222. Pollard, T. D. & Mooseker, M. S. Direct measurement of actin polymerization rate constants by electron microscopy of actin filaments nucleated by isolated microvillus cores. *J. Cell Biol.* **88,** 654–659 (1981).
223. Pollard, T. D. Rate constants for the reactions of ATP- and ADP-actin with the ends of actin filaments. *J. Cell Biol.* **103,** 2747–2754 (1986).
224. Purves D, Augustine GJ, Fitzpatrick D, et al., E. Neuroscience. *Sunderl. Sinauer Assoc.* (2001).
225. Purves, D. *et al.* Neuroscience. 2nd edition. *Sunderland (MA): Sinauer Associates; 2001.* 109–12 (2001). doi:978-0878937257
226. Qiang, L. Tau Protects Microtubules in the Axon from Severing by Katanin. *J. Neurosci.* **26,** 3120–3129 (2006).
227. Rakic, P. Radial versus tangential migration of neuronal clones in the developing cerebral cortex. *Proc. Natl. Acad. Sci. U. S. A.* **92,** 11323–11327 (1995).
228. Ramsden, M. Age-Dependent Neurofibrillary Tangle Formation, Neuron Loss, and Memory Impairment in a Mouse Model of Human Tauopathy (P301L). *J. Neurosci.* **25,** 10637–10647 (2005).
229. Rizzu, P. *et al.* High Prevalence of Mutations in the Microtubule-Associated Protein Tau in a Population Study of Frontotemporal Dementia in the Netherlands. *Am. J. Hum. Genet.* **64,** 414–421 (1999).
230. Rodríguez-Martín, T. *et al.* Tau phosphorylation affects its axonal transport and degradation. *Neurobiol. Aging* **34,** 2146–2157 (2013).

231. Roll-Mecak, A. & McNally, F. J. Microtubule-severing enzymes. *Current Opinion in Cell Biology* **22,** 96–103 (2010).
232. Roll-Mecak, A. & Vale, R. D. The Drosophila homologue of the hereditary spastic paraplegia protein, spastin, severs and disassembles microtubules. *Curr. Biol.* **15,** 650–655 (2005).
233. Rudy, J. W. Context representations, context functions, and the parahippocampal-hippocampal system. *Learning and Memory* **16,** 573–585 (2009).
234. Ryan, S. D. *et al.* Microtubule stability, Golgi organization, and transport flux require dystonin-a2-MAP1B interaction. *J. Cell Biol.* **196,** 727–742 (2012).
235. Sahay, A. *et al.* Increasing adult hippocampal neurogenesis is sufficient to improve pattern separation. *Nature* **472,** 466–470 (2011).
236. Sahay, A., Wilson, D. A. & Hen, R. Pattern Separation: A Common Function for New Neurons in Hippocampus and Olfactory Bulb. *Neuron* **70,** 582–588 (2011).
237. Sanes, J. R. & Lichtman, J. W. Developement of the vertebrate neuromuscular junction. *Annu. Rev. Neurosci.* **22,** 389–442 (1999).
238. Saxe, M. D. *et al.* Ablation of hippocampal neurogenesis impairs contextual fear conditioning and synaptic plasticity in the dentate gyrus. *Proc. Natl. Acad. Sci.* **103,** 17501–17506 (2006).
239. Saxe, M. D. *et al.* Paradoxical influence of hippocampal neurogenesis on working memory. *Proc. Natl. Acad. Sci.* **104,** 4642–4646 (2007).
240. Scharfman, H. E. & Hen, R. Is more neurogenesis always better? *Science* **315,** 336–338 (2007).
241. Schmued, L. C., Albertson, C. & Slikker, W. Fluoro-Jade: A novel fluorochrome for the sensitive and reliable histochemical localization of neuronal degeneration. *Brain Res.* **751,** 37–46 (1997).
242. Schulz, P. E., Cook, E. P. & Johnston, D. Changes in paired-pulse facilitation suggest presynaptic involvement in long-term potentiation. *J. Neurosci.* **14,** 5325–5337 (1994).
243. Schuyler, S. C. & Pellman, D. Microtubule 'plus-end-tracking proteins': The end is just the beginning. *Cell* **105,** 421–424 (2001).
244. Scoville, W. B. & Milner, B. LOSS OF RECENT MEMORY AFTER BILATERAL HIPPOCAMPAL LESIONS. *J. Neurol. Neurosurg. Psychiatry* **20,** 11–21 (1957).
245. Seo, D. -o., Carillo, M. A., Chih-Hsiung Lim, S., Tanaka, K. F. & Drew, M. R. Adult Hippocampal Neurogenesis Modulates Fear Learning through Associative and Nonassociative Mechanisms. *J. Neurosci.* **35,** 11330–11345 (2015).
246. Sept, D. Microtubule Polymerization: One Step at a Time. *Current Biology* **17,** (2007).
247. Seri, B., Garcia-Verdugo, J. M., McEwen, B. S. & Alvarez-Buylla, A. Astrocytes give rise to new neurons in the adult mammalian hippocampus. *J. Neurosci.* **21,** 7153–7160 (2001).
248. Shariati, S. a *et al.* APLP2 regulates neuronal stem cell differentiation during cortical development. *J Cell Sci* **126,** 1268–77 (2013).
249. Shors, T. J. *et al.* Neurogenesis in the adult is involved in the formation of trace memories. *Nature* **410,** 372–376 (2001).
250. Shors, T. J., Townsend, D. A., Zhao, M., Kozorovitskiy, Y. & Gould, E. Neurogenesis may relate to some but not all types of hippocampal-dependent learning. *Hippocampus* **12,** 578–584 (2002).
251. Siegel, G. J., Agranoff, B. W., Albers, R. W., Fisher, S. K. & Uhler, M. D. in *Basic Neurochemistry : Molecular , Cellular and Medical Aspects . 6th edition .* (Philadelphia: Lippincott-Raven, 1999). doi:10.1046/j.1471-4159.1995.64031424.x
252. Sirajuddin, M., Rice, L. M. & Vale, R. D. Regulation of microtubule motors by tubulin isotypes and post-translational modifications. *Nat. Cell Biol.* **16,** 335–344 (2014).
253. Skruber, K., Read, T.-A. & Vitriol, E. A. Reconsidering an active role for G-actin in cytoskeletal regulation. *J. Cell Sci.* **131,** jcs203760 (2018).

254. Smart, I. H. Proliferative characteristics of the ependymal layer during the early development of the mouse neocortex: a pilot study based on recording the number, location and plane of cleavage of mitotic figures. *J. Anat.* **116,** 67–91 (1973).
255. Smart, I. H. M., Dehay, C., Giroud, P., Berland, M. & Kennedy, H. Unique Morphological Features of the Proliferative Zones and Postmitotic Compartments of the Neural Epithelium Giving Rise to Striate and Extrastriate Cortex in the Monkey. *Cereb. Cortex* **12,** 37–53 (2002).
256. Smart, I. H. M. & McSherry, G. M. Growth patterns in the lateral wall of the mouse telencephalon. II. Histological changes during and subsequent to the period of isocortical neuron production. *J. Anat.* **134,** 415–42 (1982).
257. Smart, I. H. M. & Smart, M. Growth patterns in the lateral wall of the mouse telencephalon: I. Autoradiographic studies of the histogenesis of the isocortex and adjacent areas. *J. Anat.* **134,** 273–298 (1982).
258. So, J. H. *et al.* Intense Exercise Promotes Adult Hippocampal Neurogenesis But Not Spatial Discrimination. *Front. Cell. Neurosci.* **11,** (2017).
259. Söhl, G. & Willecke, K. Gap junctions and the connexin protein family. *Cardiovascular Research* **62,** 228–232 (2004).
260. Solnica-Krezel, L. & Sepich, D. S. Gastrulation: Making and Shaping Germ Layers. *Annu. Rev. Cell Dev. Biol.* **28,** 687–717 (2012).
261. Sorrells, S. F. *et al.* Human hippocampal neurogenesis drops sharply in children to undetectable levels in adults. *Nature* **555,** 377–381 (2018).
262. Spalding, K. L. *et al.* Dynamics of Hippocampal Neurogenesis in Adult Humans. *Cell* **153,** 1219–1227 (2013).
263. Spitzer, N. C. Neurotransmitter Switching? No Surprise. *Neuron* **86,** 1131–1144 (2015).
264. Sternlicht, H., Yaffe, M. B. & Farr, G. W. A model of the nucleotide-binding site in tubulin. *FEBS Lett.* **214,** 226–235 (1987).
265. Stevens, R. & Cowey, A. Effects of dorsal and ventral hippocampal lesions on spontaneous alternation, learned alternation and probability learning in rats. *Brain Res.* **52,** 203–224 (1973).
266. Stiess, M. & Bradke, F. Neuronal polarization: The cytoskeleton leads the way. *Dev Neurobiol* **71,** 430–444 (2010).
267. Su, L. K. & Qi, Y. Characterization of human MAPRE genes and their proteins. *Genomics* **71,** 142–149 (2001).
268. Südhof, T. C. The presynaptic active zone. *Neuron* **75,** 11–25 (2012).
269. Sudo, H. & Baas, P. W. Acetylation of Microtubules Influences Their Sensitivity to Severing by Katanin in Neurons and Fibroblasts. *J. Neurosci.* **30,** 7215–7226 (2010).
270. Sudo, H. & Baas, P. W. Strategies for diminishing katanin-based loss of microtubules in tauopathic neurodegenerative diseases. *Hum. Mol. Genet.* **20,** 763–778 (2011).
271. Sussel, L., Marin, O., Kimura, S. & Rubenstein, J. L. Loss of Nkx2.1 homeobox gene function results in a ventral to dorsal molecular respecification within the basal telencephalon: evidence for a transformation of the pallidum into the striatum. *Development* **126,** 3359–3370 (1999).
272. Takano, T., Xu, C., Funahashi, Y., Namba, T. & Kaibuchi, K. Neuronal polarization. *Development* **142,** 2088–2093 (2015).
273. Tan, X. & Shi, S. H. Neocortical neurogenesis and neuronal migration. *Wiley Interdisciplinary Reviews: Developmental Biology* **2,** 443–459 (2013).
274. Tao, J., Feng, C. & Rolls, M. M. The microtubule-severing protein fidgetin acts after dendrite injury to promote their degeneration. *J. Cell Sci.* **129,** 3274–3281 (2016).
275. Tischfield, M. A. *et al.* Human TUBB3 Mutations Perturb Microtubule Dynamics, Kinesin Interactions, and Axon Guidance. *Cell* **140,** 74–87 (2010).

276. Toyo-Oka, K. *et al.* Recruitment of katanin p60 by phosphorylated NDEL1, an LIS1 interacting protein, is essential for mitotic cell division and neuronal migration. *Hum. Mol. Genet.* **14,** 3113–3128 (2005).
277. Tsien, J. Z. *et al.* Subregion- and cell type-restricted gene knockout in mouse brain. *Cell* **87,** 1317–1326 (1996).
278. Vale, R. D. Severing of stable microtubules by a mitotically activated protein in xenopus egg extracts. *Cell* **64,** 827–839 (1991).
279. Vemu, A., Atherton, J., Spector, J. O., Moores, C. A. & Roll-Mecak, A. Tubulin isoform composition tunes microtubule dynamics. *Mol. Biol. Cell* mbc.E17–02–0124 (2017). doi:10.1091/mbc.E17-02-0124
280. Wegner, A. Head to tail polymerization of actin. *J. Mol. Biol.* **108,** 139–150 (1976).
281. Weingarten, M. D., Lockwood, A. H., Hwo, S. Y. & Kirschner, M. W. A protein factor essential for microtubule assembly. *Proc. Natl. Acad. Sci. U. S. A.* **72,** 1858–62 (1975).
282. Weisenberg, R. C., Deery, W. J. & Dickinson, P. J. Tubulin-Nucleotide Interactions during the Polymerization and Depolymerization of Microtubules. *Biochemistry* **15,** 4248–4254 (1976).
283. Wichterle, H., Garcia-Verdugo, J. M., Herrera, D. G. & Alvarez-Buylla, A. Young neurons from medial ganglionic eminence disperse in adult and embryonic brain. *Nat. Neurosci.* **2,** 461–466 (1999).
284. Witte, H. & Bradke, F. The role of the cytoskeleton during neuronal polarization. *Current Opinion in Neurobiology* **18,** 479–487 (2008).
285. Witte, H., Neukirchen, D. & Bradke, F. Microtubule stabilization specifies initial neuronal polarization. *J. Cell Biol.* **180,** 619–632 (2008).
286. Witter, M. P., Groenewegen, H. J., Lopes da Silva, F. H. & Lohman, A. H. M. Functional organization of the extrinsic and intrinsic circuitry of the parahippocampal region. *Prog. Neurobiol.* **33,** 161–253 (1989).
287. Wloga, D. *et al.* Hyperglutamylation of tubulin can either stabilize or destabilize microtubules in the same cell. *Eukaryot. Cell* **9,** 184–193 (2010).
288. Wloga, D., Joachimiak, E. & Fabczak, H. Tubulin post-translational modifications and microtubule dynamics. *International Journal of Molecular Sciences* **18,** (2017).
289. Wojtowicz, J. M. Irradiation as an experimental tool in studies of adult neurogenesis. *Hippocampus* **16,** 261–266 (2006).
290. Wojtowicz, J. M., Askew, M. L. & Winocur, G. The effects of running and of inhibiting adult neurogenesis on learning and memory in rats. *Eur. J. Neurosci.* **27,** 1494–1502 (2008).
291. Wolf, S. a, Melnik, a & Kempermann, G. Physical exercise increases adult neurogenesis and telomerase activity, and improves behavioral deficits in a mouse model of schizophrenia. *Brain. Behav. Immun.* **25,** 971–980 (2011).
292. Yang, Y., Wang, X. -b., Frerking, M. & Zhou, Q. Spine Expansion and Stabilization Associated with Long-Term Potentiation. *J. Neurosci.* **28,** 5740–5751 (2008).
293. Ye, B. *et al.* Differential regulation of dendritic and axonal development by the novel Krüppel-like factor dar1. *J. Neurosci. Off. J. Soc. Neurosci.* **31,** 3309–3319 (2011).
294. Ye, J. *et al.* Primer-BLAST: a tool to design target-specific primers for polymerase chain reaction. *BMC Bioinformatics* **13,** 134 (2012).
295. Yu, I., Garnham, C. P. & Roll-Mecak, A. Writing and reading the tubulin code. *J. Biol. Chem.* **290,** 17163–17172 (2015).
296. Yu, W. *et al.* Regulation of Microtubule Severing by Katanin Subunits during Neuronal Development. *J. Neurosci.* **25,** 5573–5583 (2005).
297. Zehr, E. *et al.* Katanin spiral and ring structures shed light on power stroke for microtubule severing. *Nat. Struct. Mol. Biol.* **24,** 717–725 (2017).
298. Zhang, D. *et al.* Drosophila katanin is a microtubule depolymerase that regulates cortical-microtubule plus-end interactions and cell migration. *Nat. Cell Biol.* **13,** 361–372 (2011).

299. Zhang, J. & Jiao, J. Molecular Biomarkers for Embryonic and Adult Neural Stem Cell and Neurogenesis. *BioMed Research International* **2015,** (2015).
300. Zhao, C., Deng, W. & Gage, F. H. Mechanisms and functional implications of adult neurogenesis. *Cell* **132,** 645–660 (2008).
301. Zhou, J., Shu, H. B. & Joshi, H. C. Regulation of tubulin synthesis and cell cycle progression in mammalian cells by gamma-tubulin-mediated microtubule nucleation. *J Cell Biochem* **84,** 472–483 (2002).
302. Zucker, R. S. & Regehr, W. G. Short-Term Synaptic Plasticity. *Annu. Rev. Physiol.* **64,** 355–405 (2002).

8. Appendix

8.1. List of figures

8.2. List of abbreviations

ACSF	Artificial cerebrospinal fluid
AD	Alzheimer's disease
ADP	Adenosine 5'-diphosphate
AF	Actin filaments
AMPA	α-amino-3-hydroxy-5-methyl-4-isoxazolepropionic acid
ATAT	Alpha-tubulin acetyltransferase
ATP	Adenosine triphosphate
BrdU	Bromodeoxyuridine
BSA	Bovine Serum Albumin
C-terminal	Carboxy-terminal
CA1	Cornu ammonis area 1

CA3	Cornu ammonis area 3
CAM(s)	Cell adhesion molecules
Camk	Ca^{2+}/calmodulin-dependent protein kinase
cl-PARP	Cleaved-PARP
CNS	Central nervous system
CP	Cortical plate
CRE	Cre recombinase
CS	Conditioned stimulus
Cy(2)	Cyanine
DAB	3,3'-Diaminobenzidine
DAPI	4',6-diamidino-2-phenylindole
DCX	Doublecortin
DG	Dentate gyrus
DH5-alpha	Douglas Hanahan5-alpha
DiI	1,1'-dioctadecyl-3,3,3'3'-tetramethylindocarbocyanine perchlorate
DIV(12)	Days in vitro (12)
DMEM	Dulbecco modified eagle medium
DNA	Deoxyribonucleic acid
dNTPs	Deoxyribonucleotide triphosphate
E.(15)	Embryonic day-(15)
E.M.	Electron microscopy
EB3	End-binding protein 3
EC	Enthorinal cortex
ECL	Enhanced chemiluminescence
EDTA	Ethylenediaminetetraacetic acid
EGFP	Enhanced green fluorescent protein
EGTA	Ethylene glycol-bis(b-aminoethyl ether)-N,N,N',N'-tetraacetic acid
EPM	Elevated-plus maze
EtOH	Ethanol
F-actin	Filamentous actin
FC	Fear conditioning
fEPSPs	Field-excitatory postsynaptic potentials
Flp	Flippase
FRT	Flippase recognition target
FTD	Frontotemporal dementia

fx	flox
G-actin	Globular actin
G-phase	Gap-phase
GAPDH	Glyceraldehyde-3-phosphate dehydrogenase
GCL	Granule Cell Layer
GDP	Guanosine diphosphate
GFAP	Glial fibrillary acidic protein
GFP	Green fluorescent protein
GTP	Guanosine triphosphate
HBSS	Hank's balanced salt solution
HDAC	histone deacetylase
HEPES	4-(2-hydroxyethyl)-1-piperazineethanesulfonic acid
HRP	Horseradish peroxidase
HSP	Hereditary Spastic Paraplegia
IF	Intermediate filaments
IF	Immunofluorescence
IgG	Immunoglobulin G
IHC	Immunohistochemistry
IHC	immunohistochemistry
IPC	Intermediate progenitor cells
kDa	Kilodaltons
KO	knockout
Lac Z	Lac operon gene Z
LB	Luria
LDT	Light-dark transition
loxP	Cre recombinase target sequence from bacteriophage P1
LTP	Long-term potentiation
LV	Lateral ventricle
MAM	methylazoxymethanol acetate
MAP(s)	MT-associated proteins
MeOH	Methanol
ML	Molecular Layer
mM	Milimolar
mRNA	Messenger RNA
MT(s)	Microtubule(s)

MZ	Marginal zone
N-terminal	Amino-terminal
N2a	Neuro2a cells from mouse neuroblastoma
neo	Neomycin
NeuN	Neuronal nuclei, Fox3
NIH	National institutes of health
NMDA	N-Methyl-D-aspartic acid
NPC	Neuronal precursor cell
NSC(s)	Neuronal Stem Cell(s)
OB	Olfactory bulb
OF	Open field
p(21)	Post-natal day (21)
PAGE	Polyacrylamide gel electrophoresis
PARP	Poly (ADP-ribose) polymerase
PBS	Phosphate buffered saline
PCR	Polymerase chain reaction
PFA	paraformaldehyde
PHF	Paired helical filaments
P_i	Inorganic phosphate
polyE	Poly-glutamylated
PP	Preplate
PTM(s)	Post-translational modification(s)
qPCR	Quantitative PCR
RGC	Radial Glia cells
RGL(s)	Radial Glia-like cells
RMS	Rostral migratory stream
RNA	Ribonucleic acid
ROI	Region of interest
rTg	Regulatable transgene
S-phase	DNA synthesis-phase
S.E.M.	Standard error of means
S.O.C.	Super optimal broth with catabolite repression
S1	Postnuclear supernatant fraction 1
SDS	Sodium dodecyl sulfate
SGZ	Subgranular zone

SHH	Sonic Hedgehog
SNP	Short neuronal precursors
SP	Subplate
SVZ	Subventricular zone
TAE	Tris-acetate-EDTA
TBS	Tris-buffered saline
TBs	Theta burst stimulation
TBS-T	Tris-buffered saline + Tween
Tg	Transgenic
TTLL	Tubulin tyrosine ligase-like
TUBA4A	Human Tubulin a-4 A chain
TUBB3	Human Tubulin b-3
US	Unconditioned stimulus
VZ	Ventricular zone
WD40	Beta-transducin repeat
wt	wildtype
ZMNH	Zentrum für Molekulare Neurobiologie Hamburg

9. Statement of contributions

Experiments that required collaborators contributions:

Knockout first animals with conditional potential generation:
Laura Ruschkies, Dr. Torben Hausrat, PD Dr. Irm Hermans-Borgmeyer

mRNA quantification:
Planned the experiments: Franco Luis Lombino and Sabine Hoffmeister-Ullerich
Performed the experiments: Priv.-Doz. Dr. rer. nat. Sabine Hoffmeister-Ullerich
Quantified the experiments: Priv.-Doz. Dr. rer. nat. Sabine Hoffmeister-Ullerich

Venus in-utero electroporation for cortical neuronal migration:
Planned the experiments: Franco Luis Lombino
Electroporation: Dr. Melanie Richter, Dr. Froylan Calderon de Anda
Tissue collection and processing: Franco Luis Lombino
Quantified the experiments: Franco Luis Lombino
Interpretation of results: Franco Luis Lombino

BrdU staining for SGZ neuronal proliferation:
Planned the experiments: Franco Luis Lombino
BrdU intraperitoneal injection: Dr. David Lutz
Tissue collection and processing: Franco Luis Lombino
Quantified the experiments: Franco Luis Lombino
Interpretation of results: Franco Luis Lombino

Sox2/GFAP staining for SGZ neuronal proliferation:
Planned the experiments: Franco Luis Lombino
Animals perfusion and brain harvesting: Edda Thies and Franco Luis Lombino
Performed the experiments: Dr. Monika Brill
Quantified the experiments: Dr. Monika Brill
Interpretation of results: Franco Luis Lombino

Behavioral experiments:
Planned the experiments: Dr. Mary Muhia and Franco Luis Lombino
Performed the experiments: Franco Lombino
Quantified the experiments: Franco Lombino
Statistical analysis: Dr. Mary Muhia and Franco Luis Lombino
Interpretation of results: Dr. Mary Muhia and Franco Luis Lombino

Electron Microscopy of p60-DEID dominant negative:

Planned the experiments: Franco Luis Lombino

Cells preparation and overexpression: Franco Luis Lombino

Tissue preparation and imaging: Dr. Michaela Schweizer.

Interpretation of results: Franco Luis Lombino

EB3 dynamics in dendrites upon p60-DEID overexpression:

Planned the experiments: Prof. Dr. Matthias Kneussel, Franco Luis Lombino

Cells seeding, overexpression and imaging: Edda Thies

Data analysis: Franco Luis Lombino

Interpretation of results: Franco Luis Lombino

Schaffer collaterals LTP measurments of CamKII-a-CRE-katna1 fx/fx animals:

Planned the experiments: Franco Luis Lombino

Tissue preparation and electrophysiological recordings: Sabine Graf and Christine Gee

Data analysis: Sabine Graf and Dr. Christine Gee

Interpretation of results: Franco Luis Lombino

Dendritic spines number upon p60-DEID overexpression in hippocampal neurons:

Planned the experiments: Franco Luis Lombino

Cells seeding: Edda Thies

Performed the experiments: Franco Luis Lombino

Data analysis: Franco Luis Lombino

Interpretation of results: Franco Luis Lombino

EB3 puncta in dendritic spines upon p60-DEID overexpression in hippocampal neurons:

Planned the experiments: Franco Luis Lombino

Cells seeding: Edda Thies

Performed the experiments: Franco Luis Lombino

Data analysis: Franco Luis Lombino

Interpretation of results: Franco Luis Lombino

Dendritic spines morphology upon glutamate uncaging in p60-DEID-overexpressing in hippocampal neurons:

Planned the experiments: Franco Luis Lombino and Dr. Kira Gromova

Cells seeding: Edda Thies

Overexpression: Franco Luis Lombino

Performed the experiments: Dr. Kira Gromova

Data analysis: Franco Luis Lombino

Interpretation of results: Franco Luis Lombino and Dr. Kira Gromova

P60 katanin protein levels in Tau transgenic animals:

Planned the experiments: Franco Luis Lombino

Tissue collection: Dr. Astrid Sydow from Prof. E. Mandelkow laboratory.

Performed the experiments: Franco Luis Lombino

Data analysis: Franco Luis Lombino

Interpretation of results: Franco Luis Lombino

10. Acknowledgements

Getting to the end of a period is a great personal achievement, but before I go forward, I want to remember every step that drove me here. For that, I want to thank my previous supervisors Dr. Comi C. and Dr. D'Adamio L. The first, supported since the beginning my wish to learn. I'll be always grateful. The next, shared with me his passion and love for every experiment performed in the lab. His inspiration was a boost for my career.

I'm very grateful to Prof. Matthias Kneussel, because he gave me the chance to reach my goals. He also allowed me to follow my curiosity and explore different aspects of the field.

During this period, I had the chance to collaborate with different groups. All of them listened to me and were ready to help. I thank them too.

I want to thank all my colleagues from the Molecular Neurogenetics lab, at ZMNH. I went to most of them with questions and concerns, and they were always available for discussion. Thanks to Dr. Kira Brune, because of her spontaneous collaboration. Thanks to Dr. Mary Muhia, because she patiently introduced me to a new field. I tried to catch as much as I could from her infinite knowledge. I also thank Dr. Wolfgang Wagner because collaborating with him in other studies gave me the chance to dig into other topics.
I'm extremely thankful to Edda Thies. Scientific discussions with her were valuable for me. Besides, she was always ready to listen or give a hand when needed.

The people that surround us everyday play a major role in achieving a goal. For that, I want to thank my friends. First Mauro, the moments we spent together are just unique. I thank him for everything what he gave me without even realizing. I thank the Argentineans Carlos and Juan, because they're always close despite the distance. Thanks to the Italians Carlo, Lorenzo, Massimo and Matteo because we met playing, and so we did until now.

Thanks to Claudia, because she never let me down and supported me in a patient and constant manner. Her simplicity and love helped me to go forward and face every single obstacle. She remembered me who I am and helped me keeping my feet on the floor since the beginning of this experience. I do not know how many lives I should live to thank her.

Finally, I also thank my father, because he encouraged me to realize my dreams. I thank my siblings Augusto, Sara and Vale. They are models for me. I feel peace every time I see them or talk with them. Special thanks to my mother, because she showed me how to fight for my dreams and how to stand up when things are not perfect. She showed me what strength is.